



5-2023

## **TCF4 Is a Key Mediator of Cell Identity and Oncogenesis in Neuroblastoma**

Nour Aljouda  
*University of Tennessee Health Science Center*

Follow this and additional works at: <https://dc.uthsc.edu/dissertations>



Part of the [Investigative Techniques Commons](#), [Medical Cell Biology Commons](#), [Medical Genetics Commons](#), and the [Neoplasms Commons](#)

---

### **Recommended Citation**

Aljouda, Nour (<https://orcid.org/0000-0001-5259-1293>), "TCF4 Is a Key Mediator of Cell Identity and Oncogenesis in Neuroblastoma" (2023). *Theses and Dissertations (ETD)*. Paper 642. <http://dx.doi.org/10.21007/etd.cghs.2023.0627>.

This Dissertation is brought to you for free and open access by the College of Graduate Health Sciences at UTHSC Digital Commons. It has been accepted for inclusion in Theses and Dissertations (ETD) by an authorized administrator of UTHSC Digital Commons. For more information, please contact [jwelch30@uthsc.edu](mailto:jwelch30@uthsc.edu).

---

# TCF4 Is a Key Mediator of Cell Identity and Oncogenesis in Neuroblastoma

## Abstract

Neuroblastomas (NB) are embryonal childhood tumors that derive from the multipotent neural crest cells (NCCs) of the peripheral nervous system. NB accounts for more than 15% of all childhood cancer-related deaths. Despite the most intensive multimodal therapy, more than 50% of patients with high-risk NB relapse with often fatal, resistant disease. Novel therapies are desperately needed to improve cure rates. Previous studies proposed that the deregulation of normal neural crest developmental programs contributes to NB oncogenesis by retaining the highly migratory and proliferative traits of NCCs. Thus, activation or repression of neural crest developmental pathways have been implicated in NB pathogenesis. Recent data reported two identities in neuroblastoma cell lines: one establishing a more proliferative adrenergic (ADRN) cell state and a second establishing a more invasive, therapy-resistant mesenchymal (MES) cell state. Super-enhancer-associated transcription factor (TF) networks define cell identities in neuroblastoma (NB). Dysregulation of these TFs contributes to the initiation and maintenance of NB by enforcing early developmental identity states. We report the bHLH transcription factor TCF4 (E2-2) is a critical NB dependency gene that significantly contributes to these identity states through its heterodimerization with cell identity specific bHLH TFs. Mechanistically, we show that TCF4 promotes cell proliferation through direct transcriptional regulation of a MYC/MYCN oncogenic program. To identify potential therapeutic vulnerabilities, we characterized the TCF4 regulatory interactome and identified multiple epigenetic factors including HDACs and KDM1A. We determined that inhibitors to both HDACs and KDM1A, which often form complexes together, reduce TCF4 protein stability. Our work suggests that loss of TCF4 protein expression is an important biological readout for determining the efficacy of these epigenetic inhibitors in treating patients and could lead to improved patient outcomes.

## Document Type

Dissertation

## Degree Name

Doctor of Philosophy (PhD)

## Program

Biomedical Sciences

## Research Advisor

Kevin W. Freeman, PhD

## Keywords

Cell identity, Core regulatory circuitries, Neuroblastoma, Super-enhancer, Targeting epigenetics

## Subject Categories

Analytical, Diagnostic and Therapeutic Techniques and Equipment | Diseases | Investigative Techniques | Medical Cell Biology | Medical Genetics | Medical Sciences | Medicine and Health Sciences | Neoplasms

UNIVERSITY OF TENNESSEE HEALTH SCIENCE CENTER

DOCTORAL DISSERTATION

---

**TCF4 Is a Key Mediator of Cell Identity and  
Oncogenesis in Neuroblastoma**

---

*Author:*  
Nour Aljouda

*Advisor:*  
Kevin W. Freeman, PhD

*A Dissertation Presented for The Graduate Studies Council of  
The University of Tennessee Health Science Center  
in Partial Fulfillment of the Requirements for the Doctor of Philosophy degree from  
The University of Tennessee*

*in*

*Biological Sciences: Genetics, Genomics, and Informatics  
College of Graduate Health Sciences*

*May 2023*

Appendix A © 2023 by Nour A. Aljouda, Dewan Shrestha, Satyanarayana Alleboina, et al.  
Appendix B © 2021 by American Society of Gene & Cell Therapy.  
All other material © 2023 by Nour Aljouda.  
All rights reserved.

## **DEDICATION**

To my husband, Abdul, who supported me throughout the years and encouraged me to work harder. To my wonderful kids, Riyad, Yasmine, Leen and Omar, for providing me with endless joy to distract from the hard days. I never could have done this without your love, and support throughout the years. To my mother and my father for their unconditional love and support.

## ACKNOWLEDGEMENTS

First, I am so grateful to my mentor Dr. Kevin Freeman for his guidance and support throughout the years. He always challenged me to do more, ask the right questions and acquire the skills and approaches to problem solving. His patience, guidance and commitment helped me evolve into a more confident, and thoughtful scientist.

I appreciate the time and help from my committee members: Dr. Ankush Gosain, Dr. Liza Makowski, Dr. Susan Amy Miranda, and Dr. Ramesh Narayanan. You all have always provided amazing feedback and contributed to my scientific training. I am extremely grateful for your help and support.

I would like to thank my previous and current lab members. Special thanks to Dr. Megan Walker, a previous post-doctoral scientist I had the privilege of working with and learning from. Also, Dr. Satyanarayana Alleboina for the contributions he made to this project. My fellow graduate students, Pamela and Chelsea, thank you both for providing an amazing, shared lab environment.

I would like to thank my colleague Dewan Shrestha for his valuable contributions in analyzing the RNA and the ChIP- sequencing data, and his mentor Dr. Yong Cheng for his support of this project and scientific guidance.

Finally, I am also thankful for the staff of the Molecular Resource Center (MRC) Core and the Flow Cytometry and Cell Sorting (FCCS) Core at The University of Tennessee Health Science Center (UTHSC) for their dedication and expertise.

## PREFACE

The body of this dissertation is organized in a way that first introduces readers to our rationale for choosing the research topic, hypothesis, and specific aims—as well as to present an overview of neuroblastoma. A discussion of the materials and methods used then leads to a presentation of the research and final analysis with a discussion of our findings. A concluding chapter relates all research elements back to our final thoughts about the findings and their significance.

For readers to have immediate access to the full presentation of our previously published research studies, the articles are presented in the appendices. This mode of presentation allows for Chapters 3 and 4, which use them as their basis, to focus more narrowly on a summary and discussion of those articles in Appendices A and B and to show specifically how they relate to the dissertation’s larger goals. Chapter 3 also references five **Supplementary Tables**. References in the chapters to relevant sections, tables, or figures in these appendices look like the following example. The Chapter 4 callout to **Figure B-S1** refers to Supplementary Figure 1 in **Appendix B**. The blue highlight links to the appendix figure to return to the Chapter 4 callout page, see the PDF navigation note next.

**NOTE ON PDF NAVIGATION:** Document navigation is greatly facilitated by using Adobe Acrobat’s “Previous view” and “Next view” functions. For “Previous view,” use quick keys Alt/Ctrl+Left Arrow on PC or Command+Left Arrow on Mac. For “Next view,” use Alt/Ctrl+Right Arrow on PC or Command+Right Arrow on Mac. Using these quick keys in tandem allows the reader to toggle between document locations. Since every scroll represents a new view; depending on how much scrolling is done for a specific view destination, more than one press of the back or forward arrows may be needed. For additional navigational tips, click View at the top of the PDF, then Page Navigation. These Adobe Acrobat functions may not be functional for other PDF readers or for PDFs opened in web browsers.

## ABSTRACT

Neuroblastomas (NB) are embryonal childhood tumors that derive from the multipotent neural crest cells (NCCs) of the peripheral nervous system. NB accounts for more than 15% of all childhood cancer-related deaths. Despite the most intensive multimodal therapy, more than 50% of patients with high-risk NB relapse with often fatal, resistant disease. Novel therapies are desperately needed to improve cure rates. Previous studies proposed that the deregulation of normal neural crest developmental programs contributes to NB oncogenesis by retaining the highly migratory and proliferative traits of NCCs. Thus, activation or repression of neural crest developmental pathways have been implicated in NB pathogenesis.

Recent data reported two identities in neuroblastoma cell lines: one establishing a more proliferative adrenergic (ADRN) cell state and a second establishing a more invasive, therapy-resistant mesenchymal (MES) cell state. Super-enhancer-associated transcription factor (TF) networks define cell identities in neuroblastoma (NB). Dysregulation of these TFs contributes to the initiation and maintenance of NB by enforcing early developmental identity states. We report the bHLH transcription factor TCF4 (E2-2) is a critical NB dependency gene that significantly contributes to these identity states through its heterodimerization with cell identity specific bHLH TFs. Mechanistically, we show that TCF4 promotes cell proliferation through direct transcriptional regulation of a MYC/MYCN oncogenic program. To identify potential therapeutic vulnerabilities, we characterized the TCF4 regulatory interactome and identified multiple epigenetic factors including HDACs and KDM1A. We determined that inhibitors to both HDACs and KDM1A, which often form complexes together, reduce TCF4 protein stability. Our work suggests that loss of TCF4 protein expression is an important biological readout for determining the efficacy of these epigenetic inhibitors in treating patients and could lead to improved patient outcomes.



## TABLE OF CONTENTS

|  |           |
|--|-----------|
| <b>CHAPTER 1. INTRODUCTION</b> .....   | <b>1</b>  |
| Neuroblastoma .....  | 1         |
| Neural Crest Cells Fate Decision.....  | 2         |
| Core Regulatory Circuitries and Super Enhancers (SEs) in Cancer.....   | 4         |
| CRC Factors in Cancer .....  | 4         |
| CRC Factors in NB .....  | 5         |
| MYCN .....   | 5         |
| The E Protein TCF4.....  | 6         |
| Targeting Epigenetic Transcriptional Regulators in Cancer.....   | 9         |
| HDAC Inhibitors.....   | 9         |
| KDM1A Inhibitors.....  | 10        |
| BET Inhibitors .....   | 11        |
| Hypothesis and Specific Aims.....  | 12        |
| Aim 1: To determine if TCF4 is a critical NB dependency factor that is shared<br>across the different NCC lineage states ..... | 12        |
| Aim 2: To determine the TCF4 interactome in neuroblastoma .....  | 12        |
| Aim 3: To test the possibility to drug TCF4 in NB expressing cell lines using<br>different epigenetic drugs .....              | 12        |
| <b>CHAPTER 2. METHODOLOGY</b> .....  | <b>13</b> |
| Cell Lines.....  | 13        |
| RNA-Seq Library Preparation and Sequencing.....  | 13        |
| Doxycycline-Inducible shRNA Systems .....  | 13        |
| Real-Time Quantitative PCR.....  | 14        |
| Western Blot Analysis .....  | 14        |
| Co-Immunoprecipitation and Western Blotting Analysis .....   | 14        |
| CyQuant Assay .....  | 15        |
| Annexin V/PI Flow Cytometry Assay .....  | 15        |
| Ectopic Expression of TCF4.....  | 15        |
| Colony Formation in Soft Agar .....  | 16        |
| In Vivo Tumor Models .....   | 16        |
| Chromatin Immunoprecipitation ChIP-Seq.....  | 16        |
| Target Genes .....   | 17        |
| ATAC-Seq Data Processing .....   | 17        |
| Promoter Capture Hi-C.....   | 17        |
| Genomic Annotation.....  | 17        |
| Public Data.....   | 17        |
| Data Availability.....   | 18        |
| Immunoprecipitation-Mass Spectrometry Analysis .....   | 18        |
| Statistical Analysis.....  | 18        |

|  |            |
|--|------------|
| <b>CHAPTER 3. TCF4 IS A KEY MEDIATOR OF CELL IDENTITY AND ONCOGENESIS IN NEUROBLASTOMA .....</b> | <b>19</b>  |
| Introduction.....  | 19         |
| Summary.....   | 19         |
| Discussion.....  | 23         |
| <b>CHAPTER 4. CRC DISRUPTION FACILITATES NB DIFFERENTIATION.....</b>                             | <b>25</b>  |
| Introduction.....  | 25         |
| Summary.....   | 26         |
| Discussion.....  | 27         |
| <b>CHAPTER 5. INFLUENCE OF TCF4 LOSS ON HAND2 PROTEIN INTERACTIONS.....</b>                      | <b>29</b>  |
| Introduction.....  | 29         |
| Immunoprecipitation-Mass Spectrometry Analysis .....   | 30         |
| Results.....   | 30         |
| Discussion.....  | 34         |
| <b>CHAPTER 6. CONCLUSIONS AND FUTURE DIRECTION .....</b>   | <b>35</b>  |
| <b>LIST OF REFERENCES.....</b>   | <b>38</b>  |
| <b>APPENDIX A. CHAPTER 3 ARTICLE .....</b>   | <b>48</b>  |
| Introduction.....  | 48         |
| Article .....  | 48         |
| <b>APPENDIX B. CHAPTER 4 ARTICLE .....</b>   | <b>79</b>  |
| Introduction.....  | 79         |
| Article .....  | 79         |
| <b>VITA.....</b>   | <b>105</b> |

## LIST OF FIGURES

|   |    |
|---|----|
| Figure 1-1. Neural crest cells lineage specification.....   | 3  |
| Figure 1-2. Structure of class I bHLH proteins. ....  | 7  |
| Figure 3-1. Inhibition of CRC TFs following the treatment of NB cells and mouse<br>NCCs with the BET-inhibitors, JQI and SJ018..... | 20 |
| Figure 3-2. TCF4 interactions validation.....   | 22 |
| Figure 3-3. TCF4 interacts with MYCN.....   | 22 |
| Figure 5-1. HAND2 interactors affected following TCF4 loss. ....  | 32 |
| Figure 5-2. PANTHER gene ontology analysis of HAND2-interacting proteins<br>following TCF4 loss.....                                | 33 |

## LIST OF ABBREVIATIONS

|          |   |
|----------|---|
| ADRN     | Adrenergic  |
| ARID1A   | AT-rich interactive domain-containing protein 1A          |
| ASCL1    | Achaete-scute homolog 1                                   |
| BET      | Bromodomain and extra-terminal motif proteins             |
| BHLH     | Basic Helix-Loop-Helix                                    |
| CHD4     | chromodomain helicase DNA binding protein 4               |
| ChIP-seq | Chromatin immunoprecipitation coupled to sequencing       |
| CoREST   | Chromatin-modifying corepressor complex 9                 |
| CRCs     | Core regulatory circuitries                               |
| DNMTs    | E1/3 ubiquitin ligases and DNA methyltransferases         |
| DRG      | Dorsal root ganglia                                       |
| EMT      | Epithelia to mesenchymal transition                       |
| ESCs     | Embryonic stem cells                                      |
| EZH2     | Enhancer of zeste homolog 2                               |
| GSEA     | Gene Set Enrichment Analysis                              |
| HAND2    | Heart- and neural crest derivatives-expressed protein 2 i |
| HATs     | Histone acetyltransferase                                 |
| HDACs    | Histone deacetylases                                      |
| IP-MS    | Immuno-precipitation coupled to mass spectrometry         |
| ISL1     | Insulin gene enhancer protein                             |
| JMJD     | Jumonji C domain-containing demethylases                  |
| Jmjd6    | Arginine demethylase                                      |
| KDM1A    | Lysine-specific histone demethylase 1A                    |
| KMTs     | Lysine methyltransferases                                 |
| LSD1     | lysine-specific demethylase                               |
| MES      | Mesenchymal   |
| NB       | Neuroblastoma   |
| NCCs     | Neural crest cells  |
| Nsd3     | Lysine methyltransferase                                  |
| NuRD     | Nucleosome Remodeling and Deacetylation                   |
| PKMTs    | protein lysine methyltransferases                         |
| Pol II   | RNA polymerase II   |
| PRMTs    | Protein arginine methyltransferases                       |
| PRRX1    | Paired related homeobox 1                                 |
| PTM      | Post translational modification                           |
| RA       | Retinoic acids  |
| RT-PCR   | Reverse transcriptase polymerase chain reaction           |
| SCID     | Severely compromised immunodeficient                      |
| SE       | Super enhancer  |
| SEdb     | Super-enhancer database                                   |
| ShRNA    | Short hairpin RNA   |
| SNS      | Sympathetic nervous system                                |
| SWI/SNF  | ATP-dependent nucleosome-remodeling enzyme                |

|        |                         |
|--------|-------------------------|
| TCF4   | Transcription factor 4  |
| TFs    | Transcription factors   |
| TSA    | Ttrichostatin A         |
| TWIST1 | Twist-related protein 1 |
| WB     | Western blot            |

## CHAPTER 1. INTRODUCTION

**NOTE:** When using Adobe Acrobat, return to the last viewed page using quick keys Alt/Ctrl+Left Arrow on PC or Command+Left Arrow on Mac. For the next page, use Alt/Ctrl or Command + Right Arrow. See [Preface](#) for further details.

### Neuroblastoma

Neuroblastoma (NB) is an aggressive pediatric malignancy that encompasses around 7-10% of all childhood cancers, and up to 15% of all pediatric cancer deaths<sup>1</sup>. NB mainly affects children less than 5 years old<sup>2</sup>. It originates from the sympathoadrenal lineage of the trunk neural crest cells (NCCs) during development<sup>3</sup>. NB arise at any final site of the migrating trunk NCCs, more commonly in the adrenal gland<sup>4</sup>. According to the International Neuroblastoma Staging System Patients are classified clinically in to 5 different stages: (1–4 and 4S)<sup>5</sup>. Stages 1 and 2, tumors do not metastasize to the lymph nodes, and /or bones and can be treated with surgery, chemotherapy, and/or radiation. High risk NB tumors (stages 3 and 4) are highly metastatic. Despite intensive treatment with chemotherapy, radiation therapy, and surgery, most high-risk NB patients relapse and develop a highly resistant disease with a median survival rate of 5 years after the time of diagnosis<sup>6</sup>. The fifth stage of metastatic NB tumors (4S), regresses spontaneously due to delayed differentiation<sup>7</sup>. Many prognostic markers are also used alongside the stage to predict the risk group, this includes the age of diagnosis, tumor histology, MYCN amplification status, and chromosome changes<sup>8</sup>. Patients with poor prognosis show undifferentiated tumors, may have MYCN amplification (20%), and or copy number alterations such as 17q gain (15%), 1p deletion (20%), and 11q deletion (30%). In contrast, low risk patients have matured and differentiated tumors<sup>9</sup>. This tumor variability well reflects NB tumor heterogeneity which is typical for this cancer<sup>10</sup>.

Over the past decade, major studies have reported a mutation frequency of 0.60 per megabase (0.48 non-silent) and few mutated genes in NB<sup>11</sup>. The most frequent ones include, activating mutation in ALK (9.2% of cases), PTPN11 (3%), ATRX (2.5%), and N-Myc mutations with approximately 2% of NBs. Furthermore, inactivating mutations include, PHOX2B in (4%), ATRX in (2.5%) of NBs, BRCA2 mutations ( 1%) of NBs and ARID1A/1B mutations in approximately 3% of NBs, p53 mutations (2%) of primary and around 10% of relapsed NBs<sup>12,13</sup>. Additionally, pathogenic germline mutations were found to be significantly enriched in ALK, , BARD1, CHEK2, and PINK1<sup>11</sup>. The relatively stable genome of NB tumors provides challenges to the use of current therapeutic strategies dependent on oncogenic drivers that are frequently altered. The heterogeneity of NB along with the paucity of genetic mutations emphasizes the need to comprehend the interplay between genetic elements and epigenetic alterations of this disease. Thus, the major goal of our study is to illuminate novel epigenetic therapeutic targets for NB through identifying new dependency factors that are shared across the different lineage states of NB.

## Neural Crest Cells Fate Decision

Current models propose that NB arises from a developmental block in NCC differentiation along the sympathoadrenal nervous system lineage leading to uncontrolled cell growth<sup>4,14</sup>. This has raised interest in studying the cell of origin of NB and the tumor's epigenetic regulation. NCCs are highly proliferative migratory cell population, found only in vertebrates and can differentiate to give rise to a wide range of cells and tissue types<sup>15,16</sup>. There are four main classifications of neural crest cells: cranial, vagal, sacral and trunk neural crest. Cranial neural crest migrates dorsolaterally and gives rise to the craniofacial mesenchyme cells such as facial cartilage and bone, cranial neurons, glia, and pigment cells. The vagal and sacral neural crest cells generate the parasympathetic (enteric) ganglia of the gut. On the other hand, trunk neural crest cells might take one of two pathways. Some of the delaminating trunk NCCs move ventrally and form the dorsal root ganglia (DRG) neurons. Cells that continue more ventrally give rise to the developing sympathetic nervous system (SNS) including the sympathetic neurons, Schwann cells, and chromaffin cells of the adrenal medulla. While the trunk NCCs that migrate dorsolaterally induce melanocytes (**Figure 1-1**)<sup>17,18</sup>.

Experimental embryology uses a variety of advancing technologies to study NCC fates<sup>19,20</sup>. Soldatov et al. use single cell RNA-sequencing (scRNA-seq) and spatial transcriptomics coupled with lineage tracing to investigate transient states and binary bifurcation points associated with cell fate decision in neural crest cells<sup>19</sup>. During early stages of embryogenesis, NCCs delaminate from the neural plate border and undergo epithelial to mesenchymal transition (EMT), migrate to multiple distal sites, and differentiate<sup>19</sup>. It has been shown that the NC induction and specification is controlled by Wnt/ $\beta$  catenin, bone morphogenesis protein (BMP), Fibroblast growth factor (FGF), and Notch signalings<sup>21</sup>. Following delamination, premigratory trunk NCCs express FoxD3 and the SoxE transcription factors (Sox8, Sox9, and Sox10). Upon arrival at the dorsal aorta at approximately day E 9.5, NCCs receive an inductive BMP signal to induces the specification of the sympathoadrenal lineage<sup>22</sup>. This leads to an increase in the expression of ASCL1 and PHOX2B. PHOX2B then activates HAND2, GATA3, and other transcription factors (TFs) expression<sup>23,24</sup>. At this stage, cells are SNS neuroblasts. Loss of ASCL1 expression induce the expression of TH generating the sympathetic neurons that can form the sympathetic ganglia at E11<sup>25</sup>. The E protein TCF4 has been shown to play a role in NCC differentiation and development, it heterodimerizes with ASCL1, TWIST1, and HAND2 and trans activate target genes<sup>26,27</sup>. TFAP2A/2B are BMP independent TF that appear to be important in the development of migratory NC cells<sup>28</sup>. Collectively, lineage TFs promote proliferation and survival during different stages of SNS differentiation.

The development of NCC is firmly regulated with the coordinated expression of both pro-proliferative and pro-differentiation factors. Thus, activation or repression of neural crest developmental pathways has the potential to be an initiator or driver for NB pathogenesis<sup>3,29</sup>. This led to many studies investigating the super-enhancer (SE) mediated transcriptional core regulatory circuits (CRCs) controlling gene expression programs that drive NB growth and survival.

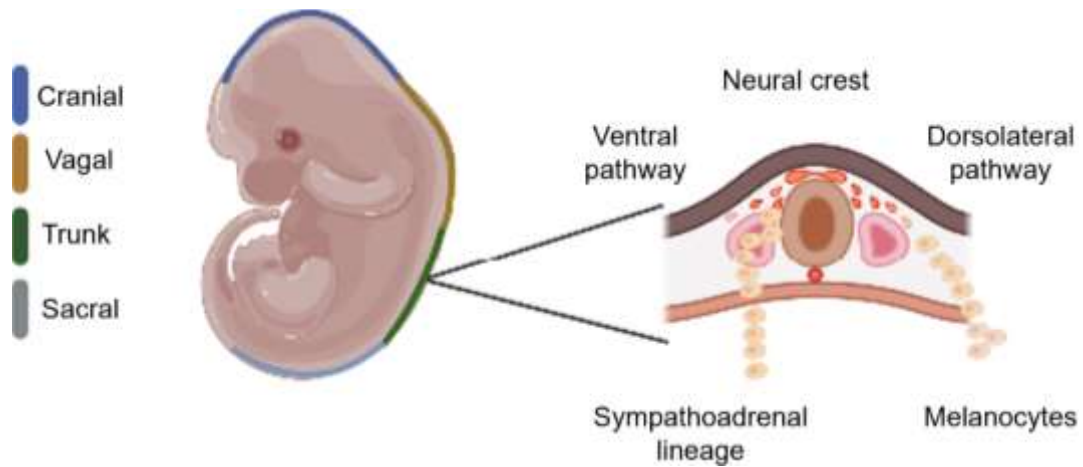


**Figure 1-1. Neural crest cells lineage specification.**

Schematic of human embryo showing the different varieties of neural crest cells (NCCs). Neuroblastomas arise from the trunk neural crest cells and have both neuronal and mesenchymal cell populations. Cells that continue more ventrally give rise to the developing sympathetic nervous system (SNS), while the trunk NCCs that migrate dorsolaterally induce melanocytes.



## Core Regulatory Circuitries and Super Enhancers (SEs) in Cancer

Almost 2000 TFs have been identified in humans, however a small proportion of master TFs control the transcriptional program that dictates cell identity<sup>30</sup>. The gene expression programs in embryonic stem cells (ESCs) are under the control of small set of core TFs including OCT4, SOX2 and NANOG<sup>31,32</sup>. These factors form interconnected auto-regulatory loops where they enforce each other's gene expression known as core regulatory circuitry (CRC TFs)<sup>33</sup>. Typically, CRC factors show co-occupancy pattern of genomic binding through direct protein-protein interactions or co-existence within protein complexes<sup>34,35</sup>. Studies have shown that CRC factors are driven by super enhancers (SEs), which create an opportunity to define candidate CRC factors in different cell types via SEs mapping<sup>36</sup>. Violaine et.al. investigated CRC TFs of different human cell types by identifying genes that are associated with SEs. Those genes bind to their own SEs, and also bind to the enhances of other core TFs<sup>37</sup>. Another valuable source to explore the transcriptional regulatory networks is a comprehensive online database called CRC Mapper dbCoRC (<http://dbcorc.cam-su.org>). This database developed circuitries in more than 230 human/murine samples.

### CRC Factors in Cancer

In cancers, CRC factors have been shown to be essential for establishing and maintaining cell identity state<sup>35</sup>. Mechanistically, CRC TFs recruit acetylation writers, readers, and erasers, and regulate the placement of acetylation deposits around a panel of CRC TF binding motifs, thus creating super-enhancers (SEs)<sup>38,39</sup>. SEs are large stretches of enhancers, densely occupied by transcription factors, BET proteins including BRD4, co-activators such as the Mediator complex, RNA polymerase II complex, and chromatin regulators<sup>40,41</sup>. Thereby, SEs drive high levels of transcription of their target genes<sup>42</sup>. Importantly, multiple genetic variations were identified within SEs in several cancer subtypes<sup>43</sup>. Moreover, studies have shown that SEs can drive expression of both oncogenes (e.g., N-Myc) and regulators of cell identity<sup>44,45</sup>. This indicates that cancer cells are highly dependent on SEs driven transcriptional program.

As cells differentiate, they transition between different identity states governed by different sets of CRC TFs<sup>10</sup>. Changes in CRC TFs can cause barriers to differentiation and promote malignant cell states in multiple pediatric malignancies<sup>46</sup>. Further different cell identity states contribute to tumor heterogeneity which can facilitate cancer's escape from therapy<sup>47</sup>. Thus, understanding the molecular dependencies of CRCs is essential to improve current therapies and preventing therapy escape leading to disease relapse. Next, we summarize identified CRCs in some human cancers.

In human T-cell acute lymphoblastic leukemia (T-ALL), Sanda et al. identified TAL1 complex (E2A, MYB, HEB, LMO1/2), RUNX1, and GATA3 as core components of the circuitry<sup>48</sup>. Medulloblastoma, the most common pediatric brain tumor, has four identified subgroups according to the molecular signature: WNT (WNT/wingless), SHH (Sonic hedgehog), Subgroup 3, Subgroup 4<sup>49</sup>. Lin et al. identified MAF, RUNX2, LEF1,

and EMX2 as core TFS driving WNT subgroup, while MAFF, OTX1, GLI2, and BARHL2 as core TFs in SHH subgroup<sup>50</sup>. The core TFs controlling subgroup 3 include OTX2, NRL, and CRX, and subgroup 4 depend on the CRC TFs LHX2, LMX1A, and EOMES<sup>35,50</sup>. Moreover, emerging evidence suggest that the master TFs, ELF3, EHF, and TGIF1, form the CRC TFs driven by SEs in lung adenocarcinoma<sup>51</sup>. Overall, knowledge of master TFs in cancer is fundamental to understanding transcriptional programs in cancer and providing important insight into therapeutics. Master transcription factors are playing a major role in tumor progression, thus identifying inhibitors to disrupt the transcriptional circuitry shows a prominent anti-tumor effect.

## **CRC Factors in NB**

In NB, recent data reported two phenotypically distinct differentiation states controlled by different regulatory circuits, one establishing a more proliferative adrenergic (ADRN) cell state and a second establishing a more invasive mesenchymal (MES) cell state<sup>46,52</sup>. Cells have the capacity to shift dynamically between the two states, providing these tumors with remarkable transcriptional plasticity, though little is known about how cells transition between these two states<sup>10</sup>. The mesenchymal cell types are chemotherapy-resistant, suggesting that lineage fate decisions are key drivers in relapse and refractory disease<sup>47</sup>. Pioneering work on NB CRCs has uncovered the transcription factors PHOX2B, HAND2, TBX2, ISL1, and GATA3 as essential factors for maintaining the ADRN subtype<sup>46,53</sup>. A recent addition to the ADRN CRC factors includes the bHLH factor ASCL1, which is directly regulated by LMO1, MYCN and other CRC members<sup>54</sup>. Further studies identified TFAP2 $\beta$  as a key member that co-binds the DNA with different ADRN CRC TFs in NB, and help recruiting EP300 to establish malignant cell state<sup>55</sup>. The CRC regulating the MES subtype in NB express MES marker genes, such as SNAI2, and AP-1<sup>46</sup>. Other members of this CRC including the NOTCH family, when lost has been shown to induce transdifferentiation to the ADRN state via remodeling of the H3K27ac landscape<sup>56</sup>. Further, Groningen et al. showed that overexpression of the MES CRC factor PRRX1 could reprogram the ADRN transcriptional landscape towards a MES state, highlighting the critical role of the CRC TFs as potent inducers of cell identity and fate<sup>56</sup>. Several attempts have been made to disrupt the CRCs in NB using multiple epigenetic drugs such as the BET protein inhibitor (JQ1) and HDAC inhibitors<sup>45,57</sup>.

In this work, our findings suggest that TCF4 links MYCN to the CRCs to drive NB oncogenic program. Surprisingly, we discovered a non-canonical role of HDACs and KDM1A inhibitors in regulating TCF4 protein stability.

## **MYCN**

Myc proteins are basic helix-loop-helix leucine zipper transcription factors. The MYC family includes: MYC, MYCN and MYCL. MYC and MYCN share many regions of homology, and are known to heterodimerize with MAX<sup>58</sup>. This heterodimer binds to the DNA at specific E-box sequences and facilitates transcription of genes essential for

proliferation, apoptosis and differentiation<sup>59</sup>. Studies have shown that MYC proteins are critical drivers of human tumorigenesis<sup>58,60</sup>. Studies also revealed that MYC proteins have oncogenic activity through inhibiting or inducing the expression of specific target genes or work as global amplification of transcription<sup>61</sup>. MYCN has been shown to be overexpressed in five nervous system cancers, and in six non-neuronal tumors<sup>62</sup>. The most common genetic alteration in NB is the MYCN gene amplification, which is found in around 20% of the cases and is correlated with poor prognosis<sup>63</sup>. At physiological levels, MYCN mainly binds with the E-box binding motifs at promoters. However, when MYCN is amplified it binds to both gene promoters and enhancers in a model characterized by Zeid et al. as enhancer invasion<sup>64</sup>. This model represents one mechanism by which MYCN contributes to driving NB tumorigenesis. Accordingly, loss of MYCN expression leads to global decrease in gene expression levels and specifically MYCN direct target genes<sup>65</sup>.

Despite MYCN being an attractive therapeutic target, till now there is no clinically approved drug that can directly target MYCN<sup>66,67</sup>. The development of drugs targeting MYCN has been challenging due to its complex structure<sup>66</sup>. To overcome these issues, studies have been focusing on targeting MYCN indirectly by controlling MYCN transcriptional regulatory networks. Numbers of the proposed approaches to indirectly target MYCN include: (1) destabilizing MYCN through targeting the cofactor AURKA<sup>68</sup> (2) targeting the upstream pathway of MYC such as PI3K<sup>69,70</sup> (3) inhibition of the bromodomain and extraterminal domain (BET) which has been shown to inhibit MYCN transcription and seems to be one of the most promising drugs in targeting NB<sup>71-73</sup>.

### **The E Protein TCF4**

Transcription factor 4 (TCF4) is a member of the E proteins, a family of class I bHLH transcription factors, that bind to the Ephrussi-box (E-box) sequences (CANNTG)<sup>74</sup>. TCF4 is also referred to as E2-2, immunoglobulin transcription factor 2 (ITF2), or SEF2-1<sup>75</sup>. In some articles there is some confusion between the TCF4 (Gene ID: 6925) and TCF7L2 (Gene ID: 6934) since they share the TCF4 symbol. TCF4 is the official name for TCF4, the protein discussed in this dissertation. TCF4t is also a widely used alternative name for T-cell-specific TCF4 (TCF7L2). Here, we have taken considerable attention to include only the data that apply to the bHLH TCF4.

E proteins include TCF3, TCF4, and TCF12, and function as heterodimer partners with class II basic Helix-Loop-Helix (bHLH) proteins<sup>76</sup>. TCF4 and other E-proteins contain two conserved activation domains (AD1 and AD2)<sup>77</sup>. AD1 is located at the N-terminus, while AD2 is located at the center of the protein (**Figure 1-2**). E proteins also contain a highly conserved dimerization domain formed by two amphipathic  $\alpha$ -helices separated by a loop (HLH)<sup>78</sup>. The HLH domain facilitates DNA binding and transcriptional activity. The b in bHLH is the C-terminal basic domain<sup>79</sup>.

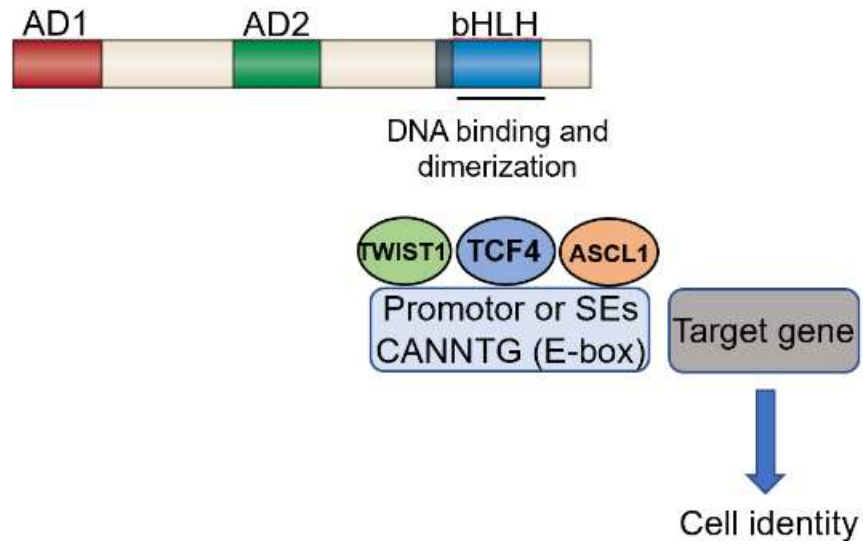


**Figure 1-2. Structure of class I bHLH proteins.**

Schematic diagram of E proteins showing the main protein domains: The activation domains (AD1 and AD2), and the basic helix loop helix (bHLH) domain. The E protein TCF4 dimerizes with multiple class I bHLH factors including the mesenchymal factor TWIST1, and the adrenergic factor ASCL1, and binds to the E-box CANNTG sequence in target genes to regulate cell identity.

The human TCF4 gene is located on chromosome 18 and contains 41 exons. Among them 20 are alternative 5' exons, 20 are internal coding exons, and 1 is the 3' terminal non-coding exon. Expression of TCF4 gene can generate up to 18 N-terminally distinct protein isoforms. Different isoforms can activate transcription in different ways, thus their function may vary during development<sup>80</sup>. Two main distinct TCF4 isoforms have been reported; TCF4-A, TCF4-B. Each isoform has the bHLH domain and a transcription activation domain (AD2). However, TCF4-B has an additional transcription activation domain in its N-terminus (AD1)<sup>81,82</sup>. It has been shown that different TCF4 isoforms differ in two ways: first, their intracellular distribution is regulated by the nuclear localization signal (NLS); second, their capacity to activate the E-box controlling transcription depends on having one or two transcriptional activation domains<sup>76</sup>. Lingbeck et al. showed that presence of NLS in TCF4 isoforms appears to be essential for their nuclear export and cytoplasmic localization. Mutation in the second half of the NLS reduced the nuclear import of TCF4<sup>83</sup>. TCF4 isoforms that lack an NLS are transported to the nucleus in a heterodimeric complex with a partner protein, that contains an NLS. Once in the nucleus, the TCF4 isoforms can either remain there or be directed to the cytoplasm by forming dimers with NES-containing proteins<sup>84</sup>. In this way, the TCF4 isoforms are able to regulate gene expression in both the nucleus and the cytoplasm. A study also suggested that AD1 acts synergistically with the AD2, and that TCF4-B isoform is more potent transactivator than the other isoforms<sup>76</sup>.

TCF4 forms homo or heterodimers with itself or other bHLH TFs forming transcriptional networks that regulate the differentiation of several distinct cell types<sup>85,86</sup>. For efficient binding to the DNA, class II bHLH factors need to heterodimerize with the class I bHLH proteins<sup>87</sup>. Class II bHLH proteins are known as potent regulators of cell specification and cell identity. Studies have shown that E-proteins such as TCF4 are the predominant interacting partners of several class II bHLH factors known to be involved in tissue development, cell differentiation, and pathological disease<sup>87,88</sup>. TCF4 is one of the top dimerization partners and transcriptional modulators of TWIST1, a critical determinant of mesenchymal development<sup>27</sup>. Further, TCF4 heterodimerizes with proneuronal TFs such as ASCL1, ATOH1 and NEUROG2 facilitating their ability to regulate differentiation of neuronal progenitor<sup>88,89</sup>. Class I bHLH proteins heterodimerize also with class V and class VI factors and have a strong effect on their activities<sup>90</sup>. Additionally, many studies reported the essential role of TCF4 in EMT<sup>91</sup>, human nervous system development<sup>87,88</sup>, B and T cell development<sup>92,93</sup>, and regulating neural stem cells (NSCs) identity<sup>94</sup>. In cancer, TCF4 has been shown to play a critical role in plasmacytoid dendritic cell (pDC) development and identified as a master transcriptional regulator that sustains Malignancy in Blastic Plasmacytoid Dendritic Cell Neoplasm (BPDCN) viability<sup>95</sup>. Additionally, TCF4 contributes to aggressive bone colonization in human lung carcinoma cell lines<sup>96</sup> and high expression is associated with worse outcome in acute myeloid leukemia<sup>97</sup>. These studies suggest that E-proteins especially TCF4 might be the primary transcriptional modulators of many class II bHLH factors regulating various lineage states during development. Considering the impact of class I bHLH proteins on overall bHLH function, we decided to delineate the unrecognized function of TCF4 in NB oncogenesis and in mediating the different NB lineage states.

## Targeting Epigenetic Transcriptional Regulators in Cancer

Dysregulation of transcriptional programs is a hallmark of cancer<sup>98</sup>. Studying transcriptional dependencies usually not identified through cancer genome sequencing is an alternative approach to understand cancer and identify new therapeutic targets<sup>99</sup>. Studies have shown that almost 20% of all oncogenes identified so far are TFs<sup>100</sup>. TFs were considered undruggable targets. Recently, deep understanding of TFs structure, function, and binding to DNA led to the development of new therapies targeting TFs<sup>101</sup>. Different ways to target TFs have been proposed in cancers including inducing their degradation or modifying their expression level, by interfering with protein-protein interactions, or preventing TFs binding to the DNA<sup>100–102</sup>.

The level of TF's expression can be modulated through epigenetics<sup>103</sup>. Epigenetics is the study of heritable changes caused by modification of gene expression that is not attributed to DNA sequence variations<sup>104</sup>. The key players associated with these modifications include writers, readers, and erasers<sup>105</sup>. Writers regulate the addition of epigenetic marks to the DNA or histone proteins such as methyl, acetyl, or phosphate groups. Important examples are the histone acetyltransferases (HATs) including EP300/CBP, histone methyltransferases such as protein lysine methyltransferases (PKMTs) and protein arginine methyltransferases (PRMTs), and the E1/3 ubiquitin ligases and DNA methyltransferases (DNMTs)<sup>106</sup>. Erasers remove epigenetic mark added by the writers such as the histone deacetylases (HDACs), the lysine-specific demethylase 1 (LSD1), and the Jumonji C domain-containing demethylases (JMJD)<sup>107</sup>. Readers recognize specific epigenetic marks and induce the activation or repression of transcription level including the bromodomain and extra-terminal motif (BET) proteins (e.g., BRD4), and AT-rich interactive domain-containing protein 1A (ARID1A)<sup>45,108</sup>. Studies have now revealed that changes in these epigenetic tool's regulation play a crucial role in tumorigenesis<sup>109</sup>.

### HDAC Inhibitors

The HDAC family consists of 18 members grouped in four classes. The most studied groups are class I HDACs (HDAC 1, 2, 3, and 8), and class II HDACs (HDAC 4, 5, 7, and 9)<sup>110</sup>. Acetylation of histones is balanced by the opposite effect of histone acetyltransferases (HAT) and histone deacetylases (HDACs)<sup>111</sup>. The canonical role of HDACs in controlling the levels of histone acetylation plays a major role in chromatin remodeling and regulating gene transcription<sup>112,113</sup>. Histone acetylation induces a more open chromatin and gene activation, while histone deacetylation induces transcriptional repression<sup>111</sup>. HDACs and HATs were shown to be dysregulated in cancer<sup>39,55,114</sup>. HDAC inhibitors (HDACi) are potent anti-cancer drugs that not only can induce hyperacetylation of histones, but also can inhibit gene expression<sup>57,110</sup>. Numerous HDACi have been reported to date, some of them such as romidepsin, Vorinostat, Panobinostat are FDA-approved HDACi<sup>115</sup>.

Recently, HDAC inhibitors were shown to induce the acetylation of non-histone proteins, such as TFs, hormone receptors, proteins of the cytoskeleton, and signal transducers affecting cell proliferation, survival, and apoptosis thus affecting downstream signaling controlling tumorigenesis<sup>116</sup>. Modulating the abnormal acetylation balance of non-histone proteins has been suggested to be an interesting therapeutic approach in cancer<sup>117</sup>. The non-canonical role of HDACs through acetylation of non-histone proteins can alter their function through affecting their stability, interactions, and cellular localization<sup>118</sup>. Prominent examples of acetylation of non-histone proteins include: the tumor suppressor P53, NF- $\kappa$ B p65, and STAT proteins<sup>119,120</sup>. Moreover, several studies suggested that acetylation of HIF-1 $\alpha$  and FOXO1 by HDACi can promote their binding to the enzymes of the ubiquitin-pathway and induce their proteasomal degradation<sup>121</sup>. Another example is the WT1 transcription factor, which has been shown to be downregulated by HDACi at the mRNA and protein level<sup>122</sup>. Trichostatin A (TSA) an inhibitor of class I and class II HDACs induces the proteasomal degradation of the WT1 protein which was found to be correlated with increased expression of the E2 ubiquitin-conjugase Ubc8. Targeting the expression of Ubc8 using siRNA reverses the TSA-mediated WT1 degradation<sup>122</sup>. This highlights the significance of proteasomal degradation for HDACi in modulating protein stability. In NB, HDAC inhibitors induce cell cycle arrest, apoptosis, differentiation, and suppress clonogenic growth of NB cells<sup>123</sup>. Multiple studies suggested that the anti-cancer effects of HDACi in NB involve modulating the acetylation level and function of non-histone proteins, activation of differentiation pathways and targeting epigenetic repression of tumor suppressor genes<sup>124,125</sup>.

## **KDM1A Inhibitors**

Lysine-specific demethylase 1 (LSD1/KDM1A) catalyzes the demethylation of histone lysine residues H3K4me1/2 and H3K9 me1/2. Histone methylation is regulated by methyltransferases (e.g., KMTs) and demethylases (e.g., KDMs)<sup>126</sup>. Abnormal over-expression of KDM1A has been reported in multiple solid tumors and acute myeloid leukemia where it promotes proliferation, invasion, stem cell self-renewal, and inhibits differentiation and associated with a poor prognosis of tumors<sup>127,128</sup>. Thus, KDM1A has emerged as an attractive therapeutic target for cancer treatment<sup>129</sup>. Several KDM1A inhibitors are in clinical trials for the treatment of solid tumors and leukemia such as ORY-1001, IMG7289 and INCB059872<sup>129,130</sup>. Studies have shown that KDM1A as a histone eraser could regulate gene expression in cancer by targeting non histone substrate such as p53, DNMT1, E2F1, and STAT3<sup>131,132</sup>. KDM1A inhibits transcription through binding to the chromatin-modifying corepressor complex 9 (CoREST) or the Nucleosome Remodeling and Deacetylation (NuRD complex)<sup>133,134</sup>. It can also induce transcriptional activation through binding to the androgen receptor (AR) or the estrogen receptor (ER)<sup>135</sup>. ORY-1001 is a highly potent and selective KDM1A inhibitor and has excellent oral bioavailability<sup>130</sup>. A recent study found that ORY 1001 induced the NOTCH signaling and inhibited ASCL1 expression and small cell lung cancer (SCLC) tumorigenesis<sup>136</sup>. Maes et al. reported a therapeutic potential of ORY-1001 in the treatment of melanoma<sup>130</sup>, and Shan et al. showed that ORY-1001 suppressed the growth

and increased apoptosis of lung cancer cells<sup>137</sup>. These findings and others highlight the KDM1A inhibitors as attractive therapy in cancer.

## **BET Inhibitors**

Targeting epigenetic readers like bromodomain and extra-terminal motif (BET) proteins has emerged as a powerful therapeutic strategy in NB<sup>45</sup>. BET proteins recognize and bind histone acetylation at super-enhancer sites across the genome to recruit transcriptional complexes and facilitate the expression of associated genes<sup>71</sup>. BET proteins consist of Brd2, Brd3, Brd4, Brdt, and play roles in regulating transcription by RNA polymerase II (Pol II)<sup>138</sup>. Upon their interaction with acetylated chromatin, BET proteins recruit other regulatory complexes (e.g., mediator complex) to affect gene expression<sup>139</sup>. BRD4 is the most studied BET proteins in many cancers and has been shown to be implicated in the onset and progression of malignant cancers<sup>140</sup>. Studies suggested that BRD4 alters chromatin structure and regulate transcription through interacting with multiple histone modifiers including the ATP-dependent nucleosome-remodeling enzyme SWI/SNF<sup>141</sup>, chromodomain helicase DNA binding protein 4 (CHD4), arginine demethylase (Jmjd6), and the lysine methyltransferase (Nsd3)<sup>142</sup>.

Studies of BETi showed a wide array of possible application in several cancers<sup>143</sup>. Bradner et al. developed a potent and selective inhibitor of BRD4<sup>144</sup>. The drug was tested in a mouse model of NUT-midline carcinoma and found to increase survival and then was found to be effective in several other cancers<sup>144</sup>. BET inhibitors (e.g., JQ1) can target cell identity by suppressing BET protein-mediated recruitment of TFs to SEs, regulatory elements closely associated with genes that determine cell identity<sup>145</sup>. It has been shown that genes regulated by SEs are specifically sensitive to BET inhibitors<sup>40</sup>. JQ1, a thienotriazolo-1, 4-diazapine competitively occupies the acetyl lysine-binding pocket and displaces BRD4 from chromatin<sup>145</sup>. JQ1 has anti-tumor effects and has been shown to be effective against several malignant tumors, including gastric, lung, and colon cancer, in addition to hepatocellular carcinoma<sup>72,146</sup>. JQ1 inhibits proliferation and cell invasion and induces apoptosis<sup>139</sup>. Interestingly, NB was found to be one of the most sensitive cancers to BET inhibitors<sup>45</sup>. Studies have shown that JQ1 causes cell cycle arrest, induces apoptosis, and promotes neural differentiation in NB<sup>53,147</sup>. Puissant et al. shows that JQ1 inhibits N-myc expression, and reported a significant correlation between MYCN amplification and sensitivity to BETi<sup>73</sup>. Another drug birabresib (MK-8628) known as OTX015, has been shown to target BRD4 and reduce MYCN expression, and found to be effective against mouse and human NB tumors<sup>45</sup>. While NB sensitivity to BET inhibition was attributed to MYCN amplification in many studies, the ectopic expression of MYCN did not compromise the effects of BRD4 inhibition suggesting the importance of other targets of BET inhibition in NB<sup>45</sup>. Given the recently proposed identity states in NB, we set out to investigate if there are universal SE-marked TFs that are expressed across NB and shared by both lineage states. Our primary finding begins to shed light on the E-box transcription factor TCF4 as a master transcriptional regulator of NB oncogenesis program. Therefore, we decided to study TCF4 in-depth to determine its importance in NB oncogenesis, in maintaining NB identity and as a future therapeutic target.



## Hypothesis and Specific Aims

Although NB sensitivity to BET inhibitors was originally attributed to MYCN repression and oncogene addiction, our group and others have shown that MYCN oncogene addiction does not explain sensitivity to BET inhibition. Since BET inhibitors can target cell identity by suppressing TFs from super-enhancers, we propose that NB sensitivity to BET inhibition depends on targeting the developmental pathways active in the neural crest lineage. In line with this idea, our recent data suggest that the class I basic helix-loop-helix transcription factor (bHLH) TCF4 is a critical target of JQ1 mediated cell death in NB and silencing of TCF4 leads to a significant decrease in cell viability potentially indicating a role of TCF4 in NB oncogenic program. Here, we hypothesize that TCF4 is a cell dependency gene in NB that is crucial for determining NB identity. To validate our hypothesis, we decided to investigate the following specific aims.

### **Aim 1: To determine if TCF4 is a critical NB dependency factor that is shared across the different NCC lineage states**

We would like to investigate if silencing TCF4 will lead to loss of NB cell viability. We would also like to map TCF4-dependent regulatory network in NB and identify TCF4 genomic binding sites by combined analysis of TCF4 ChIP-seq data and gene expression changes following TCF4 knockdown. This work will investigate if TCF4 is a universal factor that is shared across different NB lineage states and if silencing TCF4 affects both identity states.

### **Aim 2: To determine the TCF4 interactome in neuroblastoma**

Here, we would like to better understand the mechanism(s) TCF4 might play in determining NB identity. We propose to identify for the first time the protein binding partners of TCF4 and its functional modules in NB cell lines using immunoprecipitation coupled to mass spectrometry (IP-MS). In this aim, we will use TCF4 as an anchor point and the IP-MS methodology to visualize the protein interactome necessary for NB development and pathology to establish potential therapeutic targets.

### **Aim 3: To test the possibility to drug TCF4 in NB expressing cell lines using different epigenetic drugs**

We will investigate the effect of different epigenetics drugs alone or in combination on TCF4 mRNA, protein level, and TCF4 function in NB. The IP-MS analysis will help highlight potential epigenetic factors that can affect TCF4 function in different NB cell lines.

## CHAPTER 2. METHODOLOGY

**NOTE:** When using Adobe Acrobat, return to the last viewed page using quick keys Alt/Ctrl+Left Arrow on PC or Command+Left Arrow on Mac. For the next page, use Alt/Ctrl or Command + Right Arrow. See [Preface](#) for further details.

### Cell Lines

All neuroblastoma cell lines were obtained from ATCC. Kelly, SK-N-AS and IMR32 neuroblastoma cells were cultured in RPMI, DMEM or EMEM respectively, supplemented with 10% fetal bovine serum (Atlanta Biologicals). Primary mouse NCC lines were isolated and cultured as described previously<sup>108,148</sup>. Mouse NCCs were grown in CDM, which contains Iscove's modified Dulbecco's medium/Ham's F-12, 1X chemically defined lipid concentrate (GIBCO), 1X mg/ml Insulin-transferrin-selenium (Thermo Fisher Scientific), 450 mM onothioglycerol (Sigma), 5 mg/ml purified BSA (Sigma), 7 mg/ml Insulin (Thermo Fisher Scientific), and penicillin/streptomycin (Invitrogen).

### RNA-Seq Library Preparation and Sequencing

For RNA-Seq on the Kelly, SK-N-AS, IMR32 human neuroblastoma cell lines, total RNA was extracted using the RNeasy Mini Kit (QIAGEN). cDNA libraries were sequenced using the Illumina NovaSeq platforms, which utilize a paired-end 150 bp sequencing strategy (Novogene). STAR (version 2.5.3a) with default setting was used to map the sequencing data for cell lines (Kelly, SK-N-AS, and IMR32) using human reference genome (hg38). Gene abundance count was calculated using featureCounts (subread version 1.5.1). The parameter '-p' was used for featureCounts to get fragment-based counts instead of reads. Gencode v41 (hg38) was used to get the gene level quantification. DeSeq2 from R-package was used to identify differentially expressed genes. Low-coverage genes were removed if the median value for the gene is less than 0. Batch information along with treatment conditions was used as design matrix. Genes differentially expressed after knockdown of each transcription factor were selected using the following criteria: adjusted p value < 0.05, log 2-fold change < -0.58 or > 0.58. DeSeq2 normalized data was used as input for GSEA (version 4.2.2) for gene ontology analysis against the hallmark database (version 7.5.1). Human Ensembl Gene MSigDb (version 7.5.1) was used for ChIP platform parameter.

### Doxycycline-Inducible shRNA Systems

The shRNA sequences were designed according to the TRC1 library (Sigma-Aldrich, TRCN0000274214, TRCN0000274213, TRCN0000274161 referred in the manuscript as sh1, sh2, sh3 respectively) targeting TCF4. The shRNAs were cloned into

the lentiviral vector Tet-pLKO-puro (Plasmid #21915) at the Age I and EcoR I digestion sites. Each individual shRNA vector was co-transfected into 293T cells with the 2nd generation lentiviral systems and seeded into 10 cm plate 24 h before transfection, using the FuGENE 6 transfection reagent (Roche) according to the manufacturer's instruction. The media was changed 24 h after transfection. 48 h after transfection supernatants containing lentivirus was collected and filtered through a 0.45  $\mu\text{m}$  nitrocellulose filter (Thermo). The Kelly and SK-N-AS cells were infected with lentivirus in the presence of polybrene (4  $\mu\text{g}/\text{mL}$ :Millipore). Selection was performed by adding puromycin (0.5  $\mu\text{g}/\text{mL}$  for Kelly cell line; 1  $\mu\text{g}/\text{mL}$  for SK-N-AS neuroblastoma cell line) 48 hours after the infection.

### **Real-Time Quantitative PCR**

Total RNA was extracted using RNeasy Mini Kit (QIAGEN) according to the manufacturer's instructions. On-column DNase treatment was performed, and concentration was determined with Nanodrop (Thermo Scientific). cDNA synthesis was performed using High-Capacity cDNA Reverse Transcription Kit (Thermo Scientific). Real-time quantitative polymerase chain reaction (qPCR) was performed using the TaqMan Real-Time PCR Master Mix according to supplier recommendations. The housekeeping gene B2M was used for normalization. The following human probes: Hs00972432\_m1 for TCF4, and Hs00187842\_m1 for B2M, and the mouse probes: Mm00443210\_m1 for TCF4, and Mm00437762\_m1 were used.

### **Western Blot Analysis**

Cells were lysed in RIPA Buffer (#J62524, Thermo Scientific) with Halt Protease and Phosphatase Inhibitor Cocktail (#1861281). Equal amounts of protein were resolved by SDS-PAGE gel after boiling for 5 min at 95  $^{\circ}\text{C}$  with Laemmli sample buffer (Bio-Rad), then blotted onto a PVDF membrane (Bio-Rad). Membranes were blocked with 5% nonfat milk for 1 h followed by incubation with primary antibody diluted in 2.5% nonfat milk overnight at 4  $^{\circ}\text{C}$ . Next day, the membranes were washed with washing buffer (PBS-Tween 0.1%) and incubated with secondary antibody for 1 h at room temperature. HRP-labeled anti-rabbit (7074, Cell Signaling Technologies) and anti-mouse (7076P2, Cell Signaling) antibodies were used. Proteins were visualized by enhanced chemiluminescence (ProSignal® Femto ECL Reagent). Immunoblotting was carried out with the following antibodies: TCF4 (Abcam, ab217668), Cleaved PARP (Cell Signaling Technologies, #9661), and  $\beta$ -actin (Cell Signaling Technologies, #8457).

### **Co-Immunoprecipitation and Western Blotting Analysis**

Total protein was extracted from Kelly and SK-N-AS cells using Pierce IP lysis buffer (Thermo Fisher Scientific #87787) supplemented with Halt Protease and phosphatase Inhibitor Cocktail (#1861281). Whole cell lysate was incubated with TCF4

antibody (Abcam, ab217668), or Normal Rabbit IgG (CST #2729) with rotation overnight at 4°C. Next day, 50 µl of Pierce Protein A/G Magnetic Beads (Thermo Fisher Scientific # 88803) were moved to a clean tube and washed three times with 500 µl of 1X Pierce lysis buffer. The overnight cell lysate was mixed with 50µl of the pre-washed magnetic beads and incubated with rotation for 2 hours at 4°C. Next, beads were separated from the lysate using a magnetic separation rack, the beads were then washed three times with 500 µl of 1X IP lysis buffer. The IP products were eluted by 60 µl 4X SDS sample buffer and boiled at 95°C for 5 min. 15 µl of each sample was used for western blotting detection and 10% cell lysate was used as Input. Proteins were separated by SDS-PAGE gel. The following antibodies were used to detect the protein-protein interaction, TCF4 (Abcam, ab217668), ASCL1 (Santa Cruz, #sc-390794), HAND2 (Abcam, ab200040), and TWIST1 (Abcam, ab50887).

### **CyQuant Assay**

Neuroblastoma cells were seeded into 96-well plates (10000 cells/well) and plated in 100 µl media per well. 24 hours after plating, drugs were diluted to a 2x concentration in plating media and then 100µL was added to each well. Plates were incubated for 4 days and then submitted to CyQuant Cell Direct Proliferation Assay (Thermo Fisher Scientific) according to the manufacturer's instructions and read with Cytation 5 plate reader (BioTek).

### **Annexin V/PI Flow Cytometry Assay**

Kelly and SK-N-AS cells transduced with shRNA against TCF4 (sh1, sh2, sh3) were treated with 1 µg/ml doxycycline for 5 and 7 days respectively. Control cells (media with puromycin only) were also included in this experiment. After the incubation, cells were collected and washed twice with cold PBS then cells were re-suspended in 1 mL of 1X binding buffer (cell concentration  $1 \times 10^6$  cells per mL). Next, 100 µl of cell suspension was transferred to a flow tube, the cells were incubated with FITC-Annexin V and PI for 15 min. Annexin V-FITC/PI detection kit was obtained from Biolegend (cat # 640914). Cells were then analyzed by flow cytometry.

### **Ectopic Expression of TCF4**

For TCF4 overexpression, TCF4/E2-2 cDNA ORF Clone (Sino Biologica # HG12096-CF) was transfected into SK-N-AS cells using FuGENE 6 transfection reagent (Roche). Forty-eight hours after transfection, DMEM media with the selection antibiotic Hygromycin (500 µg/ml) was added and replaced every three days. After one month, antibiotic-resistant clones were generated and expanded. TCF4 overexpression was confirmed by real-time PCR.

## Colony Formation in Soft Agar

Kelly and SK-N-AS cells transduced with shRNA against TCF4 (Sh2, Sh3) were split and seeded (5000 cells/well) in a 0.30% noble agar (Sigma) mixed with culture medium (on the top of 0.6% noble agar with medium) in 6-well plates. Cells were cultured at 37°C for another 3 weeks. Cells were incubated for 21 days in media only or Doxycycline, changing the media every 2 days. Colonies were photographed (Nikon, Microphot FX) by treating the plates with 0.1% crystal violet and subsequent gentle washing with PBS.

## In Vivo Tumor Models

This study was performed in strict accordance with the recommendations in the Guide for the Care and Use of Laboratory Animals of the National Institute of Health. All animal experiments were approved by the Institutional Animal Care and Use Committee (IACUC) at UTHSC. 6–8 weeks old female severe combined immunodeficiency (SCID) mice were obtained from The Jackson Laboratory and subcutaneously injected in the flanks at  $2 \times 10^6$  cells per mouse in 100  $\mu$ l total volume. Kelly and SK-N-AS cells transduced with shRNA against TCF4 (sh2) were injected in a 1:1 mix of cells and Matrigel (BD Biosciences). One week after the injection mice were randomly assigned to the control (standard diet) or the treatment (15 mg/kg body weight (BW) of doxycycline) groups. Tumors were measured by calipers at least twice weekly, and tumor volume was calculated using the formula  $1/2 * (\text{length} * \text{width}^2)$ . Animals were sacrificed according to institutional guidelines when tumors reached ~2000 mm in length or width.

## Chromatin Immunoprecipitation ChIP-Seq

A total of  $3 \times 10^7$  cells were crosslinked with 1% formaldehyde (Sigma) while shaking for 10 min at room temperature. Crosslinking was quenched with 125 mM glycine (Sigma #G8898). DNA was sheared by sonication to obtain approximately 500 bp. To pre-bind antibodies to protein A/G agarose beads (ThermoFisher# 20423), we rotated to 50  $\mu$ l protein A/G agarose bead slurry mixed with 10  $\mu$ g of Anti-TCF4 antibody (Abcam, ab217668), or anti-H3K27ac (ab4729) overnight. Next day, chromatin fragments were immunoprecipitated by mixing the pre-cleared chromatin with the antibody:bead complex and rotating for 4 h at 4°C. protein A/G bound complexes were washed 6 times, once with (20 mM Tris-HCl pH8, 50mM NaCl, 1% Triton X-100, 0.1% SDS, 2 mM EDTA), twice with (20 mM Tris-HCl pH8, 500mM NaCl, 1% Triton X-100, 0.1% SDS, 2 mM EDTA), once with (10 mM Tris-HCl pH8, 250 mM LiCl, 1% NP40, 1% Deoxycholic acid, 1 mM EDTA), twice with TE pH 8.0 and finally resuspended in 100  $\mu$ l TE pH8. Total chromatin samples were processed in parallel as input reference. To each DNA sample add 370 mM NaCl, RNase, and 0.26mg/mL Proteinase-K. Reverse cross-link was performed overnight at 65°C. Final DNA purification was performed with Qiagen MinElute PCR Purification kit (# 28004). ChIP DNA was used to generate ChIP-Seq libraries. The sequencing of the TCF4 ChIP-Seqs was performed on Illumina PE150

sequencer (Novogene). BWA-MEM (version 0.7.16a) with default parameters were used to map sequence data to human genome (hg38). MACS2 (version 2.2.1) was used to call the peaks. For TCF4 ChIP-seq data IDR (version 2.0.3) peaks were called with idr threshold of 0.05. For all the peaks called, the peak regions were further filtered out removing the blacklisted regions. Homer motif analysis was carried out using IDR peaks generated from TCF4 ChIP-seq data. Region's size of 200 and allowed mismatch of 2.

### **Target Genes**

TCF4 ChIP-seq data along with promoter capture Hi-C data was integrated with RNA-seq data to identify the target genes. Differentially expressed genes with a fold-change threshold of 1.5 and p-value < 0.05 were only used for this analysis. If the promoter region or gene body overlaps with the coordinates of the TCF4 peak region or if based on promoter capture Hi-C data if the region overlapping with TCF4 peaks have interaction with the genes, those genes are defined as the target genes.

### **ATAC-Seq Data Processing**

Using previously published ATAC-seq data, BWA-MEM (version 0.7.16a) with default parameters were used to map sequence data to human genome (hg38). SAMtools (version 1.9) was used to remove the duplicate reads from mapped file. CPM normalization was used to generate the signal track (bigwig file) using bamCoverage (version 3.5).

### **Promoter Capture Hi-C**

Adrenal gland associated promoter capture Hi-C interaction data was downloaded from Jung et al.<sup>149</sup> Significant interactions between promoter-other and promoter-promoter.

### **Genomic Annotation**

Promoters were defined based on 1000 bp upstream of the transcription start site (hg38 gencode v41) based on strand information. Enhancers for respective cell lines were defined based on the overlap between H3K27ac and H3K4me1 peaks using bedtools intersect.

### **Public Data**

ATAC Seq data (SRA: SRR10215668, SRR10215669) and H3K4me1 data (SRA: SRR10217411, SRR10217413) for KELLY was downloaded from NCBI GEO. ChIP-seq

data for GATA3, ISL1, HAND2, n-Myc, PHOX2B and TBX2 data for KELLY was downloaded from NCBI GEO. ATAC Seq data (SRA: SRR10215682, SRR10215683), H3k4me1 and HK3K27ac (SRA: SRR10217389, SRR10217391, SRR10217393) data for SKNAS was downloaded from NCBI GEO.

### **Data Availability**

RNA, ChIP and ATAC sequencing data are available online through the Gene Expression Omnibus (GEO) portal. The accession numbers of this SuperSeries is GSE222212, GSE222212, GSE222214.

<https://www.ncbi.nlm.nih.gov/geo/query/acc.cgi?acc=GSE222212>,  
<https://www.ncbi.nlm.nih.gov/geo/query/acc.cgi?acc=GSE222213>  
<https://www.ncbi.nlm.nih.gov/geo/query/acc.cgi?acc=GSE222214>

### **Immunoprecipitation-Mass Spectrometry Analysis**

Kelly and SK-N-AS cell lines were cultured to 90% confluency in 15 cm dishes per biological replicate prior to harvesting. Immunoprecipitation of TCF4 was performed as described earlier in the Co-immunoprecipitation method section. IP-MS protocol was performed using 1 mg of whole cell lysate immunoprecipitations in triplicate plus IgG control. Antibody: bead complex samples were sent to the University of Tennessee Health Science Center Proteomics Core for Label Free Quantification (LFQ) mass spectrometry protein identification. We performed On-bead Trypsin Digestion by adding 1  $\mu$ L of 1  $\mu$ g/ $\mu$ L MS grade trypsin, then incubated with the sample overnight at 37 °C while rocking on a nutator. Mass spectrometry protein identification results were analyzed with Proteome Discoverer 2.4, (Thermo Fisher). Peptide Abundance represents MS Peak Area, normalization mode is the total peptide amount, and the protein abundance is the summed abundances of assigned peptides. TCF4 interaction partners are included in the final list (**Supplementary Table 4**) if they are present in at least two out of three TCF4 complex purifications and show at least two-fold enrichment by protein abundance in the TCF4 purified sample over the control sample.

### **Statistical Analysis**

We used the unpaired, two-tailed Student t test to determine the statistical significance using GraphPad Prism 9.0 software. A p-value of less than 0.05 was considered statistically significant.

## CHAPTER 3. TCF4 IS A KEY MEDIATOR OF CELL IDENTITY AND ONCOGENESIS IN NEUROBLASTOMA<sup>1</sup>

**NOTE:** This chapter refers frequently to content in **Appendix A**. When using Adobe Acrobat, after going there, return to the last viewed page using quick keys Alt/Ctrl+Left Arrow on PC or Command+Left Arrow on Mac. For the next page, use Alt/Ctrl or Command + Right Arrow. See **Preface** for further details.

### Introduction

This chapter summarizes the research focused on investigating: 1) If TCF4 is a critical dependency factor in NB and shared across the different NCC lineage states; 2) The TCF4 interactome in NB; and 3) If TCF4 expression or function in NB cell lines can be targeted using different epigenetic drugs. As shown in the article TCF4 is a key mediator of cell identity and oncogenesis in neuroblastoma (**Appendix A**), we found that TCF4 is a critical mediator of NB cell identity and is a core facilitator of a MYC/MYCN driven oncogenic program for neuroblastoma. We also found that TCF4 is vulnerable to protein degradation induced by multiple clinically promising epigenetic therapies in NB.

### Summary

MYCN amplification serves as an oncogenic driver found in ~20% of high-risk NB. Targeting epigenetic regulators like BET proteins has emerged as a powerful therapeutic strategy in cancer treatment. Interestingly, NB was found to be one of the most sensitive cancers to BETi, and this vulnerability to BET inhibition has been attributed to MYCN amplification. Our ability to transform mouse NCC's line into NB enabled us to test and confirm that NB sensitivity to BET inhibition is not due to oncogenic addiction suggesting that other factors predominantly mediate this sensitivity (**Figure A-1a**). This observation is consistent with previous studies, and the sensitivity of wild-type NCCs to JQ1 indicated a role of cell identity factors in NB. Thus, we decided to determine if there are TFs whose expression is sensitive to BETi, found across NBs and shared by both NB subtypes. Here, we performed RNA-seq analysis using ADRN and MES NB cell lines after JQ1 treatment. **Figure 3-1** and **Supplementary Table 1** show that acute JQ1 treatment prompted a robust change in transcription. Shared TFs were arranged in a heatmap based on the number of SEs identified for each factor in multiple NB cell lines using the super-enhancer database (SEdb) (**Figure A-S1b**). TCF4 has the highest number of SEs identified in multiple NB cell lines compared to other identified shared factors.

---

<sup>1</sup>Prepared Word manuscript reused with authors' permission. Nour A. Aljouda, Dewan Shrestha, Satyanarayana Alleboina, Rachelle R. Olsen, Megan Walker, Yong Cheng, Kevin W. Freeman. TCF4 is a key mediator of cell identity and oncogenesis in neuroblastoma, 2023 (**Appendix A**).



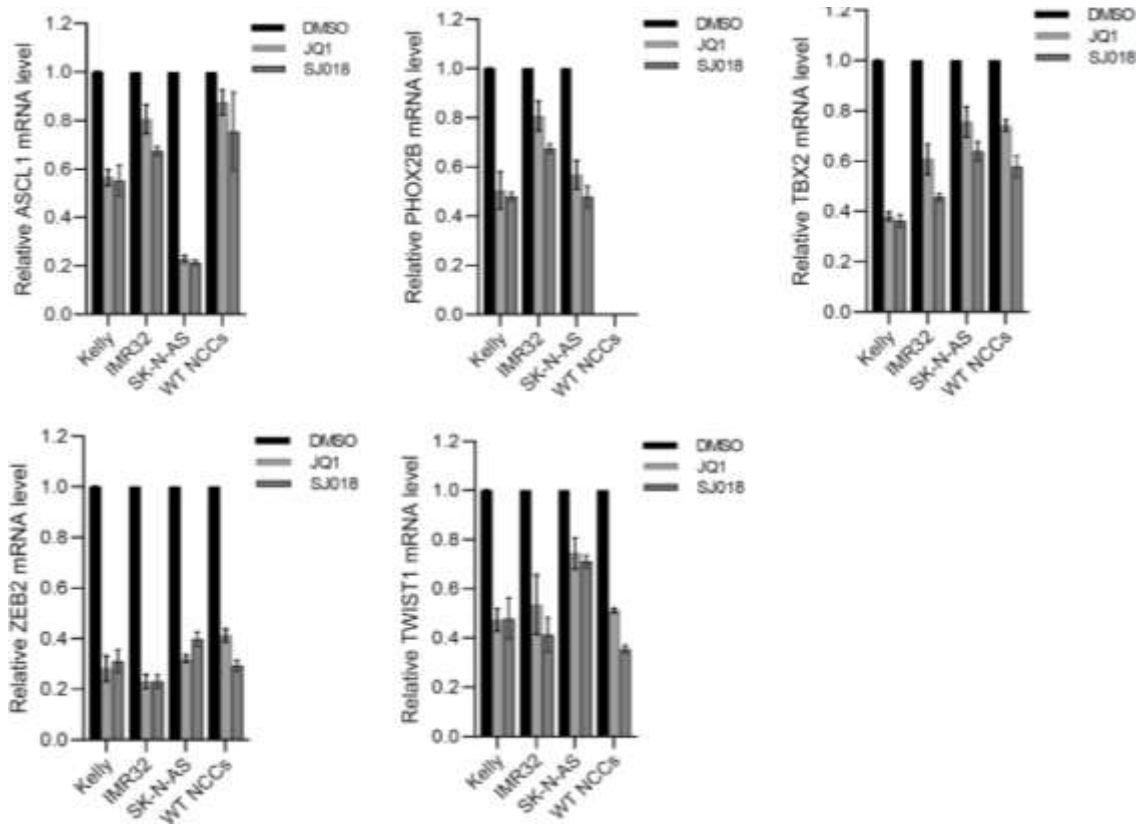


**Figure 3-1. Inhibition of CRC TFs following the treatment of NB cells and mouse NCCs with the BET-inhibitors, JQ1 and SJ018.**

The adrenergic factors ASCL1, PHOX2B, TBX2, and the mesenchymal factors TWIST1, and ZEB2 mRNA levels were determined by quantitative real-time PCR after neuroblastoma cell lines and primary NCCs were treated with DMSO, 1 $\mu$ M JQ1 or SJ018 for 3 hours. Expression values are shown relative to the DMSO condition for each cell line.

Moreover, TCF4 has the highest expression in NB of all cancer types found in the Cancer Cell Line Encyclopedia (CCLE) database (**Figures A-1d** and **S1b**). Additionally, we also confirmed that JQ1 and SJ018, a structurally distinct BETi, suppress TCF4 by performing quantitative PCR in all three human NB cell lines and primary mouse NCCs (**Figure A-S1c-d**). Next, we validated TCF4 interactors in NB, and showed using IP-Western (IP-WB) that TCF4 interacts with ASCL1, HAND2 and TWIST1 in Kelly and SK-N-AS NB cell lines (**Figure A-1d**). Furthermore, we performed reverse immunoprecipitation using TWIST1 and ASCL1 antibodies for the same cell lines and confirmed their interaction with TCF4 (**Figure 3-2**). Therefore, we propose to study TCF4 in-depth to determine its importance: 1. in NB oncogenesis, 2. in maintaining NB identity and 3. as a future therapeutic target.

To study the role of TCF4 in NB, we silenced TCF4 expression in Kelly and SK-N-AS cells using three different shRNAs. Quite consistently, across both the ADRN and the MES cell lines, TCF4 loss resulted in a significant inhibition of proliferation (**Figures A-2c** and **S2a**), colony formation capacity (**Figures A-2d** and **S2b**), and cell growth in soft agar (**Figure A-3a-b**). Silencing of TCF4 also induced apoptosis (**Figures A-2f** and **S2d**) and cell cycle arrest (**Figures A-2e** and **S2c**) *in vitro* and impedes tumor growth *in vivo* (**Figure A-3c-d**).

We next investigated the TCF4 transcriptional regulated network in both NB cells (**Supplementary Table 2**). Gene Set Enrichment Analysis (GSEA) following TCF4 knockdown in both Kelly and SK-N-AS cells showed significantly downregulated gene sets enriched in EMT and cell cycle pathways including G2/M checkpoint, E2F, and MYC targets (**Figure A-S3a-b**). These observations suggest that TCF4 control regulatory network driving proliferation and implicate lineage dependency role for TCF4 in the ADRN and the MES NB cell lines.

Next, to identify TCF4 direct targets in NB cells, we performed ChIP-seq analysis using anti-TCF4 antibody in both cell lines. Intersection of ChIP-seq and RNA-seq datasets for TCF4 knockdown uncovered direct targets of TCF4 (**Figure A-4a**). Moreover, TCF4 regulates E2F-FOXM1 core members, and other DREAM complex members involved in cell cycle regulation (**Figure A-4a** and **Supplementary Table 3**). Next, we performed HOMER motif analysis we found that regions bound by TCF4 were also enriched for several CRC factors (**Figure A-4c**). Further, we observed a strong MYCN intensity signal at TCF4 binding sites (**Figures A-4d** and **S4a**). In addition, we confirmed using IP-WB that TCF4 interacts with MYCN (**Figure 3-3**).

We discovered that TCF4 peaks that overlap with MYCN peaks at SEs in Kelly and SK-N-AS cells show enrichment for many CRC TFs such as HAND2 and TBX2 (**Figure A-S4d-e**). These data suggest collaborative roles among these factors and TCF4 in regulating NB gene expression programs and potentially a physical interaction.

On the other hand, we did not see a strong overlap of TCF4 peaks summits with binding sites of ADRN CRC factors at the TCF4 locus (**Figure A-S4b**). Moreover, in our RNA-seq data, we do not observe a strong effect of TCF4 KD on the expression of

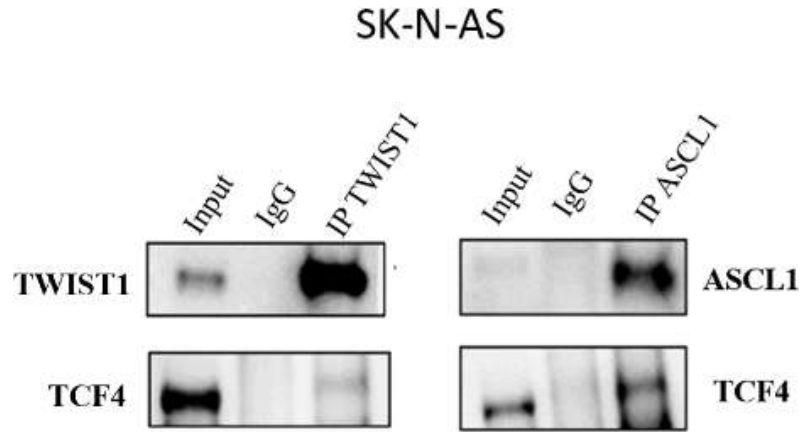


**Figure 3-2. TCF4 interactions validation.**  
 Immunoprecipitation of TWIST1 and ASCL1 using SK-N-AS cell line's whole cell lysate. Control using rabbit IgG and 10% input are also shown.

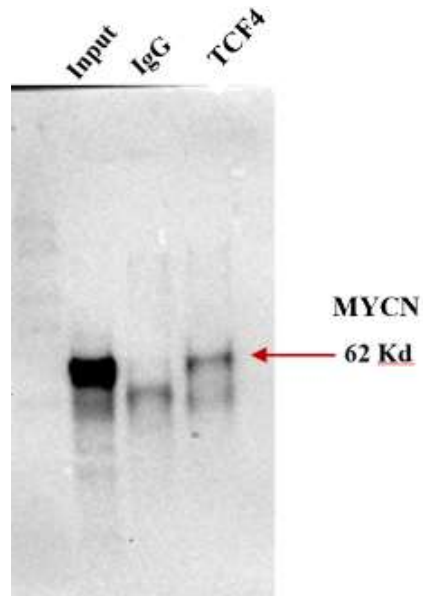


**Figure 3-3. TCF4 interacts with MYCN.**  
 Immunoprecipitation of TCF4 using Kelly neuroblastoma cell line's whole cell lysate, followed by Western blot using MYCN primary antibody. Control using rabbit IgG and 10% input are also shown.

known CRC members (**Supplementary Table 2**). Collectively, these data suggest that TCF4 is not a canonical CRC member but is regulated in parallel to these CRCs and facilitates their downstream effects. Hence, we propose that TCF4 is a member of the extended regulatory network (ERN), reported as SE-associated genes whose enhancers and promoters are bound by the CRC TFs and work downstream of these factors to modulate their effect.

Finally, we performed TCF4 immunoprecipitation coupled to mass spectrometry (IP-MS) in Kelly and SK-N-AS cells to determine the TCF4 interactome in NB (**Supplementary Table 4**). TCF4 interaction network in NB comprises many ADRN and MES CRC TFs and multiple chromatin remodeling complexes, such as the nucleosome remodeling and deacetylase (NuRD) complex and the SWI-SNF complex (**Figure A-5**). Interestingly, there was a strong overlap between TFs identified as part of the TCF4 interactome in NB cell lines and motifs enriched in our TCF4 ChIP-seq (**Figure A-5**).

Though TCF4 is not directly targetable, we observed multiple therapeutic targets that complex with TCF4 (**Figure A-5**). HDAC 1 and 2 were present in the TCF4 (IP-MS). Surprisingly, the pan-HDACi trichostatin A (TSA) led to loss of TCF4 protein 24 hours post-treatment in both cell lines (**Figure A-6a**). The Class I HDAC specific inhibitor romidepsin caused degradation of TCF4 in both cell lines (**Figure A-6b**). We found no significant change in TCF4 gene expression following romidepsin treatment for 24 hours (**Figure A-S5b**). The proteasome inhibitor MG132 blocked the loss of TCF4 which confirms that the effects of HDAC inhibition are post-translational and based on protein stability (**Figure A-S5c**). SK-N-AS cells overexpressing TCF4 reduced the effects of romidepsin (**Figures A-6c** and **S5d**) indicating that TCF4 is a sensitive and central component of romidepsin toxicity in NB.

Finally, we assessed if KDM1A, identified in the IP-MS, also has a role in regulating TCF4 protein stability. We found that ORY-1001, a clinically relevant KDM1A inhibitor similarly caused reduced TCF4 protein stability (**Figure A-6e**). Taken together, found that TCF4 is central to the effects of multiple epigenetic factors through their regulation of TCF4 protein stability.

## Discussion

Neuroblastoma tumors display startling heterogeneity, compromising populations of both the ADRN and MES lineage<sup>46</sup>. This heterogeneity provides NB with high transcriptional plasticity allowing tumors to escape therapeutic treatment or to relapse<sup>10</sup>. NB identity is determined by lineage-specific transcription factors, driven by cell type specific SEs<sup>54,73,150</sup>. In this work, we identified TCF4 as a critical NB dependency gene, which is shared across the different NB lineage states. Our functional analysis demonstrated that loss of TCF4 dramatically decreases cell proliferation, induces apoptosis, and inhibits tumor growth in vivo.

To determine how TCF4 regulates these oncogenic programs we integrated our TCF4 ChIP-seq data and publicly available data for CRC ADRN factors in Kelly cells and found a high concordance of DNA occupancy by TCF4 with HAND2, MYCN, and TBX2 proteins. To test whether TCF4 and CRC TFs physically interact, we performed IP-MS analysis and identified TCF4 protein-protein interactions from two NB cell lines. The analysis showed enrichment in the network of multiple ADRN and MES NB CRC factors. When MYCN is highly expressed, it works as an “enhancer invader” and reinforces the gene expression program of the ADRN CRC<sup>64</sup>. TWIST1 and HAND2 factors collaborate with MYCN to drive oncogenic enhancer-driven transcription<sup>125</sup>. Our data further indicates TCF4 as a collaborative factor involved in facilitating TF-DNA binding for MYCN with TWIST1 and or HAND2 to regulate downstream oncogenic programs. Further, we found that TCF4 KD in NB cells caused downregulation in the expression of E2F genes, and genes kept silenced by the DREAM complex during quiescence including FOXM1 and MYBL2. E2Fs, FOXM1 and MYBL2 coordinately regulate multiple stages of cell cycle progression including the G2M transition<sup>151,152</sup>. MYBL2 and FOXM1 are important oncogenic factors with MYBL2 known to coregulate MYCN in NB<sup>153</sup>. Further, recent work identified TBX2 as a member of the ADRN CRC that similarly regulates E2Fs, MYBL2 and FOXM1<sup>150</sup>. Our results propose a role for TCF4 in regulating FOXM1/E2F-driven gene regulatory networks controlling proliferation in cooperation with MYCN, TBX2 and TCF4 dimerization partners HAND2 and TWIST1.

We have determined that multiple epigenetic therapies (BETi, HDACi and KDM1Ai) converge on TCF4. Despite the potential of HDACi in cancer therapy, why certain cancers are especially vulnerable to HDACi is not well understood. A pan-cancer study that tested two HDAC inhibitors (romidepsin and vorinostat) across 8 different cancer types found that the therapeutic effects of HDACi poorly associated with global histone changes suggesting that non-histone targets contribute to their effect<sup>154</sup>. Our finding that TCF4 protein stability is affected by HDACs and KDM1A inhibitors identifies an additional vulnerability of NB to these inhibitors. Across multiple cancer types, understanding the contribution of TCF4 to the therapeutic responses of patients toward certain epigenetic therapies is an important new avenue of research.

A model that fits our findings would suggest signaling to KDM1A would facilitate its demethylation of the MTA1 subunit of the NuRD complex causing NuRD to bind p300 to counteract the destabilizing acetylation of TCF4 by p300. Conversely, loss of demethylation of MTA1 achieved by KDM1A would lead to the NuRD complex affiliating with histones which would fulfill its traditional role of deacetylating histones to promote a transition to a close chromatin state. Concomitantly, loss of the counteracting effect of the NuRD HDACs would lead to the acetylation of TCF4 by p300 and its degradation, which would disrupt transcriptional complexes that are dependent on TCF4. This model possibly explains how neural crest cells are capable of rapidly transitioning between identity states during development by coupling transcription regulation to chromatin remodeling through the signaling axis of KDM1A, the NuRD complex and TCF4.

## CHAPTER 4. CRC DISRUPTION FACILITATES NB DIFFERENTIATION<sup>2</sup>

**NOTE:** This chapter refers frequently to content in **Appendix B**. When using Adobe Acrobat, after going there, return to the last viewed page using quick keys Alt/Ctrl+Left Arrow on PC or Command+Left Arrow on Mac. For the next page, use Alt/Ctrl or Command + Right Arrow. See **Preface** for further details.

### Introduction

NB arises from a block in NCC differentiation during development<sup>17,29</sup>. NB accounts for more than 15% of all childhood cancer-related deaths. Despite the most intensive multimodal therapy, more than 50% of patients with high-risk NB relapse with often fatal, resistant disease. Maintenance therapy using retinoic acid (RA) decreases the risk of recurrent disease after intensive multimodal treatment<sup>155</sup>. Clinically, high-risk NB patients are treated with high-dose 13-cis-RA (isotretinoin) as maintenance therapy, which converts into ATRA and 9-cisRA, a stereoisomer of ATRA<sup>156,157</sup>. The introduction of RA has been shown to induce differentiation and reduce the proliferation of neuroblastoma cells<sup>158</sup>. However, only a subset of NB patients responds to it. Studies have described the role of CRC factors in the establishment and maintenance of NB identity states<sup>36</sup>. The two identity states in NB, adrenergic and mesenchymal, capture NCCs early in their commitment to the sympathoadrenal lineage<sup>38,46</sup>. NCCs undergo an epithelial to mesenchymal transition (EMT) program and give rise to neuroblasts that are highly proliferative<sup>19,20</sup>. In normal development, these cells would respond to differentiation cues like RA to become mature neurons and Schwann cells of the sympathetic nervous system<sup>159</sup>. One strategy to treat NB is to push cells to differentiate<sup>160</sup>. RA has been shown to drive maturation of some NB tumors through transition of an immature CRCs to a more differentiated CRC<sup>161</sup>. Moreover, BETi disrupt CRCs and also show prominent anticancer activity in NB including promoting cellular differentiation in some NB cell lines<sup>72,162</sup>. Here, we hypothesize that blocks in differentiation are due to pathogenic CRCs, caused by multiple mechanisms and that these interfere with RA-mediated differentiation.

This chapter summarizes the research focused on investigating a therapeutic strategy for NB based on the hypothesis that blocks in differentiation are due to pathogenic CRCs. Overexpression and that these interfere with RA mediated differentiation<sup>163</sup>. Data are presented in the article “Therapeutically targeting oncogenic cell regulatory circuitries facilitates induced differentiation of neuroblastoma by retinoic acid and BET bromodomain inhibitor.” (**Appendix B**).

---

<sup>2</sup> Final submission reused with permission. Alleboina S, Aljouda N, Miller M, Freeman KW. Therapeutically targeting oncogenic CRCs facilitates induced differentiation of NB by RA and the BET bromodomain inhibitor. *Mol Ther Oncolytics*. 2021 Sep 25;23:181-191. DOI: <https://doi.org/10.1016/j.omto.2021.09.004><sup>163</sup> (**Appendix B**).

## Summary

MYCN gene amplification is a common mutation in high-risk NB<sup>53,63</sup>. MYCN amplification drives high ASCL1 expression, which blocks cell differentiation of sympathoadrenal neuroblasts into mature neurons<sup>164</sup>. ASCL1 has been identified as part of the ADRN CRC factors. First, we investigated the basal protein expression of the ADRN CRC factors, and SOX10, TWIST1, PRRX1, SNAI2, and vimentin, which are prominent MES markers in four different NB cell lines with different MYCN amplification status. We confirmed that Kelly cells are showing high protein expression level of ASCL1 and PHOX2B and low protein expression level of the MES markers SOX10, TWIST1, SNAI2, and vimentin (**Figure B-S1**). On the other hand, SKNAS showed a significantly lower basal protein expression of ASCL1 and PHOX2B and higher protein expression of SOX10, TWIST1, PRRX1, SNAI2, and vimentin, indicating a more mesenchymal type of identity (**Figure B-S1**). The other cell lines SK-N-BE2, GIMEN, and SY5Y showed an intermediate identity with a more mixed expression of ADRN and ME markers (**Figure B-S1**). Kelly cells, an MYCN-amplified NB, had higher ASCL1 expression and the most adrenergic type of identity, thus were chosen for our ASCL1 study.

First, we investigated the effect of ASCL1 knockdown on the expression of ADRN and MES CRC factors using ASCL1 sh6 and sh8 dox-inducible cell lines. We found that ASCL1 loss induces a significant effect on gene expression of core TFs with an upregulation in ADRN versus MES identity (**Figure B-1f**). This suggests a loss of stemness and gain of both more MES and ADRN differentiation. We also found that loss of ASCL1 caused a gain of multiple sympathoadrenal markers, TBX2, GATA3, and TH, at 96 h (**Figure B-1g-h**). However, we did not observe obvious and consistent increases in the MES markers suggesting that silencing of ASCL1 promotes sympathoadrenal differentiation.

We next tested if the differentiating agent ATRA would augment differentiation when ASCL1 is silenced. We observed that ATRA reduces ASCL1 gene expression to almost the same extent as caused by silencing of ASCL1 (**Figure B-2a**). We also observed a significant upregulation in TH when ASCL1 silencing was combined with ATRA (**Figure B-2b**). Using WB, we showed that ATRA inhibits ASCL1 expression and causes a further increase in TH expression when combined with ASCL1 silencing (**Figure B-2c**). Finally, we observed a significant decrease in proliferation by either ASCL1 knockdown or ATRA treatment in both Sh-ASCL1 cell lines. The effect on proliferation was more significant when ASCL1 knockdown was combined by ARTA treatment (**Figure B-2d**).

To investigate if broad disruption of CRCs using the BETi in combination with ATRA, we first determined the optimum dose of JQ1, ATRA, and JQ1+ATRA (**Figure B-S2a**). MYCN protein expression in Kelly, SKNAS, GIMEN, and SY5Y cells were also investigated (**Figure B-S2b**). We found that treatment of ATRA in the presence of JQ1 in Kelly and SY5Y cells showed a significant decrease in ASCL1 expression, and SOX10,

and a significant increase in GATA3 expression (**Figure B-3a-b**). A significant increase of both TH and myelin basic protein was observed in Kelly and SY5Y (**Figure B-4a-b**) after combinatorial JQ1/ATRA treatment. While SKNAS showed a significant increase in TH expression (**Figure B-4a**), and no change in MBP expression (**Figure B-4b**). Overall, we did not see that ATRA affect MYCN expression (**Figure B-S2c**), and we observe a significant reduction of SOX10 protein expression across the cell lines after the combination treatment (**Figure B-4c-e**), suggesting a loss of MES/stem identity. Using immunofluorescence staining of TH, we showed an increase in differentiation with the combination treatment across the three genetically diverse NB cell lines (**Figure B-S3a**).

We next investigated the effect of combinatorial treatment of ATRA with JQ1 on cell proliferation. We found that the combinational treatment is synergistic in inhibiting proliferation in Kelly (**Figure B-5a**), SY5Y (**Figure B-5b**), and SKNAS (**Figure B-5c**) versus single-agent treatments. Using 9-cisRA versus ATRA in combination with JQ1, we found that both drugs in combination with JQ1 cause induction of TH and GATA3 expression and loss of ASCL1 and SOX10 expression, indicating similar effects on cell differentiation (**Figures B-S3** and **3c**). We also showed that the combination of both drugs with JQ1 is synergistic in both Kelly (**Figure B-5d**), and SKNAS (**Figure B-5e**). When Kelly and SKNAS cells were treated with high doses of JQ1 and lower doses of ATRA the effect was antagonistic (**Figure B-5f-g**). The same results were observed when 9-cis-RA was combined with JQ1 (**Figure B-S4a-d**).

Using the colony-forming assay and the tumor-sphere assay, we found that the combinational treatment of ATRA and JQ1 cause a significant inhibition of colony forming capacity (**Figures B-6a** and **S5**), and tumor-sphere formation and growth in soft agar (**Figure B-6b**). These data suggest that BETi in combination with ATRA reduced stem/progenitor behavior in NB cells.

## Discussion

Changes in the CRC members in NB drive phenotypic changes such as proliferation, differentiation and drug resistance<sup>36</sup>. 13-cis RA, an important component of current maintenance treatment protocols for high risk NB patients has been shown to inhibit cell growth and induce differentiation<sup>156,157</sup>. Zimmerman et al. showed that RA results in rewiring of the CRC, leading to the loss of the ADRN CRC and acquiring of new members such as SOX4 and MEIS1 leading to NB differentiation<sup>165</sup>. Here, we identified a strategy to improve the efficacy of retinoids. Silencing of ASCL1 in combination with ATRA increased the differentiation marker TH and inhibited proliferation in Kelly cells. This suggests that disrupting the developmental block caused by high ASCL1 expression in combination with ATRA is an effective strategy to drive differentiation of Kelly cells. Further, combination of JQ1 and retinoids (ATRA or 9-cis RA) caused a significant loss in the key neural stem cell marker SOX10, a gain of the differentiation marker TH, and a robust suppression of cell growth in multiple *in vitro* assays.



Both Kelly and SY5Y show similar responses for the markers we have analyzed to the JQ1/ATRA combination, suggesting SY5Y might have a similar developmental block as Kelly cells. However, SKNAS shows a different response to this combination suggesting a different developmental block in this cell line. Taken together, these data suggest that overcoming a developmental block by the JQ1/ATRA combination could be useful in treating different NB with different underlying mutations.

In our study, we observed a similar response to ATRA and 9-cis-RA, the two main metabolites of 13-cis-RA (isotretinoin), with ATRA showing a more potent effect. Interestingly, we observed antagonistic effect of high doses of JQ1 to lower doses of both retinoids. We anticipate that the ability of ATRA to establish a more differentiated CRC is interrupted by high doses of JQ1. This suggests that timing and dosing of BETi with retinoids will be critical in their effectiveness and should be further explored in preclinical models.

## CHAPTER 5. INFLUENCE OF TCF4 LOSS ON HAND2 PROTEIN INTERACTIONS

**NOTE:** When using Adobe Acrobat, return to the last viewed page using quick keys Alt/Ctrl+Left Arrow on PC or Command+Left Arrow on Mac. For the next page, use Alt/Ctrl or Command + Right Arrow. See [Preface](#) for further details.

### Introduction

Regulation of transcription is under the control of multiple TFs. These factors collaborate together to achieve efficient binding to the DNA, thus regulates gene transcription and directs the development lineage specification<sup>30,166</sup>. Protein function is mainly determined by its interactions with other proteins<sup>167</sup>. Protein-protein interactions control many biological processes, thus disruption of the interactome for a specific protein may lead to pathway dysregulation and potentially contribute to development of diseases<sup>168,169</sup>.

In our study, we established the role of the E protein TCF4 as a critical NB dependency gene. We also validated the interaction of TCF4 with multiple class II bHLH TFs, including the master MES factor TWIST1, and the master ADRN factors ASCL1 and HAND2. By combining ChIP-seq, RNA-seq and IP-Mass spectrometry, we have shown that TCF4, through its heterodimerization partners, is a critical mediator of cell identity and is a core facilitator of a MYC/MYCN driven oncogenic program for NB. A recent study reported that when MYCN is highly expressed, it works as “enhancer invader” and reinforces the gene expression program of the ADRN CRC<sup>64</sup>. Two recent studies have shown that TWIST1 and HAND2 factors collaborate with MYCN to drive oncogenic enhancer-driven transcription<sup>64,125</sup>. Xu et al. show that HAND2 helps MYCN to invade enhancers through an indirect cooperative TF-DNA mechanism<sup>125</sup>. The way MYCN invades the enhancers, and the contribution of other master factors in this process still needs to be elucidated. HAND2 (dHAND) is a basic helix-loop-helix (bHLH) transcription factor. HAND2 is an essential factor expressed during development in multiple tissues such as the heart, and a subset of neural crest derivatives<sup>170</sup>. HAND2 is known to form homodimers, but also has been shown to work as a transcription activator through binding the E-boxes as a heterodimer with E-proteins such as TCF4<sup>171,172</sup>. In NB HAND2 has been shown to be a members of the transcriptional core regulatory circuitry that maintains cell identity state in MYCN-amplified NB<sup>53</sup>.

Since we have confirmed that TCF4 interacts with HAND2 and MYCN, we anticipate that TCF4 play an important role in this collaborative interaction and contribute to MYCN oncogenic role. To address this, we developed an IP/MS method to delaminate TCF4’s role in this process by studying the impact of TCF4 knockdown on HAND2 protein-protein interactions. This work will help understand what TCF4 is bringing to HAND2, and how losing TCF4 would affect HAND2 protein-protein interactions.

## Immunoprecipitation-Mass Spectrometry Analysis

Kelly cells transduced with shRNA against TCF4 (sh2) were treated with 1 µg/ml doxycycline for 3 days. Cells cultured in media with puromycin only were included in this experiment as a control. N=3 biological replicates for each cell line were used. Kelly TCF4 shRNA#2 cell lines were cultured to 90% confluency in 15 cm dishes per biological replicate prior to harvesting. After the incubation, cells were collected and washed twice with cold PBS. Total protein was extracted from cells using Pierce IP lysis buffer (Thermo Fisher Scientific #87787) supplemented with Halt Protease and phosphatase Inhibitor Cocktail (#1861281). Whole cell lysate was incubated with HAND2 antibody (Abcam, ab20004), or Normal Rabbit IgG (CST #2729) for each group with rotation overnight at 4°C. Next day, 50 µl of Pierce Protein A/G Magnetic Beads (Thermo Fisher Scientific # 88803) were moved to a clean tube and washed three times with 500 µl of 1X Pierce lysis buffer. The overnight cell lysate (~1 mg of whole cell lysate) was mixed with 50ul of the pre-washed magnetic beads and incubated with rotation for 2 hours at 4°C. Next, beads were separated from the lysate using a magnetic separation rack, the beads were then washed three times with 500 µl of 1X IP lysis buffer. The IP antibody: bead complex samples were sent to the University of Tennessee health science center Proteomics Core for Label Free Quantification (LFQ) mass spectrometry protein identification. On-bead Trypsin Digestion was performed by adding 1 µL of 1 µg/ µL MS grade trypsin. Mixed gently and incubated with the sample overnight at 37 °C while rocking on a nutator. Mass spectrometry protein identification results were analyzed with Proteome Discoverer 2.4, (Thermo Fisher). Peptide Abundance represents MS Peak Area, normalization mode is the total peptide amount, and the protein abundance is the summed abundances of assigned peptides. HAND2 interaction partners before and after adding doxycycline are included in the final list if they are present in at least two out of three HAND2 complex purifications and show at least two-fold enrichment by protein abundance in the HAND2 purified sample over the control sample (**Supplementary Table 5**). Cytoskeletal and cytoplasmic proteins (Uniprot) were removed. Proteins found in the negative IgG control were also removed.

## Results

In this study, we used the Kelly TCF4 shRNA (#2) cell line which shows around 65% TCF4 knockdown. Since we are not completely knocking down TCF4, we are investigating proteins that are lost after TCF4 knockdown, but we are also interested in proteins in which their abundance is going down or up with the dox treatment. Here TCF4 sh#2 cell line were treated with doxycycline to induce TCF4 knockdown followed by performing IP/MS using HAND2 antibody. We found that some HAND2 interactors were completely lost after knocking down TCF4. Those include many genes involved in survival (MECOM, TRAF2, MCM5), neuronal development (FMR1, TBC1D24, ASCC1, LDB1, PSIP1, NUMB), RNA Pol II and III (GTF3C4, HEXIM2, GTF3C3.), and chromatin remodeling (CHD6, CHD1L, SMARCA1, RBBP7). Another factor that disappeared following TCF4 knockdown among HAND2 interactors is SMAD4, which has been shown to suppresses NB tumorigenesis and aggressiveness via inhibiting the

expression of heparinase. SMARCA1 a member of the chromatin remodeling complex SWI/SNF, and GATAD2A a member of the NuRD complex involved in pluripotency, lineage commitment was also lost following TCF4 loss. Another interesting group of proteins lost from the HAND2 interactors are members of the CoREST family. The human CoREST family consists of three proteins that are encoded by separate genes (CoREST1, CoREST2, and CoREST3)<sup>173</sup>. RCOR2 and RCOR3 are known to be involved in neurodevelopment process<sup>134</sup>. The CoREST complex also encompasses the plant homeodomain (PHD) finger protein BHC80, and the histone deacetylases 1/2 (HDAC1/2). So, they combine LSD1 and HDAC1/2. HDAC-induced deacetylation positively influences the LSD1 activity thus induces the affinity of the entire complex for chromatin, and promotes the removal of methyl marks from target lysine residues by demethylase<sup>173</sup>. CoREST proteins have been shown to induce transcriptional repression through recruiting KDM1A and HDAC1/2<sup>129</sup>.

Moving to the list of proteins showings less abundance level following TCF4 loss based on the cutoff of FC>2, and P-value<0.05 (**Supplementary Table 5**), we confirmed the knockdown of TCF4, which consequently induces a decrease in HAND2 protein abundance. Multiple other proteins were identified including the TFs (MAZ, TFAP2B, ZEB2, TWIST1), the RNA polymerase II subunit POLR2B, the chromatin organization proteins (RUVBL1, WDR6, CHD7) and the NuRD complex members (HDAC2, MTA3 and GATAD2B) (**Figure 5-1**). The nucleosome remodeling and deacetylase (NuRD) complex has been shown to regulate the transcription through chromatin compaction and decompaction<sup>174</sup>. NuRD also plays a critical role in neurodevelopment. It is a known epigenetic regulator controlling gene expression in neural progenitor cell fate decisions in brain development<sup>175</sup>. Collectively, these data suggest that TCF4 is a major player in affecting HAND2 protein-protein interactions with multiple cell identity factors and critical epigenetic regulators.

To evaluate the functional significance of the HAND2 interactors affected following TCF4 knockdown, we performed gene ontology analysis of these proteins using the PANTHER database ([www.pantherdb.org](http://www.pantherdb.org)). We identified multiple significantly enriched pathways/compartments in each gene ontology category. Results showed that the most significantly enriched biological process, cellular component and molecular function in each cell line were regulation of transcription by RNA polymerase II, chromatin, and DNA binding respectively (**Figure 5-2**). The identification of the regulation of the DNA binding, gene expression, and cell fate among the most significantly enriched biological process coincides with our hypothesis that TCF4 is playing a role in regulating binding of different proteins related to chromatin remodeling and transcriptional regulation. Many of these proteins were identified in our study such as the NuRD complex member, HDAC2, the SWI/SNF-related regulator of chromatin, SMARCA1, and multiple cell fate transcription factors. These data highlight a cooperative role between HAND2 and TCF4 in NB oncogenic program. Future experiments are needed to confirm this collaborative interaction.

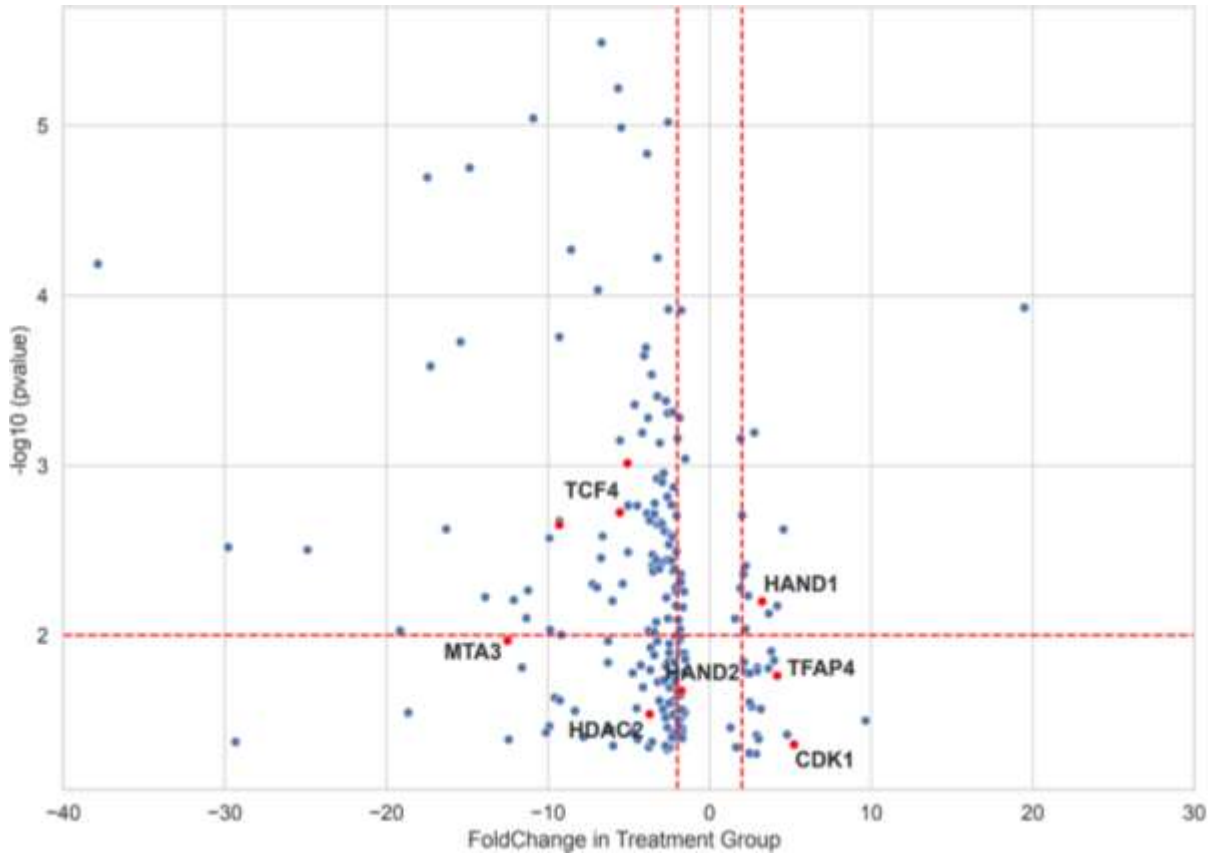


**Figure 5-1. HAND2 interactors affected following TCF4 loss.**

Volcano plot from the HAND2 IP mass spectrometry data demonstrates the magnitude and significance of the cellular proteins following TCF4 knockdown in Kelly sh#2 cell line.

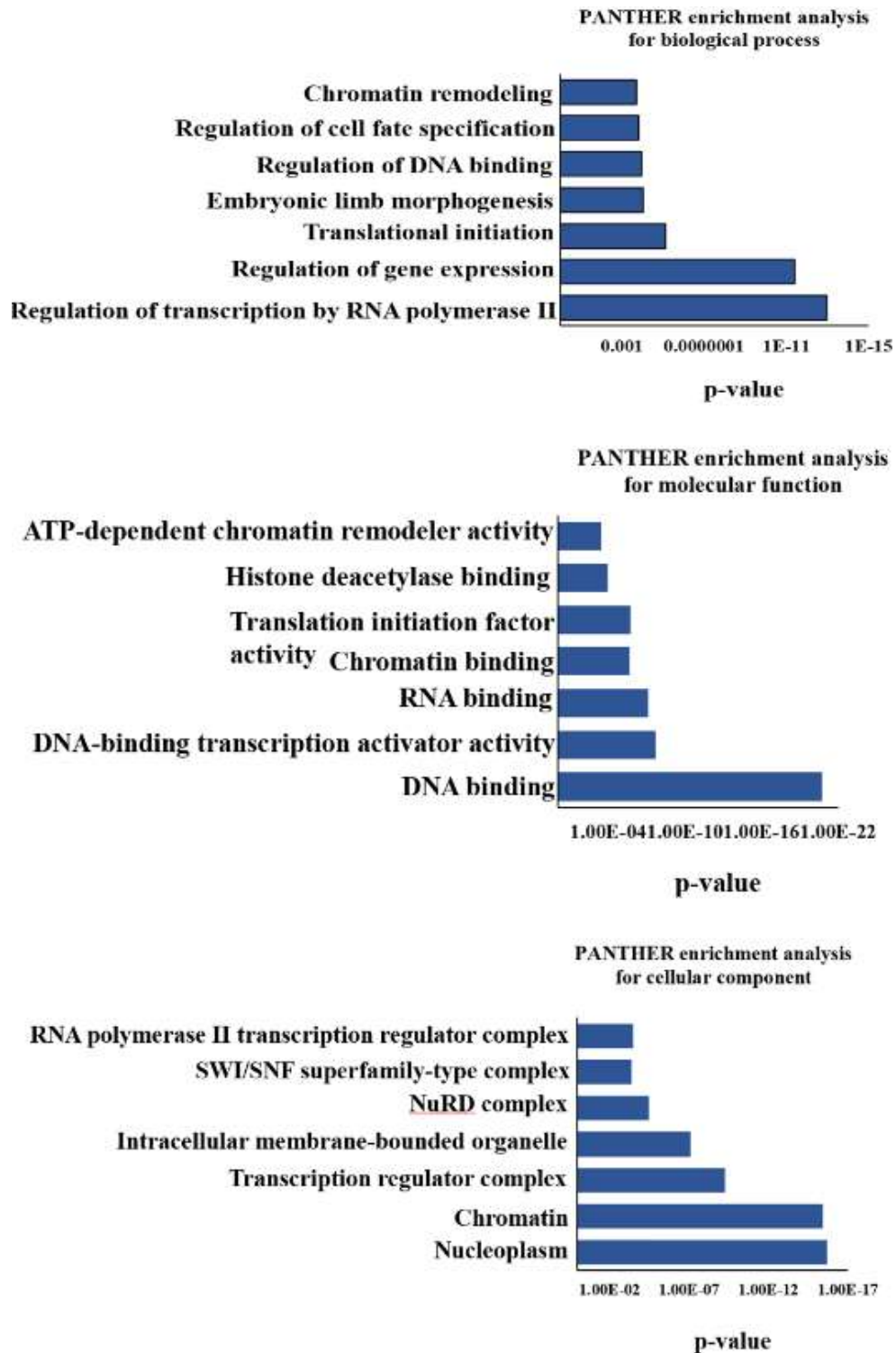


**Figure 5-2. PANTHER gene ontology analysis of HAND2-interacting proteins following TCF4 loss.**

The 7 most significantly enriched biological processes, cellular components and molecular functions in Kelly cells are shown.

## Discussion

HAND2 is a basic helix-loop-helix transcription factor, expressed in the neural crest derivatives and play major role in the autonomic nervous system development including sympathetic neurons<sup>170</sup>. HAND2 is highly expressed in NB, and has been shown to function as transcriptional activator through binding to the E-box as a heterodimer<sup>171</sup>. In our work, we demonstrated using IP-MS that TCF4 heterodimerizes with multiple class II bHLH TFs including HAND2. A recent study showed that HAND2 assists MYCN to invade enhancer and shape NB cell identity<sup>125</sup>. Since our data suggest that TCF4 colocalizes with MYCN and HAND2 and physically interact, we decided to determine the effect of TCF4 loss on HAND2 protein interactions with MYCN and other factors.

Knockdown of TCF4 prompted multiple changes in HAND2 interactome in NB Kelly cells. This includes many TFs, RNA polymerase and chromatin remodeling proteins. Among the list of proteins affected are HDAC2 and the CoREST complex proteins RCOR2 and RCOR3. In a previous study Song et al. showed that the CoREST complex encloses the HDAC1/2 and KDM1A, and that the two enzymes are coupled within the CoREST complex. The CoREST complex has been shown to bind one substrate at a time. However, the activity of both enzymes within the CoREST complex is closely correlated. The TCF4 interactome we identified in NB cell lines confirmed the binding of TCF4 to both HDAC2 and KDM1A. Recently, a study showed that c-MYC is deacetylated via the HDACs leading to improvement of c-MYC DNA binding in a c-MYC amplified medulloblastoma (brain tumor)<sup>176</sup>. Herein, our data support a model in which TCF4 contributes to MYCN oncogenic program through recruiting CoREST through heterodimerization with HAND2. This brings HDAC2 interacting with TCF4 close to MYCN protein. We anticipate that deacetylation of MYCN via HDACs leads to its stabilization and improves its DNA binding in MYCN amplified NB. Following from this work, multiple experiments could be performed to investigate this hypothesis. One suggested experiment is knocking down TCF4 using the established cell lines, at the same time treat Kelly cells with the HDACi romidepsin to compare the level of total MYCN and the acetylated MYCN proteins following TCF4 loss and romidepsin treatment. This experiment will determine if TCF4 loss would have a comparable effect to romidepsin in affecting acetylation of MYCN and thus its overall binding. Multiple experiments are also needed to confirm this model.

## CHAPTER 6. CONCLUSIONS AND FUTURE DIRECTION

**NOTE:** When using Adobe Acrobat, return to the last viewed page using quick keys Alt/Ctrl+Left Arrow on PC or Command+Left Arrow on Mac. For the next page, use Alt/Ctrl or Command + Right Arrow. See [Preface](#) for further details.

NB is characterized by a set of master TFs establishing cell identity<sup>46</sup>. Dysregulation of these TFs contributes to the initiation and maintenance of NB by enforcing early developmental identity states<sup>38,44</sup>. Identifying NB dependency genes is critical to provide insights into the disruption of core regulatory circuits in NB. This body of work suggest that the class I bHLH factor TCF4 is a critical NB dependency gene that significantly contributes to NB identity states through its heterodimerization with cell identity specific bHLH TFs. Mechanistically, we show that TCF4 promotes cell proliferation through direct transcriptional regulation of a MYC/MYCN oncogenic program. We also determined TCF4 regulatory genes in NB and showed that TCF4 colocalizes with multiple class II bHLH factors known to drive NB oncogenesis and establish its identity. Future studies will need to enlarge the panel of NB cell lines tested to include more ADRN and MES NB cell lines and PDXs to fully assess the importance of TCF4 across heterogenous NB lines.

Several future experiments can be done to elucidate the role of TCF4 in NB oncogenesis. It is crucial to check if TCF4 loss affects the epigenetic landscape. This could be done by performing ChIP-seq using TCF4, the histone mark H3K27ac, and RNA Pol II antibodies. In parallel, we can perform ATAC-seq to evaluate the chromatin accessibility upon TCF4 knockdown. Here, we can investigate if TCF4 loss results in a significant loss of TCF4 signal and if it is accompanied by a decrease of H3K27ac and RNA Pol II signal at the TCF4 locus. This would imply that TCF4 loss decreases enhancer activity. We can also look to see if loss of TCF4 decreases ATAC-seq signal, suggesting a decrease in chromatin accessibility. This experiment will establish if TCF4 regulates gene transcription at the epigenetic level.

Many questions still need to be answered to better develop effective approaches to target all NB subtypes. This includes identifying the master TFs controlling the NCCs, the cell of origin of NB to better understand NB tumorigenesis. Several studies reported the enrichment of MES cells at relapse tumors<sup>47,56,177</sup>. One explanation is the switching between the ADRN and MES states in NB, where chemotherapies favor switching to the MES gene expression program. In general, most studies have focused on investigating multiple therapeutic approaches in the ADRN cell lines, thus many questions still need to be investigated about the relevance of these approaches in the MES drug resistance cells.

MYCN is master TF that drives NB oncogenesis, found in ~20% of the cases and is associated with aggressive disease and poor prognosis<sup>54,64,152</sup>. Zeid et al. investigated MYCN activation and loss in NB. They found that in NB cells MYCN binds to the canonical (CACGTG) E-box sites at promoters. However, when MYCN is amplified, it starts binding to the non-canonical CANNTG E-boxes at enhancers<sup>64</sup>. Shutdown of



MYCN decreases MYCN enhancer gene signature, suggesting that MYCN amplification prompts enhancer invasion to drive NB. In this study they found that TWIST1 is required for MYCN oncogenic enhancer gene transcription. The study also showed that the related E-protein TCF3 (E2A) is needed for the growth of MYC-deregulated multiple myeloma and play a similar role to TWIST1 in NB<sup>64</sup>.

Another study reported that HAND2 collaborates with MYCN to invade enhancers<sup>125</sup>. They performed ChIP-seq for MYCN and focused on MYCN ChIP-seq peaks that overlapped with all the binding sites of the CRC components. The top ranked motifs include PHOX2A/2B, GATA3, ISL1, HAND2 and TCF4 binding motifs. Interestingly our data show that TCF4 physically interacts with HAND2, TWIST1, and MYCN. Also, our ChIP-seq data shows a high concordance of DNA occupancy by TCF4, HAND2, and MYCN, and a strong overlap of MYCN and TCF4 at enhancers. These data highlight a possible role of TCF4 among CRC TFs, via collaborative gene control with the MYCN oncoprotein. However, the role that TCF4 plays in this process still needs to be investigated. There are key experiments that could be performed to validate this collaborative interaction in driving NB tumorigenesis. First, we can use the established shRNA cell lines targeting TCF4 and perform MYCN ChIP sequencing before and after TCF4 knockdown. We will investigate if TCF4 loss in NB cell lines will influence MYCN binding by evaluating the average ChIP-seq signal of MYCN intensity. Performing ATAC-seq in parallel will inform if the decrease in the MYCN binding signal is accompanied by a decrease in the ATAC-seq signal. Moreover, we can investigate if TCF4 loss will induce downregulation of genes only with high MYCN enhancer signal, while having no or minimum effect on genes with high MYCN promotor signal. This experiment will establish if TCF4 is collaborating with MYCN to drive enhancer dependent NB gene expression program. The existence of this collaborative interaction at the genome level adds another layer of complexity of how master TFs are driving NB cell identity and will have important therapeutic implications for this pediatric cancer.

It is well established that posttranslational modifications (PTMs) are involved in regulating protein function and interactions, including acetylation, phosphorylation, and ubiquitination<sup>178</sup>. For instance, the p300/CBP associated factor (PCAF) has been shown to acetylates the class I bHLH protein TCF3 within the HLH domain to facilitate its heterodimerization with class II bHLH proteins<sup>179</sup>. In our work, through IP-MS studies, we have identified multiple promising epigenetic therapies (BETi, HDACi and KDM1A inhibitors) that control TCF4 stability at the gene expression level (BETi), and at the protein level (HDACi and KDM1A inhibitors). We found that the HDACi romidepsin and the KDM1A inhibitor ORY-1001 caused reduced TCF4 protein stability (Figure A-6e). Further, garcinol blocks both HDAC and KDM1A inhibition indicating that the HAT activity of p300 is epistatic to HDACs and KDM1A (Figure A-S5g). The proteasome inhibitor MG132 blocked the loss of TCF4 which confirms that the effects of HDAC inhibition are post-translational and based on protein stability. We found that romidepsin and ORY-1001 were synergistic with ATRA in Kelly cells (Figure A-6f and 5h). These findings indicate that TCF4 is central to the effects of multiple epigenetic factors through their regulation of TCF4 protein stability. Further, these data highlight the existence of an

additional layer of cell identity control mediated by epigenetic regulators through acetylation of a central cell identity factor, TCF4.

We confirmed with a series of experiments that the epigenetic drugs HDACi and KDM1A inhibitor induce TCF4 protein degradation. We anticipate that the acetylation of TCF4 by these drugs lead to TCF4 protein proteasomal degradation. An experiment that we suggest performing is to identify the acetylated lysine site of the endogenous TCF4 using IP-MS approach in NB. First, to induce the acetylation of the endogenous TCF4, we have to treat NB cells with romidepsin with the proteasomal inhibitor MG132. Next, we will perform immunoprecipitation of TCF4 followed by mass spectrometry and look for sites of acetylated lysine peptides in TCF4 pull down. If successful, another avenue that would be interesting to explore is to check if mutating this identified acetylated site of TCF4 followed by romidepsin or ORY-1001 treatment would cause a block or shift in these drugs inducing toxicity in NB cells. To do this, we can use the site-directed mutagenesis approach and perform a lysine to alanine mutation at the identified site to introduce a mutation within the acetylation consensus sequence in the bHLH domain. The established cell line with the mutated site will then be treated with romidepsin or ORY-1001 to determine if TCF4 is central to the toxicity of those two drugs in NB cell lines. If successful, the study will support testing combinatorial treatments using HDACi, ORY-1001 and the differentiating agent ATRA to target TCF4 function in NB and other cancers *in vitro* and *in vivo*.

It is now becoming evident that epigenetic changes are involved in cancer development<sup>98,180</sup>. Epigenetic therapies are showing promising anti-cancer effects<sup>105,109</sup>. HDAC inhibitors such as SAHA and romidepsin are used in cancer treatment, although their direct targets are still unknown<sup>57,115</sup>. Our study provides a novel explanation of the non- canonical HDACs mechanism of toxicity in NB through targeting TCF4 protein stability. Future studies should investigate the effect of HDACs and KDM1A inhibitors on TCF4 *in vivo*. It is also important to determine the therapeutic window that is selective and effective to kill tumors while having limited toxicity on normal and stem cells.

The essential role we identified for TCF4 in NB prompted us to consider investigating in the future the role of other members of the E-protein family TCF3 and TCF12 in NB. Acetylation of TCF3 in B lymphocyte did not affect its protein stability rather it causes alteration of its class II heterodimerization partners<sup>179</sup>. Future experiments may involve studying of HDACi and KDM1A inhibitors on TCF3 and TCF12 to compare the effect of acetylation of the class I factors and the influence of this acetylation on their behavior. This will be critical for therapy since different reactions of those proteins to HDAC and KDM1A inhibitors might lead to varying outcomes and sensitivities in cancer. Finally, it is essential to further investigate the role of other factors identified in the complex with IP-MS analysis to understand their contribution more fully. These include, different class II TFs, CoREST family members, KDM1A, MTA3 and GATAD2A and others. Interrogating the effects of inhibiting or silencing of individual factors in the complex is crucial to explore their potential roles in therapy.

## LIST OF REFERENCES

1. Maris, J. M., Hogarty, M. D., Bagatell, R. & Cohn, S. L. Neuroblastoma. *Lancet* **369**, 2106–20 (2007).
2. Brodeur, G. M. Neuroblastoma: biological insights into a clinical enigma. *Nat Rev Cancer* **3**, 203–16 (2003).
3. Kameneva, P. *et al.* Single-cell transcriptomics of human embryos identifies multiple sympathoblast lineages with potential implications for neuroblastoma origin. *Nat Genet* **53**, 694–706 (2021).
4. Delloye-Bourgeois, C. & Castellani, V. Hijacking of Embryonic Programs by Neural Crest-Derived Neuroblastoma: From Physiological Migration to Metastatic Dissemination. *Front. Mol. Neurosci.* **12**, 52 (2019).
5. Naranjo, A. *et al.* Statistical Framework in Support of a Revised Children’s Oncology Group Neuroblastoma Risk Classification System. *JCO Clin Cancer Inform* **2**, 1–15 (2018).
6. Smith, V. & Foster, J. High-Risk Neuroblastoma Treatment Review. *Children (Basel)* **5**, 114 (2018).
7. DuBois, S. G., Macy, M. E. & Henderson, T. O. High-Risk and Relapsed Neuroblastoma: Toward More Cures and Better Outcomes. *Am Soc Clin Oncol Educ Book* **42**, 1–13 (2022).
8. Brodeur, G. M. Spontaneous regression of neuroblastoma. *Cell Tissue Res* **372**, 277–286 (2018).
9. Carén, H. *et al.* High-risk neuroblastoma tumors with 11q-deletion display a poor prognostic, chromosome instability phenotype with later onset. *Proc Natl Acad Sci U S A* **107**, 4323–4328 (2010).
10. Meacham, C. E. & Morrison, S. J. Tumour heterogeneity and cancer cell plasticity. *Nature* **501**, 328–37 (2013).
11. Pugh, T. J. *et al.* The genetic landscape of high-risk neuroblastoma. *Nat Genet* **45**, 279–284 (2013).
12. Farina, A. R., Cappabianca, L. A., Zelli, V., Sebastiano, M. & Mackay, A. R. Mechanisms involved in selecting and maintaining neuroblastoma cancer stem cell populations, and perspectives for therapeutic targeting. *WJSC* **13**, 685–736 (2021).
13. Mossé, Y. P. *et al.* Identification of ALK as a major familial neuroblastoma predisposition gene. *Nature* **455**, 930–935 (2008).
14. Bertrand, N., Castro, D. S. & Guillemot, F. Proneural genes and the specification of neural cell types. *Nat Rev Neurosci* **3**, 517–30 (2002).
15. Artinger, K. B. & Monsoro-Burq, A. H. Neural crest multipotency and specification: power and limits of single cell transcriptomic approaches. *Fac Rev* **10**, 38 (2021).
16. Achilleos, A. & Trainor, P. A. Neural crest stem cells: discovery, properties and potential for therapy. *Cell Res* **22**, 288–304 (2012).
17. Zeineldin, M., Patel, A. G. & Dyer, M. A. Neuroblastoma: When differentiation goes awry. *Neuron* **110**, 2916–2928 (2022).
18. Gammill, L. S. & Bronner-Fraser, M. Neural crest specification: migrating into genomics. *Nat Rev Neurosci* **4**, 795–805 (2003).

19. Soldatov, R. *et al.* Spatiotemporal structure of cell fate decisions in murine neural crest. *Science* **364**, eaas9536 (2019).
20. Jing, J. *et al.* Spatiotemporal single-cell regulatory atlas reveals neural crest lineage diversification and cellular function during tooth morphogenesis. *Nat Commun* **13**, 4803 (2022).
21. Steventon, B., Araya, C., Linker, C., Kuriyama, S. & Mayor, R. Differential requirements of BMP and Wnt signalling during gastrulation and neurulation define two steps in neural crest induction. *Development* **136**, 771–779 (2009).
22. Cheung, M. *et al.* The transcriptional control of trunk neural crest induction, survival, and delamination. *Dev Cell* **8**, 179–192 (2005).
23. Häming, D. *et al.* Expression of Sympathetic Nervous System Genes in Lamprey Suggests Their Recruitment for Specification of a New Vertebrate Feature. *PLoS ONE* **6**, e26543 (2011).
24. Pei, D. *et al.* Distinct neuroblastoma-associated alterations of PHOX2B impair sympathetic neuronal differentiation in zebrafish models. *PLoS Genet* **9**, e1003533 (2013).
25. Takayama, Y. *et al.* Selective Induction of Human Autonomic Neurons Enables Precise Control of Cardiomyocyte Beating. *Sci Rep* **10**, 9464 (2020).
26. Persson, P., Jögi, A., Grynfeld, A., Pählman, S. & Axelson, H. HASH-1 and E2-2 are expressed in human neuroblastoma cells and form a functional complex. *Biochem Biophys Res Commun* **274**, 22–31 (2000).
27. Fan, X. *et al.* TWIST1 and chromatin regulatory proteins interact to guide neural crest cell differentiation. *Elife* **10**, (2021).
28. Sanchez-Ferras, O. *et al.* A coordinated progression of progenitor cell states initiates urinary tract development. *Nat Commun* **12**, 2627 (2021).
29. Ponzoni, M. *et al.* Recent advances in the developmental origin of neuroblastoma: an overview. *J Exp Clin Cancer Res* **41**, 92 (2022).
30. Lambert, S. A. *et al.* The Human Transcription Factors. *Cell* **172**, 650–665 (2018).
31. Choi, H. J. *et al.* Differential transcriptional regulation of the NANOG gene in chicken primordial germ cells and embryonic stem cells. *J Animal Sci Biotechnol* **12**, 40 (2021).
32. Chambers, I. & Smith, A. Self-renewal of teratocarcinoma and embryonic stem cells. *Oncogene* **23**, 7150–7160 (2004).
33. Marson, A. *et al.* Connecting microRNA Genes to the Core Transcriptional Regulatory Circuitry of Embryonic Stem Cells. *Cell* **134**, 521–533 (2008).
34. Sönmezer, C. *et al.* Molecular Co-occupancy Identifies Transcription Factor Binding Cooperativity In Vivo. *Molecular Cell* **81**, 255-267.e6 (2021).
35. Chen, Y., Xu, L., Lin, R. Y.-T., Müschen, M. & Koeffler, H. P. Core transcriptional regulatory circuitries in cancer. *Oncogene* **39**, 6633–6646 (2020).
36. Wei, L. *et al.* Cancer CRC: A Comprehensive Cancer Core Transcriptional Regulatory Circuit Resource and Analysis Platform. *Front Oncol* **11**, 761700 (2021).
37. Saint-André, V. *et al.* Models of human core transcriptional regulatory circuitries. *Genome Res* **26**, 385–96 (2016).
38. Jahangiri, L. *et al.* Core regulatory circuitries in defining cancer cell identity across the malignant spectrum. *Open Biol.* **10**, 200121 (2020).

39. Gryder, B. E. *et al.* Histone hyperacetylation disrupts core gene regulatory architecture in rhabdomyosarcoma. *Nat Genet* **51**, 1714–1722 (2019).
40. Tang, F., Yang, Z., Tan, Y. & Li, Y. Super-enhancer function and its application in cancer targeted therapy. *npj Precis. Onc.* **4**, 2 (2020).
41. Sabari, B. R. *et al.* Coactivator condensation at super-enhancers links phase separation and gene control. *Science* **361**, eaar3958 (2018).
42. Thandapani, P. Super-enhancers in cancer. *Pharmacology & Therapeutics* **199**, 129–138 (2019).
43. Zhang, X. *et al.* Somatic Superenhancer Duplications and Hotspot Mutations Lead to Oncogenic Activation of the KLF5 Transcription Factor. *Cancer Discovery* **8**, 108–125 (2018).
44. Hnisz, D. *et al.* Super-Enhancers in the Control of Cell Identity and Disease. *Cell* **155**, 934–947 (2013).
45. Henssen, A. *et al.* Targeting MYCN-Driven Transcription By BET-Bromodomain Inhibition. *Clin Cancer Res* **22**, 2470–81 (2016).
46. Boeva, V. *et al.* Heterogeneity of neuroblastoma cell identity defined by transcriptional circuitries. *Nat Genet* **49**, 1408–1413 (2017).
47. Westerhout, E. M. *et al.* Mesenchymal-Type Neuroblastoma Cells Escape ALK Inhibitors. *Cancer Res* **82**, 484–496 (2022).
48. Sanda, T. *et al.* Core Transcriptional Regulatory Circuit Controlled by the TAL1 Complex in Human T Cell Acute Lymphoblastic Leukemia. *Cancer Cell* **22**, 209–221 (2012).
49. Juraschka, K. & Taylor, M. D. Medulloblastoma in the age of molecular subgroups: a review. *J Neurosurg Pediatr* **24**, 353–363 (2019).
50. Lin, C. Y. *et al.* Active medulloblastoma enhancers reveal subgroup-specific cellular origins. *Nature* **530**, 57–62 (2016).
51. Zhang, T. *et al.* Aberrant super-enhancer landscape reveals core transcriptional regulatory circuitry in lung adenocarcinoma. *Oncogenesis* **9**, 92 (2020).
52. van Groningen, T. *et al.* Neuroblastoma is composed of two super-enhancer-associated differentiation states. *Nat Genet* **49**, 1261–1266 (2017).
53. Durbin, A. D. *et al.* Selective gene dependencies in MYCN-amplified neuroblastoma include the core transcriptional regulatory circuitry. *Nat Genet* **50**, 1240–1246 (2018).
54. Wang, L. *et al.* ASCL1 is a MYCN- and LMO1-dependent member of the adrenergic neuroblastoma core regulatory circuitry. *Nat Commun* **10**, 5622 (2019).
55. Durbin, A. D. *et al.* EP300 Selectively Controls the Enhancer Landscape of MYCN-Amplified Neuroblastoma. *Cancer Discov* **12**, 730–751 (2022).
56. van Groningen, T. *et al.* A NOTCH feed-forward loop drives reprogramming from adrenergic to mesenchymal state in neuroblastoma. *Nat Commun* **10**, 1530 (2019).
57. Suraweera, A., O’Byrne, K. J. & Richard, D. J. Combination Therapy With Histone Deacetylase Inhibitors (HDACi) for the Treatment of Cancer: Achieving the Full Therapeutic Potential of HDACi. *Front Oncol* **8**, 92 (2018).
58. Lourenco, C. *et al.* MYC protein interactors in gene transcription and cancer. *Nat Rev Cancer* **21**, 579–591 (2021).
59. Bretones, G., Delgado, M. D. & León, J. Myc and cell cycle control. *Biochim Biophys Acta* **1849**, 506–516 (2015).

60. Stine, Z. E., Walton, Z. E., Altman, B. J., Hsieh, A. L. & Dang, C. V. MYC, Metabolism, and Cancer. *Cancer Discov* **5**, 1024–1039 (2015).
61. Patange, S. *et al.* MYC amplifies gene expression through global changes in transcription factor dynamics. *Cell Reports* **38**, 110292 (2022).
62. Rickman, D. S., Schulte, J. H. & Eilers, M. The Expanding World of N-MYC-Driven Tumors. *Cancer Discov* **8**, 150–163 (2018).
63. Otte, J., Dyberg, C., Pepich, A. & Johnsen, J. I. MYCN Function in Neuroblastoma Development. *Front. Oncol.* **10**, 624079 (2021).
64. Zeid, R. *et al.* Enhancer invasion shapes MYCN-dependent transcriptional amplification in neuroblastoma. *Nat Genet* **50**, 515–523 (2018).
65. Wang, L. *et al.* EZH2 depletion potentiates MYC degradation inhibiting neuroblastoma and small cell carcinoma tumor formation. *Nat Commun* **13**, 12 (2022).
66. Wolpaw, A. J. *et al.* Drugging the ‘Undruggable’ MYCN Oncogenic Transcription Factor: Overcoming Previous Obstacles to Impact Childhood Cancers. *Cancer Res* **81**, 1627–1632 (2021).
67. Llombart, V. & Mansour, M. R. Therapeutic targeting of ‘undruggable’ MYC. *EBioMedicine* **75**, 103756 (2022).
68. Dauch, D. *et al.* A MYC–aurora kinase A protein complex represents an actionable drug target in p53-altered liver cancer. *Nat Med* **22**, 744–753 (2016).
69. Chen, H., Liu, H. & Qing, G. Targeting oncogenic Myc as a strategy for cancer treatment. *Sig Transduct Target Ther* **3**, 5 (2018).
70. Chen, Y., Tsai, H.-W., Tsai, Y.-H. & Tseng, S.-H. VS-5584, a PI3K/mTOR dual inhibitor, exerts antitumor effects on neuroblastomas in vitro and in vivo. *Journal of Pediatric Surgery* **56**, 1441–1448 (2021).
71. Sarnik, J., Popławski, T. & Tokarz, P. BET Proteins as Attractive Targets for Cancer Therapeutics. *Int J Mol Sci* **22**, (2021).
72. Zhou, S. *et al.* BET protein inhibitor JQ1 downregulates chromatin accessibility and suppresses metastasis of gastric cancer via inactivating RUNX2/NID1 signaling. *Oncogenesis* **9**, 33 (2020).
73. Puissant, A. *et al.* Targeting MYCN in neuroblastoma by BET bromodomain inhibition. *Cancer Discov* **3**, 308–23 (2013).
74. Murre, C. *et al.* Interactions between heterologous helix-loop-helix proteins generate complexes that bind specifically to a common DNA sequence. *Cell* **58**, 537–544 (1989).
75. Forrest, M. P., Hill, M. J., Quantock, A. J., Martin-Rendon, E. & Blake, D. J. The emerging roles of TCF4 in disease and development. *Trends Mol Med* **20**, 322–31 (2014).
76. Sepp, M., Kannike, K., Eesmaa, A., Urb, M. & Timmusk, T. Functional Diversity of Human Basic Helix-Loop-Helix Transcription Factor TCF4 Isoforms Generated by Alternative 5' Exon Usage and Splicing. *PLoS ONE* **6**, e22138 (2011).
77. Forrest, M. *et al.* Functional analysis of TCF4 missense mutations that cause Pitt-Hopkins syndrome. *Hum Mutat* **33**, 1676–1686 (2012).
78. Chen, W.-Y. *et al.* A TAF4 coactivator function for E proteins that involves enhanced TFIID binding. *Genes Dev.* **27**, 1596–1609 (2013).

79. Tarczewska, A. & Greb-Markiewicz, B. The Significance of the Intrinsically Disordered Regions for the Functions of the bHLH Transcription Factors. *IJMS* **20**, 5306 (2019).
80. Sirp, A. *et al.* Expression of alternative transcription factor 4 mRNAs and protein isoforms in the developing and adult rodent and human tissues. *Front. Mol. Neurosci.* **15**, 1033224 (2022).
81. Massari, M. E. *et al.* A Conserved Motif Present in a Class of Helix-Loop-Helix Proteins Activates Transcription by Direct Recruitment of the SAGA Complex. *Molecular Cell* **4**, 63–73 (1999).
82. Massari, M. E., Jennings, P. A. & Murre, C. The AD1 transactivation domain of E2A contains a highly conserved helix which is required for its activity in both *Saccharomyces cerevisiae* and mammalian cells. *Mol Cell Biol* **16**, 121–129 (1996).
83. Lingbeck, J. M., Trausch-Azar, J. S., Ciechanover, A. & Schwartz, A. L. E12 and E47 modulate cellular localization and proteasome-mediated degradation of MyoD and Id1. *Oncogene* **24**, 6376–6384 (2005).
84. Greb-Markiewicz, B., Kazana, W., Zarebski, M. & Ozyhar, A. The subcellular localization of bHLH transcription factor TCF4 is mediated by multiple nuclear localization and nuclear export signals. *Sci Rep* **9**, 15629 (2019).
85. Massari, M. E. & Murre, C. Helix-loop-helix proteins: regulators of transcription in eucaryotic organisms. *Mol Cell Biol* **20**, 429–440 (2000).
86. Powell, L. M. & Jarman, A. P. Context dependence of proneural bHLH proteins. *Current Opinion in Genetics & Development* **18**, 411–417 (2008).
87. Wedel, M. *et al.* Transcription factor Tcf4 is the preferred heterodimerization partner for Olig2 in oligodendrocytes and required for differentiation. *Nucleic Acids Res* **48**, 4839–4857 (2020).
88. Chen, T. *et al.* Tcf4 Controls Neuronal Migration of the Cerebral Cortex through Regulation of Bmp7. *Front Mol Neurosci* **9**, 94 (2016).
89. Flora, A., Garcia, J. J., Thaller, C. & Zoghbi, H. Y. The E-protein Tcf4 interacts with Math1 to regulate differentiation of a specific subset of neuronal progenitors. *Proc Natl Acad Sci U S A* **104**, 15382–7 (2007).
90. Sasai, Y., Kageyama, R., Tagawa, Y., Shigemoto, R. & Nakanishi, S. Two mammalian helix-loop-helix factors structurally related to *Drosophila* hairy and Enhancer of split. *Genes & Development* **6**, 2620–2634 (1992).
91. Cano, A. & Portillo, F. An emerging role for class I bHLH E2-2 proteins in EMT regulation and tumor progression. *Cell Adh Migr* **4**, 56–60 (2010).
92. Bergqvist, I. *et al.* The basic helix-loop-helix transcription factor E2-2 is involved in T lymphocyte development. *Eur J Immunol* **30**, 2857–63 (2000).
93. Bradney, C. *et al.* Regulation of E2A activities by histone acetyltransferases in B lymphocyte development. *J Biol Chem* **278**, 2370–6 (2003).
94. Quevedo, M. *et al.* Mediator complex interaction partners organize the transcriptional network that defines neural stem cells. *Nat Commun* **10**, 2669 (2019).
95. Ceribelli, M. *et al.* A Druggable TCF4- and BRD4-Dependent Transcriptional Network Sustains Malignancy in Blastic Plasmacytoid Dendritic Cell Neoplasm. *Cancer Cell* **30**, 764–778 (2016).
96. Vicent, S. *et al.* A novel lung cancer signature mediates metastatic bone colonization by a dual mechanism. *Cancer Res* **68**, 2275–85 (2008).

97. in 't Hout, F. E., van der Reijden, B. A., Monteferrario, D., Jansen, J. H. & Huls, G. High expression of transcription factor 4 (TCF4) is an independent adverse prognostic factor in acute myeloid leukemia that could guide treatment decisions. *Haematologica* **99**, e257-9 (2014).
98. Flavahan, W. A., Gaskell, E. & Bernstein, B. E. Epigenetic plasticity and the hallmarks of cancer. *Science* **357**, eaal2380 (2017).
99. Bradner, J. E., Hnisz, D. & Young, R. A. Transcriptional Addiction in Cancer. *Cell* **168**, 629–643 (2017).
100. Lambert, M., Jambon, S., Depauw, S. & David-Cordonnier, M.-H. Targeting Transcription Factors for Cancer Treatment. *Molecules* **23**, 1479 (2018).
101. Zhuang, J., Liu, Q., Wu, D. & Tie, L. Current strategies and progress for targeting the “undruggable” transcription factors. *Acta Pharmacol Sin* **43**, 2474–2481 (2022).
102. Henley, M. J. & Koehler, A. N. Advances in targeting ‘undruggable’ transcription factors with small molecules. *Nat Rev Drug Discov* **20**, 669–688 (2021).
103. Weidemüller, P., Kholmatov, M., Petsalaki, E. & Zaugg, J. B. Transcription factors: Bridge between cell signaling and gene regulation. *Proteomics* **21**, 2000034 (2021).
104. Hamilton, J. P. Epigenetics: principles and practice. *Dig Dis* **29**, 130–135 (2011).
105. Biswas, S. & Rao, C. M. Epigenetic tools (The Writers, The Readers and The Erasers) and their implications in cancer therapy. *Eur J Pharmacol* **837**, 8–24 (2018).
106. Conery, A. R., Rocnik, J. L. & Trojer, P. Small molecule targeting of chromatin writers in cancer. *Nat Chem Biol* **18**, 124–133 (2022).
107. Fang, Z. *et al.* Role of m6A writers, erasers and readers in cancer. *Exp Hematol Oncol* **11**, 45 (2022).
108. García-López, J. *et al.* Large 1p36 Deletions Affecting Arid1a Locus Facilitate Mycn-Driven Oncogenesis in Neuroblastoma. *Cell Rep* **30**, 454-464.e5 (2020).
109. Cheng, Y. *et al.* Targeting epigenetic regulators for cancer therapy: mechanisms and advances in clinical trials. *Sig Transduct Target Ther* **4**, 62 (2019).
110. Buchwald, M., Krämer, O. H. & Heinzl, T. HDACi – Targets beyond chromatin. *Cancer Letters* **280**, 160–167 (2009).
111. Lehrmann, H., Pritchard, L. L. & Harel-Bellan, A. Histone acetyltransferases and deacetylases in the control of cell proliferation and differentiation. *Adv Cancer Res* **86**, 41–65 (2002).
112. Johnstone, R. W. Histone-deacetylase inhibitors: novel drugs for the treatment of cancer. *Nat Rev Drug Discov* **1**, 287–299 (2002).
113. Iizuka, M. & Smith, M. M. Functional consequences of histone modifications. *Curr Opin Genet Dev* **13**, 154–160 (2003).
114. Yang, J., Li, D. & Zhou, J. Histone Deacetylase 6 as a Therapeutic Target in B cell-associated Hematological Malignancies. *Front Pharmacol* **11**, 971 (2020).
115. Bertino, E. M. & Otterson, G. A. Romidepsin: a novel histone deacetylase inhibitor for cancer. *Expert Opinion on Investigational Drugs* **20**, 1151–1158 (2011).
116. Yang, X.-J. & Seto, E. Lysine Acetylation: Codified Crosstalk with Other Posttranslational Modifications. *Molecular Cell* **31**, 449–461 (2008).
117. Narita, T., Weinert, B. T. & Choudhary, C. Functions and mechanisms of non-histone protein acetylation. *Nat Rev Mol Cell Biol* **20**, 156–174 (2019).



118. Glozak, M. A., Sengupta, N., Zhang, X. & Seto, E. Acetylation and deacetylation of non-histone proteins. *Gene* **363**, 15–23 (2005).
119. Ray, S., Lee, C., Hou, T., Boldogh, I. & Brasier, A. R. Requirement of histone deacetylase 1 (HDAC1) in signal transducer and activator of transcription 3 (STAT3) nucleocytoplasmic distribution. *Nucleic Acids Res* **36**, 4510–4520 (2008).
120. Nadiminty, N. *et al.* Stat3 activation of NF- $\kappa$ B p100 processing involves CBP/p300-mediated acetylation. *Proc Natl Acad Sci U S A* **103**, 7264–7269 (2006).
121. Jeong, J. W. *et al.* Regulation and destabilization of HIF-1 $\alpha$  by ARD1-mediated acetylation. *Cell* **111**, 709–720 (2002).
122. Makki, M. S., Heinzel, T. & Englert, C. TSA downregulates Wilms tumor gene 1 (Wt1) expression at multiple levels. *Nucleic Acids Research* **36**, 4067–4078 (2008).
123. De los Santos, M., Zambrano, A., Sánchez-Pacheco, A. & Aranda, A. Histone deacetylase inhibitors regulate retinoic acid receptor beta expression in neuroblastoma cells by both transcriptional and posttranscriptional mechanisms. *Mol Endocrinol* **21**, 2416–2426 (2007).
124. Witt, O., Deubzer, H. E., Lodrini, M., Milde, T. & Oehme, I. Targeting histone deacetylases in neuroblastoma. *Curr Pharm Des* **15**, 436–447 (2009).
125. Xu, M. *et al.* HAND2 assists MYCN enhancer invasion to regulate a noradrenergic neuroblastoma phenotype. *Cancer Research* CAN-22-2042 (2023) doi:10.1158/0008-5472.CAN-22-2042.
126. Forneris, F., Binda, C., Vanoni, M. A., Mattevi, A. & Battaglioli, E. Histone demethylation catalysed by LSD1 is a flavin-dependent oxidative process. *FEBS Lett* **579**, 2203–2207 (2005).
127. Ravasio, R. *et al.* Targeting the scaffolding role of LSD1 (KDM1A) poises acute myeloid leukemia cells for retinoic acid-induced differentiation. *Sci Adv* **6**, eaax2746 (2020).
128. Zhang, W. *et al.* KDM1A promotes thyroid cancer progression and maintains stemness through the Wnt/ $\beta$ -catenin signaling pathway. *Theranostics* **12**, 1500–1517 (2022).
129. Fang, Y., Liao, G. & Yu, B. LSD1/KDM1A inhibitors in clinical trials: advances and prospects. *J Hematol Oncol* **12**, 129 (2019).
130. Maes, T. *et al.* ORY-1001, a Potent and Selective Covalent KDM1A Inhibitor, for the Treatment of Acute Leukemia. *Cancer Cell* **33**, 495-511.e12 (2018).
131. Huang, J. *et al.* G9a and Glp Methylate Lysine 373 in the Tumor Suppressor p53. *Journal of Biological Chemistry* **285**, 9636–9641 (2010).
132. Zheng, Y.-C. *et al.* A Systematic Review of Histone Lysine-Specific Demethylase 1 and Its Inhibitors. *Med Res Rev* **35**, 1032–1071 (2015).
133. Wang, Y. *et al.* LSD1 Is a Subunit of the NuRD Complex and Targets the Metastasis Programs in Breast Cancer. *Cell* **138**, 660–672 (2009).
134. Yang, M. *et al.* Structural basis for CoREST-dependent demethylation of nucleosomes by the human LSD1 histone demethylase. *Mol Cell* **23**, 377–387 (2006).
135. Metzger, E. *et al.* LSD1 demethylates repressive histone marks to promote androgen-receptor-dependent transcription. *Nature* **437**, 436–439 (2005).
136. Augert, A. *et al.* Targeting NOTCH activation in small cell lung cancer through LSD1 inhibition. *Sci Signal* **12**, eaau2922 (2019).

137. Lu, Z. *et al.* ORY-1001 Suppresses Cell Growth and Induces Apoptosis in Lung Cancer Through Triggering HK2 Mediated Warburg Effect. *Front Pharmacol* **9**, 1411 (2018).
138. Taniguchi, Y. The Bromodomain and Extra-Terminal Domain (BET) Family: Functional Anatomy of BET Paralogous Proteins. *Int J Mol Sci* **17**, 1849 (2016).
139. Bhagwat, A. S. *et al.* BET Bromodomain Inhibition Releases the Mediator Complex from Select cis-Regulatory Elements. *Cell Rep* **15**, 519–530 (2016).
140. Yang, H., Wei, L., Xun, Y., Yang, A. & You, H. BRD4: An emerging prospective therapeutic target in glioma. *Molecular Therapy - Oncolytics* **21**, 1–14 (2021).
141. Alver, B. H. *et al.* The SWI/SNF chromatin remodelling complex is required for maintenance of lineage specific enhancers. *Nat Commun* **8**, 14648 (2017).
142. Rahman, S. *et al.* The Brd4 extraterminal domain confers transcription activation independent of pTEFb by recruiting multiple proteins, including NSD3. *Mol Cell Biol* **31**, 2641–2652 (2011).
143. Donati, B., Lorenzini, E. & Ciarrocchi, A. BRD4 and Cancer: going beyond transcriptional regulation. *Mol Cancer* **17**, 164 (2018).
144. Filippakopoulos, P. *et al.* Selective inhibition of BET bromodomains. *Nature* **468**, 1067–1073 (2010).
145. Jiang, G., Deng, W., Liu, Y. & Wang, C. General mechanism of JQ1 in inhibiting various types of cancer. *Mol Med Rep* **21**, 1021–1034 (2020).
146. Ding, W., Zhang, H. & Mei, G. Synergistic antitumor activity of DHA and JQ1 in colorectal carcinoma. *European Journal of Pharmacology* **885**, 173500 (2020).
147. Lee, S. *et al.* Bromodomain and extraterminal inhibition blocks tumor progression and promotes differentiation in neuroblastoma. *Surgery* **158**, 819–26 (2015).
148. Olsen, R. R. *et al.* MYCN induces neuroblastoma in primary neural crest cells. *Oncogene* **36**, 5075–5082 (2017).
149. Jung, I. *et al.* A compendium of promoter-centered long-range chromatin interactions in the human genome. *Nat Genet* **51**, 1442–1449 (2019).
150. Decaestecker, B. *et al.* TBX2 is a neuroblastoma core regulatory circuitry component enhancing MYCN/FOXM1 reactivation of DREAM targets. *Nat Commun* **9**, 4866 (2018).
151. Leone, G. *et al.* Myc requires distinct E2F activities to induce S phase and apoptosis. *Mol Cell* **8**, 105–13 (2001).
152. Liu, Y., Liu, D. & Wan, W. MYCN-induced E2F5 promotes neuroblastoma cell proliferation through regulating cell cycle progression. *Biochem Biophys Res Commun* **511**, 35–40 (2019).
153. Sadasivam, S., Duan, S. & DeCaprio, J. A. The MuvB complex sequentially recruits B-Myb and FoxM1 to promote mitotic gene expression. *Genes Dev* **26**, 474–89 (2012).
154. Luchenko, V. L. *et al.* Histone deacetylase inhibitor-mediated cell death is distinct from its global effect on chromatin. *Mol Oncol* **8**, 1379–92 (2014).
155. Reynolds, C. P., Matthay, K. K., Villablanca, J. G. & Maurer, B. J. Retinoid therapy of high-risk neuroblastoma. *Cancer Lett* **197**, 185–192 (2003).
156. Shelake, S. *et al.* Combination of 13 cis-retinoic acid and tolfenamic acid induces apoptosis and effectively inhibits high-risk neuroblastoma cell proliferation. *Int J Dev Neurosci* **46**, 92–99 (2015).

157. Sonawane, P. *et al.* Metabolic characteristics of 13-cis-retinoic acid (isotretinoin) and anti-tumour activity of the 13-cis-retinoic acid metabolite 4-oxo-13-cis-retinoic acid in neuroblastoma. *Br J Pharmacol* **171**, 5330–5344 (2014).
158. Chlapek, P. *et al.* Enhancement of ATRA-induced differentiation of neuroblastoma cells with LOX/COX inhibitors: an expression profiling study. *J Exp Clin Cancer Res* **29**, 45 (2010).
159. Muppirala, A. N., Limbach, L. E., Bradford, E. F. & Petersen, S. C. Schwann cell development: From neural crest to myelin sheath. *Wiley Interdiscip Rev Dev Biol* **10**, e398 (2021).
160. Bayeva, N., Coll, E. & Piskareva, O. Differentiating Neuroblastoma: A Systematic Review of the Retinoic Acid, Its Derivatives, and Synergistic Interactions. *J Pers Med* **11**, 211 (2021).
161. Altucci, L. & Gronemeyer, H. The promise of retinoids to fight against cancer. *Nat Rev Cancer* **1**, 181–193 (2001).
162. Slavish, P. J. *et al.* Bromodomain-Selective BET Inhibitors Are Potent Antitumor Agents against MYC-Driven Pediatric Cancer. *Cancer Res* **80**, 3507–3518 (2020).
163. Alleboina, S., Aljouda, N., Miller, M. & Freeman, K. W. Therapeutically targeting oncogenic CRCs facilitates induced differentiation of NB by RA and the BET bromodomain inhibitor. *Mol Ther Oncolytics* **23**, 181–191 (2021).
164. Wylie, L. A., Hardwick, L. J., Papkovskaia, T. D., Thiele, C. J. & Philpott, A. Ascl1 phospho-status regulates neuronal differentiation in a *Xenopus* developmental model of neuroblastoma. *Dis Model Mech* **8**, 429–41 (2015).
165. Zimmerman, M. W. *et al.* Retinoic acid rewires the adrenergic core regulatory circuitry of childhood neuroblastoma. <http://biorxiv.org/lookup/doi/10.1101/2020.07.23.218834> (2020) doi:10.1101/2020.07.23.218834.
166. Reiter, F., Wienerroither, S. & Stark, A. Combinatorial function of transcription factors and cofactors. *Current Opinion in Genetics & Development* **43**, 73–81 (2017).
167. Feng, S., Zhou, L., Huang, C., Xie, K. & Nice, E. C. Interactomics: toward protein function and regulation. *Expert Rev Proteomics* **12**, 37–60 (2015).
168. Rabbani, G., Baig, M. H., Ahmad, K. & Choi, I. Protein-protein Interactions and their Role in Various Diseases and their Prediction Techniques. *Curr Protein Pept Sci* **19**, 948–957 (2018).
169. Cheng, F. *et al.* Comprehensive characterization of protein–protein interactions perturbed by disease mutations. *Nat Genet* **53**, 342–353 (2021).
170. Firulli, A. B. A HANDful of questions: the molecular biology of the heart and neural crest derivatives (HAND)-subclass of basic helix–loop–helix transcription factors. *Gene* **312**, 27–40 (2003).
171. Yamagishi, H., Olson, E. N. & Srivastava, D. The basic helix-loop-helix transcription factor, dHAND, is required for vascular development. *J Clin Invest* **105**, 261–270 (2000).
172. Dai, Y.-S. & Cserjesi, P. The basic helix-loop-helix factor, HAND2, functions as a transcriptional activator by binding to E-boxes as a heterodimer. *J Biol Chem* **277**, 12604–12612 (2002).

173. Perillo, B., Tramontano, A., Pezone, A. & Migliaccio, A. LSD1: more than demethylation of histone lysine residues. *Exp Mol Med* **52**, 1936–1947 (2020).
174. Torchy, M. P., Hamiche, A. & Klaholz, B. P. Structure and function insights into the NuRD chromatin remodeling complex. *Cell. Mol. Life Sci.* **72**, 2491–2507 (2015).
175. Hoffmann, A. & Spengler, D. Chromatin Remodeling Complex NuRD in Neurodevelopment and Neurodevelopmental Disorders. *Front. Genet.* **10**, 682 (2019).
176. Ecker, J. *et al.* Reduced chromatin binding of MYC is a key effect of HDAC inhibition in MYC amplified medulloblastoma. *Neuro Oncol* **23**, 226–239 (2021).
177. Naiditch, J. A. *et al.* Mesenchymal change and drug resistance in neuroblastoma. *J Surg Res* **193**, 279–88 (2015).
178. Wang, H., Yang, L., Liu, M. & Luo, J. Protein post-translational modifications in the regulation of cancer hallmarks. *Cancer Gene Ther* (2022) doi:10.1038/s41417-022-00464-3.
179. Bradney, C. *et al.* Regulation of E2A activities by histone acetyltransferases in B lymphocyte development. *J Biol Chem* **278**, 2370–2376 (2003).
180. Kanwal, R., Gupta, K. & Gupta, S. Cancer epigenetics: an introduction. *Methods Mol Biol* **1238**, 3–25 (2015).

## APPENDIX A. CHAPTER 3 ARTICLE

**NOTE:** Navigation with Adobe Acrobat Reader or Adobe Acrobat Professional: To return to the last viewed page, use key commands Alt/Ctrl+Left Arrow on PC or Command+Left Arrow on Mac. For “Next view,” use Alt/Ctrl+Right Arrow on PC or Command+Right Arrow on Mac. See [Preface](#) for further details. If needed, use this link to return to **Chapter 3** after navigating within this appendix.

### Introduction

Word manuscript reused with authors’ permission. Nour A. Aljouda, Dewan Shrestha, Satyanarayana Alleboina, Rachele R. Olsen, Megan Walker, Yong Cheng, Kevin W. Freeman. TCF4 is a key mediator of cell identity and oncogenesis in neuroblastoma, 2023.

### Article

#### **TCF4 is a key mediator of cell identity in neuroblastoma and vulnerable to protein degradation by multiple epigenetic factors.**

Nour A. Aljouda<sup>1</sup>, Dewan Shrestha<sup>1,2</sup>, Satyanarayana Alleboina<sup>1</sup>, Rachele R. Olsen<sup>3</sup>, Megan Walker<sup>1</sup>, Yong Cheng<sup>2</sup>, Kevin W. Freeman<sup>1</sup>.

<sup>1</sup> Department of Genetics, Genomics and Informatics, University of Tennessee Health Science Center, Memphis, USA.

<sup>2</sup> Department of Hematology, St. Jude Children’s Research Hospital, Memphis, TN, USA

<sup>3</sup> Department of Surgery, St. Jude Children’s Research Hospital, Memphis, TN, USA

### Introduction

Neuroblastomas (NBs) are aggressive pediatric tumors that originate from the sympathoadrenal lineage of neural crest cells (NCCs). It encompasses around 7% of all childhood cancers and up to 15% of all pediatric cancer deaths<sup>1,2</sup>. NB arises from a developmental block in NCC differentiation along the sympathoadrenal nervous system lineage (SNS) leading to uncontrolled cell growth<sup>3-5</sup>. The transition between identity states in differentiation is governed by different sets of master TFs that are driven by super-enhancers (SEs), autoregulate their own gene expression, and collectively form core regulatory circuitries (CRC) that drive high expression of downstream lineage-specific genes<sup>6,7</sup>. Two differentiation states exist in NB tumors, one establishing a more proliferative adrenergic (ADRN) cell state and a second establishing a more invasive mesenchymal (MES) cell state<sup>8-10</sup>. Cells have the capacity to shift dynamically between the two states, providing these tumors with remarkable transcriptional plasticity and the ability to escape from therapy<sup>9,11,12</sup>.

High-risk NB often relapse and develop highly resistant disease, and epigenetic regulators are emerging as an option to overcome this resistance<sup>13-15</sup>. Inhibitors of the bromodomain and extra-terminal domain (BET) protein family are promising novel NB therapy<sup>14,16</sup>. NB is one of the most sensitive cancers to BET inhibitors (BETi), however, the reasons for their effectiveness in NB are not fully understood<sup>16,17</sup>. BET proteins are epigenetic readers that promote transcription and are enriched at SEs, large genomic clusters occupied by high levels of TFs and BET-dependent regulatory regions. BET proteins like BRD4 bind acetylated lysine at histones and stabilize transcriptional complexes. Importantly, SEs drive the expression of both oncogenes (e.g., N-Myc) and regulators of cell identity<sup>16,18</sup>. While the sensitivity of NB to BET inhibition was originally attributed to oncogene addiction to MYCN amplification, ectopic MYCN expression did not change the response to BRD4 inhibition suggesting there are other essential targets of BET inhibition in NB<sup>17</sup>.

To discover new NB cell lineage dependency factors, we used BET inhibitors as a tool to identify common targets between diverse NB lines and identified the E-box transcription factor TCF4 (E2-2). TCF4 is a class I basic helix-loop-helix (bHLH) TF that forms homo or heterodimers with itself or other bHLH TFs establishing transcriptional networks that regulate the differentiation of multiple cell types<sup>19,20</sup>. Studies have shown that E-proteins such as TCF4 are the predominant interacting partners of several class II bHLH factors known to be involved in tissue development, cell differentiation, and pathological disease<sup>21-23</sup>. TCF4 is one of the top dimerization partners and transcriptional modulators of TWIST1, a critical determinant of mesenchymal development<sup>23</sup>. Further, TCF4 heterodimerization with proneuronal TFs such as ASCL1 facilitating their ability to regulate the differentiation of neuronal progenitors<sup>21,22,24</sup>. Many studies reported the essential role of TCF4 in EMT<sup>25,26</sup>, human nervous system development<sup>24,27,28</sup>, B and T cell development<sup>29,30</sup>, and regulating neural stem cell (NSC) identity<sup>31</sup>. In cancer, TCF4 was identified as a master transcriptional regulator that sustains malignancy in Blastic Plasmacytoid Dendritic Cell Neoplasm (BPDCN)<sup>32</sup>. Additionally, TCF4 contributes to aggressive bone colonization in human lung carcinoma cell lines<sup>33</sup>, and high expression is associated with worse outcome in acute myeloid leukemia.

Considering the critical effect of class I bHLH proteins on bHLH function, we decided to delineate the unrecognized function of TCF4 in NB oncogenesis and in mediating the different NB lineage states. Here, we report for the first time that TCF4 is a lineage dependency factor in both ADRN and MES NB cells. A comparative analysis of TCF4 and multiple CRC factors identified TCF4 as a critical part of the extended regulator network (ERN) reported to work downstream of CRC TFs to modulate their direct effect in regulating NB pathogenesis and mediating NB identity states. Through immunoprecipitation and mass spectrometry studies, we identified multiple epigenetic factors including histone deacetylases (HDAC), histone acetyltransferases (HAT) and lysine demethylase 1A (KDM1A) that unexpectedly control TCF4 protein stability. These findings highlight the existence of an additional layer of cell identity control mediated by epigenetic regulators through acetylation of a central cell identity factor, TCF4. Histone deacetylase inhibitors (HDACi) and lysine demethylase 1A inhibitors are emerging epigenetic cancer therapies<sup>34-36</sup>. The regulation of TCF4 protein stability by HDACi and

KDM1A inhibitors changes the understanding of the effect and molecular mechanism of HDACs and KDM1A inhibitors in treating NB which should improve their clinical application.

## **Results**

### **Neuroblastoma sensitivity to BET inhibition is due to transcriptional addiction, not oncogene addiction.**

Targeting epigenetic regulators like BET proteins (e.g., BRD4) has emerged as a powerful therapeutic strategy in cancer treatment<sup>16,37</sup>. NB was found to be one of the most sensitive cancers to BETi, which was attributed to MYCN amplification, an oncogenic driver found in ~20% of high-risk NB<sup>16</sup>. However, the ectopic expression of MYCN in NB cell lines did not rescue cells from BETi<sup>17</sup>. To better understand NB response to BET bromodomain inhibition, we transformed primary murine NCCs, the presumed cell of origin of NB into NB via enforcing N-Myc expression<sup>38</sup>. Here, we generated a panel of cell lines at different stages of NB transformation including normal NCCs, NCCs with N-Myc overexpression, NCCs from a pool of p53<sup>-/-</sup> and p53<sup>+/-</sup> mice embryos (p53mixed NCCs), tumor derived cell lines (TDCL) from a NB tumor caused by N-Myc overexpression in wild-type NCCs (N-Myc Tu) and TDCLs from three independent tumors caused by N-Myc overexpression in p53mixed NCCs (N-Myc; p53mixed Tu)<sup>38</sup>. Based on the two current models for BETi cytotoxicity, an oncogene addiction model would predict that primary NCCs would be resistant to BETi while a lineage sensitivity model, also characterized as transcriptional addiction<sup>39</sup>, would predict that all NCC-derived lines would be BETi sensitive. Supporting a lineage sensitivity model, these cell lines that share a common origin but that differ in p53 status, N-Myc expression levels, and stages of transformation displayed equivalent sensitivity to JQ1 treatment (Fig. 1a). NIH3T3 cells were relatively unaffected, showing that JQ1 is not broadly toxic. NCCs were also more sensitive to JQ1 treatment than human NB cell lines (Supplementary Fig. 1a). These data suggest that the shared susceptibility of the NCC-derived lines to JQ1 is lineage-dependent and due to a transcriptional addiction, not oncogene addiction.

### **TCF4 is a critical determinant of JQ1 sensitivity in NB cells**

Recent studies have reported intratumoral heterogeneity within NB tumors, which plays a major role in therapy resistance. These heterogeneous tumors include a majority of more committed ADRN tumor cells and a minority of neural crest cell (MES/NCC)-like cells<sup>11</sup>. Based on finding lineage-dependency in NB we set out to determine if there are TFs whose expression is sensitive to BETi, found across neuroblastomas and shared by both the MES and ADRN NB subtypes.

To accomplish this, we performed genome-wide transcriptional profiling on a panel of NB cell lines with and without MYCN amplification following JQ1 treatment. These included the human Kelly, and IMR-32 NB cell lines (ADRN) and the heterogeneous SK-N-AS cell line that skews MES. We profiled cells using RNA-seq analysis three hours after treatment with JQ1 to enrich for changes due to the primary effects of JQ1. Our data confirm that JQ1 suppresses the expression of multiple lineage factors implicated in NB oncogenesis and maintenance (Supplementary Table 1). We defined candidates for universally shared

factors as (1) a TF that is expressed across all NB cell lines and (2) downregulated after JQ1 treatment (adjusted p value < 0.05, log 2-fold change < -0.58). Since a direct target of BETi would be predicted to have SEs, shared TFs were arranged in a heatmap based on the sum total of SEs identified for each factor in NB cell lines using the super-enhancer database (SEdb)<sup>40</sup>. Although other factors showed a greater fold change after JQ1 treatment, TCF4 has the highest number of SEs identified in multiple NB cell lines compared to other identified shared factors. Moreover, among all candidate genes TCF4 has the highest expression in NB of all cancer types found in the Cancer Cell line Encyclopedia (CCLE) database (Fig.1b and Supplementary Fig.1b). We confirmed that JQ1 and SJ018<sup>41</sup> suppress TCF4 by quantitative PCR (qRT-PCR) in all three human NB cell lines and primary mouse NCCs (Supplementary Fig.1c, and d). Further, we found that this set of transcriptional regulatory genes is highly connected by protein-protein interactions in the STRING database with TCF4 as part of both ADRN and MES CRC hubs (Fig. 1c). TCF4 has been shown to interact with ASCL1 and HAND2, regulators of the ADRN lineage, and TWIST1 a master regulator of the MES fate. Heterodimers formed between TCF4 and the TFs, ASCL1 and TWIST1, have been demonstrated to provide lineage-specific differentiation from embryonic stem cells<sup>21,23</sup>. To validate TCF4 interactions in NB, we purified the endogenous TCF4 by immunoprecipitation (IP) and showed using IP-Western blot (IP-WB) that TCF4 interacts with ASCL1, HAND2, and TWIST1 in Kelly and SK-N-AS NB cell lines (Fig. 1d). Our findings identify TCF4 as a promising shared TF regulated by SEs across both ADRN and MES identity states with a potential role in regulating those identity states.

### **TCF4 is essential for NB Viability**

To determine the consequences of TCF4 knockdown (KD), we transduced two representatives NB cell lines Kelly (ADRN) and SK-N-AS (MES) with three doxycycline-inducible shRNA expression vectors targeting TCF4 (sh#1, sh#2 and sh#3). An empty vector harboring only (Tet-pLKO-puro) served as a control throughout the study. Quantitative PCR (qPCR) and western blots revealed that TCF4 was significantly downregulated in the established stable cell lines after treatment with doxycycline (Dox), (Fig. 2a and b). Loss of TCF4 in both cell lines led to a significant decrease of cell proliferation and colony formation ability over time compared with the control (Fig. 2c and 2d, Supplementary Fig. 2a and b). Moreover, we show a significant G<sub>1</sub> arrest and a decrease in S-phase in both cell lines upon TCF4 KD (Fig. 2e and Supplementary Fig. 2c). Further TCF4 loss produced a marked induction of apoptosis in Kelly and SK-N-AS cell lines as confirmed by Annexin V staining (Fig. 2f and Supplementary Fig. 2d) and PARP cleavage as detected by western blotting (Supplementary Fig.2e). Collectively, our data suggest that both NB identity states, ADRN and MES, depend on TCF4 for growth and survival.

To interrogate TCF4-dependent JQ1 effects, SK-N-AS cells were transfected with a TCF4 cDNA Clone. Three different clones overexpressing TCF4 were expanded and exposed to increasing JQ1 doses for four days (Supplementary Fig.2f). JQ1-induced apoptosis was blocked in cells ectopically expressing TCF4 at doses as low as 100 nM (Fig. 2g), indicating that TCF4 is a sensitive and central component of JQ1 toxicity in NB.



### **TCF4 knockdown suppresses tumor growth in vivo**

Next, the knockdown of TCF4 in NB cells in a soft agar colony assay showed that colonies were smaller and significantly fewer in number for the TCF4 KD cells compared to the controls (Fig. 3a and b). Given our *in vitro* findings that TCF4 loss blocks NB growth and transformation, we next examined the effect of TCF4 KD on NB subcutaneous xenograft tumors. In these experiments,  $2 \times 10^6$  Kelly shTCF4 #2 and SK-N-AS shTCF4 #2 cells were implanted in the subcutaneous flank region of female SCID mice separately. One week after the injection, the mice were randomized into two groups (+Dox and -Dox). We found that decreased expression of TCF4 in Kelly and SK-N-AS cells delayed tumor growth in vivo as reflected in the mean tumor volume over time compared to the control using both cell lines (Fig. 3c and d). Tumor tissues were subsequently analyzed by western blotting for TCF4 protein expression. As shown in (Fig. 3e), Dox treatment markedly decreased TCF4 expression in tumors, whereas no significant change in TCF4 protein expression was observed in the absence of Dox in control mice. Therefore, these results confirm our *in vitro* observations and further indicate TCF4 as a critical lineage dependency factor in NB.

### **TCF4 regulates genes critical for NB pathogenesis and cell identity states**

Multiple studies have demonstrated the role of the CRC TFs in the establishment of cell identity and fate in NB<sup>7,11,42</sup>. Given our previous data highlighting TCF4 as NB cell dependency gene, we propose that TCF4 plays a critical role in modulating and facilitating CRC TFs function. To explore this, we first performed RNA-seq analysis after *TCF4 KD* in Kelly and SK-N-AS cells to identify TCF4-regulated genes. RNA-seq analyses indicate that TCF4 loss activates distinct but overlapping gene expression profiles between both cell lines (Supplementary Table 2). Supporting the TCF4 KD functional analysis described above, Gene Set Enrichment Analysis (GSEA) revealed negative enrichment for the hallmark gene sets involved in G2/M checkpoint, E2F targets, mitotic spindle, and MYC targets (FDR < 0.01, Supplementary Fig.3a and b).

We next examined the genome-wide occupancy of TCF4 by chromatin immunoprecipitation followed by (ChIP-seq) analysis in Kelly and SK-N-AS cells. The integration of ChIP-seq and RNA-seq data for TCF4 KD revealed the individual target genes directly regulated by TCF4 in both NB cells (Fig. 4a, supplementary table 3). In accordance with the putative role of TCF4 in ADRN and MES cell identity, we find enrichment for the genes of the proneuronal subtype and MES subtype amongst the TCF4 regulated targets. For instance, in Kelly (ADRN) cells, TCF4 controls factors involved in catecholamine biosynthesis and expressed in the sympathoadrenal precursors that are downstream targets of MES factors (TWIST1, PRRX1, and SNAI2) and the ADRN factor HAND1 (Supplementary Fig.3c). Our integrative analysis of TCF4 KD in SK-N-AS finds TCF4 contributes to NB oncogenesis, regulates sympathetic neurogenesis factors (HAND1, INSM1, NEUROD1, SOX11, DBH), and MES EMT markers such as SNAI2 ((Fig. 4a, Supplementary Table.3). TCF4 also regulates many genes involved in driving proliferation, like E2F-FOXM1 core members, the cell cycle regulatory DREAM complex genes, and genes of distinct oncogenic pathways required for NB proliferation (CDKN1A, E2F1, E2F2, FOXM1, MYBL2). Another cell cycle regulator EZH2 involved in epigenetic silencing of tumor-suppressor genes by H3K27 methylation<sup>43</sup> was also identified as a

putative direct target of TCF4 (Supplementary Table.3). Enrichr<sup>44</sup> analysis in SK-N-AS suggests that TCF4 regulates genes downstream of EZH2, E2F2, MYCN, and HAND2 (Supplementary Fig.3d).

Next, using H3K27ac as a marker for active chromatin we confirmed the enrichment of TCF4 binding to active promoter and enhancer regions (Fig. 4b). We then performed HOMER motif analysis using peaks bound by TCF4 in both NB cell lines. Consistent with previous evidence suggesting that TCF4 proteins heterodimerize with several ADRN and MES TFs, regions bound by TCF4 were also enriched for several CRC factors (Fig. 4c). We also recognized enrichment of the E2F motif at TCF4 binding sites in both Kelly and SK-N-AS cells (Fig. 4c). These data suggest that TCF4 regulates cell cycle progression by direct transcriptional regulation of E2F-FOXM1 and their target genes. Moreover, we found that most of the NB specific regions of open chromatin overlapped with TCF4 binding peaks in Kelly and SK-N-AS cells (Supplementary Fig. 4a, b, and c). Finally, we explored the putative role of TCF4 in the adrenergic CRC in Kelly cells. Here, we integrated the ChIP-seq tracks for TCF4 with published data reported for ADRN CRC factors in the Kelly NB cells. As shown in (Fig. 4d) several factors, including MYCN and HAND2, are enriched around TCF4 binding sites in Kelly cells. To further explore the relation between TCF4 and MYCN in-depth, we integrated previously published MYCN ChIP-seq data<sup>8,45,46</sup> with our TCF4 ChIP data. We observed a strong MYCN intensity signal at TCF4 binding sites. We also found that many TCF4 binding sites are shared with MYCN, both at promoters at enhancers, which are sites of MYCN enhancer invasion and associated with the MYCN oncogenic program (Supplementary Fig. 4a). We discovered that TCF4 peaks that overlap with MYCN peaks at SEs in Kelly and SK-N-AS cells show enrichment for many CRC TFs among which HAND2, TBX2 and MYCN are at the top of the list of enriched factors as identified by ChIP Enrichment Analysis (ChEA)<sup>44</sup>(Supplementary Fig. 4d and 4e). These data suggest collaborative roles among these factors and TCF4 in regulating NB gene expression programs and potentially a physical interaction. However, using a published data set of CRC TFs (such as PHOX2B, GATA3, and HAND2) binding peaks in Kelly cells, we did not see a strong overlap of TCF4 peaks summits with binding sites of these CRC factors at the TCF4 locus (Supplementary Fig. 4b). Moreover, in our RNA-seq data, we do not observe a strong effect of TCF4 KD on the expression of known CRC members (Supplementary Table 2). Collectively, these data suggest that TCF4 is not a canonical CRC member but is regulated in parallel to these CRCs and facilitates their downstream effects. Hence, we propose that TCF4 is a member of the extended regulatory network (ERN), reported as SE-associated genes whose enhancers and promoters are bound by the CRC TFs and work downstream of these factors to modulate their effect<sup>6</sup>.

### **TCF4 interactome in NB cell lines**

Next, we performed TCF4 immunoprecipitation coupled to mass spectrometry (IP-MS) using the total cellular extracts from Kelly and SK-N-AS cells to determine the TCF4 interactome in NB. Interacting proteins present in at least two purifications of the TCF4 protein were included (Supplementary Table 4, see the 'Materials and methods' section for inclusion criteria). A total of 436 TCF4 potential interactors were identified in Kelly cells, and 451 interactors in SK-N-AS, among which 294 proteins (~60% of overlap) were found between both lines. TCF4 interaction network in NB compromises many ADRN and MES

CRC TFs and multiple chromatin remodeling complexes, such as the nucleosome remodeling and deacetylase (NuRD) complex and the SWI-SNF complex (Fig. 5). Interestingly, there was a strong overlap between TFs identified as part of the TCF4 interactome in NB cell lines and motifs enriched in our TCF4 ChIP-seq data (Fig. 5).

Though TCF4 is not directly targetable, we observed multiple therapeutic targets that complex with TCF4 (Fig. 5). HDAC 1 and 2 were present in the TCF4 (IP-MS). Acetylation of bHLH factors was previously reported to affect the preferred heterodimerization partners of the TCF4 homolog TCF3<sup>47</sup>. In contrast to our expectations of HDAC inhibition leading to change in TCF4 interactions, our experiments revealed that treating Kelly or SK-N-AS cells with the pan-HDAC inhibitor trichostatin A (TSA), led to loss of TCF4 protein 24 hours post-treatment (Fig. 6a). Degradation was prevented if cells were treated with the histone acetyltransferase (HAT) inhibitor garcinol which inhibits both p300 and PCAF (Fig. 6a). P300 is the only HAT identified in the (IP-MS) suggesting it is the primary candidate for generating the destabilizing acetylation. The class II HDACi TMP269 had minimal effects on TCF4 (Suppl Fig. 5a), while the Class I HDAC specific inhibitor romidepsin, which preferentially targets the HDACs found in the (IP-MS) HDAC1 and 2 also caused degradation of TCF4 in Kelly and SK-N-AS cells (Fig. 6b). Since HDACi can affect gene transcription, we performed RT-PCR and found no significant change in TCF4 gene expression at 24 hours (Supplementary Fig. 5b), when loss of TCF4 protein is already observed (Fig. 6b). The proteasome inhibitor MG132 blocked the loss of TCF4 which confirms that the effects of HDAC inhibition are post-translational and based on protein stability (Supplementary Fig. 5c). SK-N-AS cells overexpressing TCF4 reduced the effects of romidepsin (Fig. 6c and Supplementary Fig. 5d) indicating that TCF4 is central to the effects of the romidepsin in SK-N-AS. Pan-cancer TCF4 expression significantly correlated with susceptibility to multiple HDAC inhibitors as determined using the Cancer Dependency Map (DepMap)<sup>48</sup> (Supplementary Fig. 5e). In previous work, we found that disruption of the adrenergic CRC by silencing of ASCL1 or using the BETi JQ1 could synergize with the differentiating agent all-trans retinoic acid (ATRA) to promote differentiation<sup>49</sup>. Therefore, we tested whether romidepsin could synergize with ATRA by disrupting the developmental block caused by the CRCs. The two agents were synergistic in killing NB cell lines and observed a significant increase in cell death when romidepsin was combined with ATRA (Fig. 6d and supplementary Fig. 5f).

There are multiple layers of crosstalk between HDACs and KDM1A in epigenetic control and transcriptional regulation<sup>50</sup>, thus we assessed if KDM1A, identified in the IP-MS, also has a role in regulating TCF4 protein stability. We found that ORY-1001, a clinically relevant KDM1A inhibitor<sup>51</sup> similarly caused reduced TCF4 protein stability (Fig. 6e). Further, that garcinol blocks both HDAC and KDM1A inhibition indicating that the HAT activity of p300 is epistatic to HDACs and KDM1A (Supplementary Fig. 5g). Similar to our romidepsin studies we found that ORY-1001 was synergistic with ATRA in Kelly cells (Fig. 6f and Supplementary Fig. 5h). We have identified that TCF4 is a critical factor in NB by being essential for the downstream effects of the key CRC ADRN and MES programs and unexpectedly that TCF4 is central to the effects of multiple epigenetic factors through their regulation of TCF4 protein stability.

## **Discussion:**

Neuroblastoma tumors display startling heterogeneity, compromising populations of both the lineage ADRN and MES cells<sup>11</sup>. This heterogeneity provides NB with high transcriptional plasticity allowing tumors to escape therapeutic treatment or relapse<sup>9,12</sup>. NB identity is determined by lineage-specific transcription factors, driven by cell type specific SEs<sup>12,52</sup>. In this work, we identified the E-box transcription factor TCF4 not reported previously to be implicated in NB as a critical NB dependency gene, that is shared across the different NB lineage states. Our functional analysis demonstrated that loss of TCF4 dramatically decreases cell proliferation, induces apoptosis, and inhibits tumor growth *in vivo*.

To determine how TCF4 regulates these oncogenic programs we integrated our TCF4 ChIP-seq data and publicly available data for CRC ADRN factors in Kelly cells and found a high concordance of DNA occupancy by TCF4 with HAND2, MYCN, and TBX2 proteins. To test whether TCF4 and CRC TFs physically interact, we performed IP-MS analysis and identified TCF4 protein-protein interactions from two NB cell lines. The analysis showed enrichment in the network of multiple ADRN and MES NB CRC factors, including TWIST1, HAND2, MYCN, and TBX2. A recent study found that when MYCN is highly expressed, it works as an “enhancer invader” and reinforces the gene expression program of the ADRN CRC. Their work indicated that TWIST1 and HAND2 factors collaborate with MYCN to drive oncogenic enhancer-driven transcription<sup>53</sup>. Our ChIP-seq and IP-MS data further indicate TCF4 as a collaborative factor involved in facilitating TF-DNA binding for TWIST1 and or HAND2 with MYCN to regulate downstream oncogenic programs. GSEA after TCF4 silencing in NB lines showed TCF4 significantly drives gene sets enriched for EMT, E2F targets, Myc targets, and G2M checkpoint pathways. Both E2F and MYCN play crucial roles in driving NB tumor cell proliferation<sup>54</sup>. We found that TCF4 KD in Kelly and SK-N-AS cells caused downregulation in the expression of E2F genes, and genes kept silenced by the DREAM complex during quiescence including FOXM1 and MYBL2. E2Fs, FOXM1 and MYBL2 coordinately regulate multiple stages of cell cycle progression including the G2M transition<sup>55</sup>. The E2F family of transcription factors are critical regulators of cell cycle and are known MYC targets<sup>56</sup>. We have previously shown that MYCN overexpression in murine NCCs generates NB and causes an increase in expression of E2Fs, MYBL2 and FOXM1, which is also a signature of MYCN-amplified NB<sup>38</sup>. MYBL2 and FOXM1 are important oncogenic factors with MYBL2 known to coregulate MYCN in NB<sup>57,58</sup>. Further, recent work identified TBX2 as a member of the ADRN CRC that similarly regulates E2Fs, MYBL2 and FOXM1<sup>59</sup>. Our results propose a role for TCF4 in regulating FOXM1/E2F-driven gene regulatory networks controlling proliferation in cooperation with MYCN, TBX2 and TCF4 dimerization partners HAND2 and TWIST1.

Our TCF4 IP-MS data identified a comprehensive list of bHLH TFs known to regulate NB cell identity. Also, we observed a remarkable concordance of DNA occupancy and physical interaction between TCF4, MYCN, HAND2, GATA3 and TBX2 in Kelly cells. However, we did not see a strong overlap of TCF4 peak summits with binding sites of these CRC TFs at the TCF4 locus. Further, we did not observe a broad loss of CRC member’s gene expression when TCF4 is silenced. Collectively, our data suggest that TCF4 is not a

canonical CRC member, hence we propose that TCF4 is part of the extended regulatory network<sup>6</sup> which serves as a downstream effector of CRC TFs via its ability to interact with the CRC factors to allow cooperative binding and directly or indirectly regulate identity states. Additionally, our IP-MS analysis revealed multiple TCF4 interacting partners implicated in a wide range of essential epigenetic regulatory processes. From this, we have determined that multiple promising epigenetic therapies (BETi, HDACi and KDM1A inhibitors) converge on the bHLH factor TCF4. Targeting of epigenetic writers and erasers for treating malignancies has focused on their role in modifying the histone code as a central mechanism of action. Although acetylation of non-histone proteins, such as p53, is recognized as a contributing factor in therapy<sup>60</sup>. Despite the potential of HDACi in cancer therapy, why certain cancers are especially vulnerable to HDACi is not well understood. A pan-cancer study that tested two HDAC inhibitors (romidepsin and vorinostat) across 18 cancer cell lines from 8 different cancer types found that the therapeutic effects of HDACi poorly associated with global histone changes suggesting that non-histone targets contribute to their effect<sup>61</sup>. Our finding that TCF4 protein stability is affected by HDACs and KDM1A inhibitors identifies an additional vulnerability of NB to these inhibitors. Clinically, the broader HDAC inhibitor panobinostat was tested in combination with ATRA in 64 pediatric cancer patients with a diverse set of cancers. Remarkably the only complete response was observed in 1 of 4 NB patients showing the promise of this therapy for NB<sup>62</sup>. Our work suggests that loss of TCF4 protein expression is an important biological readout for determining the efficacy of these epigenetic inhibitors in treating patients. We have identified a new level of cell identity regulation by epigenetic inhibitors that has implications in the application of these therapies in cancer and interestingly, TCF4 gene expression significantly correlates with cell line sensitivity to HDAC inhibitors pan-cancer (Supplementary Fig. 5e). Across multiple cancer types, understanding the contribution of TCF4 to the therapeutic responses of patients toward certain epigenetic therapies is an important new avenue of research.

## **Materials and methods**

### **Cell lines**

All neuroblastoma cell lines were obtained from ATCC. Kelly, SK-N-AS and IMR32 neuroblastoma cells were cultured in RPMI, DMEM or EMEM respectively, supplemented with 10% fetal bovine serum (Atlanta Biologicals). Primary mouse NCC lines were isolated and cultured as described previously<sup>38,63</sup>. Mouse NCCs were grown in CDM, which contains Iscove's modified Dulbecco's medium/Ham's F-12, 1X chemically defined lipid concentrate (GIBCO), 1X mg/ml Insulin-transferrin-selenium (Thermo Fisher Scientific), 450 mM onothioglycerol (Sigma), 5 mg/ml purified BSA (Sigma), 7 mg/ml Insulin (Thermo Fisher Scientific), and penicillin/streptomycin (Invitrogen). Culture dishes were coated with fibronectin (250 mg/mL) (Corning). The medium was supplemented with EGF (R&D) and FGF2 (R&D) to modulate growth factor signals and SB431542 (SB) (Sigma) as a TGF-beta signaling pathway suppressor.

### **RNA-Seq Library Preparation and Sequencing**

For RNA-Seq on the Kelly, SK-N-AS, IMR32 human neuroblastoma cell lines, total RNA was extracted using the RNeasy Mini Kit (QIAGEN). cDNA libraries were sequenced

using the Illumina NovaSeq platforms, which utilize a paired-end 150 bp sequencing strategy (Novogene). STAR (version 2.5.3a)<sup>64</sup> with default setting was used to map the sequencing data for cell lines (Kelly, SK-N-AS, and IMR32) using human reference genome (hg38). Gene abundance count was calculated using featureCounts (subread version 1.5.1)<sup>65</sup>. The parameter '-p' was used for featureCounts to get fragment-based counts instead of reads. Gencode v41 (hg38) was used to get the gene level quantification. DeSeq2<sup>66</sup> from R-package was used to identify differentially expressed genes. Low-coverage genes were removed if the median value for the gene is less than 0. Batch information along with treatment conditions was used as design matrix. Protein-protein interaction (PPI) networks among the significantly up/downregulated genes were determined by a web-based online tool, STRING V11.0 (<http://string-db.org>). Genes differentially expressed after knockdown of each transcription factor were selected using the following criteria: adjusted p value < 0.05, log 2-fold change < -0.58 or > 0.58. DeSeq2 normalized data was used as input for GSEA (version 4.2.2)<sup>67</sup> for gene ontology analysis against the hallmark database (version 7.5.1). Human Ensembl Gene MSigDb (version 7.5.1) was used for ChIP platform parameter and permutation was carried out based on gene set.

### **Doxycycline-inducible shRNA systems**

The shRNA sequences were designed according to the TRC1 library (Sigma-Aldrich, TRCN0000274214, TRCN0000274213, TRCN0000274161 referred in the manuscript as sh1, sh2, sh3 respectively) targeting TCF4. The shRNAs were cloned into the lentiviral vector Tet-pLKO-puro (Plasmid #21915) at the Age I and EcoR I digestion sites. Each individual shRNA vector was co-transfected into 293T cells with the 2nd generation lentiviral systems and seeded into 10 cm plate 24 h before transfection, using the FuGENE 6 transfection reagent (Roche) according to the manufacturer's instruction. The media was changed 24 h after transfection. 48 h after transfection supernatants containing lentivirus was collected and filtered through a 0.45 mm nitrocellulose filter (Thermo). The Kelly and SK-N-AS cells were infected with lentivirus in the presence of polybrene (4 µg/mL:Millipore). Selection was performed by adding puromycin (0.5 µg/mL for Kelly cell line; 1 µg/mL for SK-N-AS neuroblastoma cell line) 48 hours after the infection.

### **Real-time quantitative PCR.**

Total RNA was extracted using RNeasy Mini Kit (QIAGEN) according to the manufacturer's instructions. On-column DNase treatment was performed, and concentration was determined with Nanodrop (Thermo Scientific). cDNA synthesis was performed using High-Capacity cDNA Reverse Transcription Kit (Thermo Scientific). Real-time quantitative polymerase chain reaction (qPCR) was performed using the TaqMan Real-Time PCR Master Mix according to supplier recommendations. The housekeeping gene B2M was used for normalization. The following human probes: Hs00972432\_m1 for TCF4, and Hs00187842\_m1 for B2M, and the mouse probes: Mm00443210\_m1 for TCF4, and Mm00437762\_m1 were used.

### **Western blot analysis**

Cells were lysed in RIPA Buffer (#J62524, Thermo Scientific) with Halt Protease and phosphatase Inhibitor Cocktail (#1861281). Equal amounts of protein were resolved by

SDS-PAGE gel after boiling for 5 min at 95 °C with Laemmli sample buffer (Bio-Rad), then blotted onto a PVDF membrane (Bio-Rad). Membranes were blocked with 5% nonfat milk for 1 h followed by incubation with primary antibody diluted in 2.5% nonfat milk overnight at 4 °C. Next day, the membranes were washed with washing buffer (PBS-Tween 0.1%) and incubated with secondary antibody for 1 h at room temperature. HRP-labeled anti-rabbit (7074, Cell Signaling Technologies) and anti-mouse (7076P2, Cell Signaling) antibodies were used. Proteins were visualized by enhanced chemiluminescence (ProSignal® Femto ECL Reagent). Immunoblotting was carried out with the following antibodies: TCF4 (Abcam, ab217668), Cleaved PARP (Cell Signaling Technologies, #9661), and  $\beta$ -actin (Cell Signaling Technologies, #8457).

### **Co-immunoprecipitation and western blotting analysis**

Total protein was extracted from Kelly and SK-N-AS cells using Pierce IP lysis buffer (Thermo Fisher Scientific #87787) supplemented with Halt Protease and phosphatase Inhibitor Cocktail (#1861281). Whole cell lysate was incubated with TCF4 antibody (Abcam, ab217668), or Normal Rabbit IgG (CST #2729) with rotation overnight at 4°C. Next day, 50  $\mu$ l of Pierce Protein A/G Magnetic Beads (Thermo Fisher Scientific # 88803) were moved to a clean tube and washed three times with 500  $\mu$ l of 1X Pierce lysis buffer. The overnight cell lysate was mixed with 50ul of the pre-washed magnetic beads and incubated with rotation for 2 hours at 4°C. Next, beads were separated from the lysate using a magnetic separation rack, the beads were then washed three times with 500  $\mu$ l of 1X IP lysis buffer. The IP products were eluted by 60  $\mu$ l 4X SDS sample buffer and boiled at 95°C for 5 min. 15  $\mu$ l of each sample was used for western blotting detection and 10% cell lysate was used as Input. Proteins were separated by SDS-PAGE gel. The following antibodies were used to detect the protein-protein interaction, TCF4 (Abcam, ab217668), ASCL1 (Santa Cruz, #sc-390794), HAND2 (Abcam, ab200040), and TWIST1 (Abcam, ab50887).

### **CyQuant Assay**

Neuroblastoma cells were seeded into 96-well plates (10000 cells/well) and plated in 100 $\mu$ l media per well. 24 hours after plating, drugs were diluted to a 2x concentration in plating media and then 100 $\mu$ L was added to each well. Plates were incubated for 4 days and then submitted to CyQuant Cell Direct Proliferation Assay (Thermo Fisher Scientific) according to the manufacturer's instructions and read with Cytation 5 plate reader (BioTek).

### **Colony formation assays**

For colony formation assays, 50000 viable Kelly and SK-N-AS cells with or without TCF4 KD were seeded in a 6-cm dish. Cells were incubated for 10 days in media only or Doxycycline, changing the media every 2 days. After an initial evaluation under the microscope, the colonies were stained with 0.05% crystal violet.

### **Annexin V/PI flow cytometry assay**

Kelly and SK-N-AS cells transduced with shRNA against TCF4 (Sh1, Sh2, Sh3) were treated with 1  $\mu$ g/ml doxycycline for 5 and 7 days respectively. Control cells (media with puromycin only) were also included in this experiment. After the incubation, cells were

collected and washed twice with cold PBS then cells were re-suspended in 1 mL of 1X binding buffer (cell concentration  $1 \times 10^6$  cells per mL). Next, 100  $\mu$ l of cell suspension was transferred to a flow tube, the cells were incubated with FITC-Annexin V and PI for 15 min. Annexin V-FITC/PI detection kit was obtained from Biolegend (cat # 640914). Cells were then analyzed by Flow cytometry.

#### **Ectopic expression of TCF4**

For TCF4 overexpression, TCF4/E2-2 cDNA ORF Clone (Sino Biologicala # HG12096-CF) was transfected into SK-N-AS cells using FuGENE 6 transfection reagent (Roche). Forty-eight hours after transfection, DMEM media with the selection antibiotic Hygromycin (500 $\mu$ g/ml) was added and replaced every three days. After one month, antibiotic-resistant clones were generated and expanded. TCF4 overexpression was confirmed by real-time PCR.

#### **Colony formation in soft agar**

Kelly and SK-N-AS cells transduced with shRNA against TCF4 (Sh2, Sh3) were split and seeded (5000 cells/well) in a 0.30% noble agar (Sigma) mixed with culture medium (on the top of 0.6% noble agar with medium) in 6-well plates. Cells were cultured at 37C for another 3 weeks. Cells were incubated for 21 days in media only or Doxycycline, changing the media every 2 days. Colonies were photographed (Nikon, Microphot FX) by treating the plates with 0.1% crystal violet and subsequent gentle washing with PBS.

#### **In vivo tumor models**

This study was performed in strict accordance with the recommendations in the Guide for the Care and Use of Laboratory Animals of the National Institute of Health. All animal experiments were approved by the Institutional Animal Care and Use Committee (IACUC) at UTHSC. 6–8 weeks old female SCID mice were subcutaneously injected in the flanks at  $2 \times 10^6$  cells per mouse in 100 $\mu$ l total volume. Kelly and SK-N-AS cells transduced with shRNA against TCF4 (Sh2) were injected in a 1:1 mix of cells and Matrigel (BD Biosciences). One week after the injection mice were randomly assigned to the control (standard diet) or the treatment (15 mg/kg body weight (BW) of doxycycline) groups. Tumors were measured by calipers at least twice weekly, and tumor volume was calculated using the formula  $1/2 * (\text{length} * \text{width}^2)$ . Animals were sacrificed according to institutional guidelines when tumors reached ~2000 mm in length or width.

#### **Chromatin immunoprecipitation ChIP-Seq**

A total of  $3 \times 10^7$  cells were crosslinked with 1% formaldehyde (Sigma) while shaking for 10 min at room temperature. Crosslinking was quenched with 125 mM glycine (Sigma #G8898). DNA was sheared by sonication to obtain approximately 500 bp. To pre-bind antibodies to protein A/G agarose beads (Thermofischer # 20423), we rotated to 50 $\mu$ l protein A/G agarose bead slurry mixed with 10  $\mu$ g of Anti-TCF4 antibody (Abcam, ab217668), or anti-H3K27ac (ab4729) overnight. Next day, chromatin fragments were immunoprecipitated by mixing the pre-cleared chromatin with the antibody:bead complex and rotating for 4 h at 4°C. protein A/G bound complexes were washed 6 times, once with (20 mM Tris-HCl pH8, 50mM NaCl, 1% Triton X-100, 0.1% SDS, 2 mM EDTA), twice with (20 mM Tris-HCl pH8, 500mM NaCl, 1% Triton X-100, 0.1% SDS, 2 mM EDTA), once with (10 mM Tris-HCl pH8, 250 mM LiCl, 1% NP40, 1% Deoxycholic acid, 1 mM



EDTA), twice with TE pH 8.0 and finally resuspended in 100  $\mu$ l TE pH8. Total chromatin samples were processed in parallel as input reference.

To each DNA sample add 370 Mm NaCl, RNase, and 0.26mg/mL Proteinase-K. Reverse cross-link was performed overnight at 65°C. Final DNA purification was performed with Qiagen MinElute PCR Purification kit (# 28004). ChIP DNA was used to generate ChIP-Seq libraries. The sequencing of the TCF4 ChIP-Seqs was performed on Illumina PE150 sequencer (Novogene). BWA-MEM (version 0.7.16a)<sup>68</sup> with default parameters were used to map sequence data to human genome (hg38). MACS2 (version 2.2.1)<sup>69</sup> was used to call the peaks. For TCF4 ChIP-Seq data IDR (version 2.0.3) peaks were called with idr threshold of 0.05. For all the peaks called, the peak regions were further filtered out removing the blacklisted regions. Homer motif analysis was carried out using IDR peaks generated from TCF4 ChIP-Seq data. The region's size of 200 and allowed mismatch of 2.

### **Target Genes**

TCF4 ChIP-seq data along with promoter capture Hi-C data was integrated with RNA-seq data to identify the target genes. Differentially expressed genes with a foldchange threshold of 1.5 and pvalue < 0.05 were only used for this analysis. If the promoter region or gene body overlaps with the coordinates of the TCF4 peak region or if based on promoter capture Hi-C data if the region overlapping with TCF4 peaks have interaction with the genes, those genes are defined as the target genes.

### **ATAC-Seq Data Processing:**

BWA-MEM (version 0.7.16a)<sup>68</sup> with default parameters were used to map sequence data to human genome (hg38).

### **Promoter capture Hi-C**

Adrenal gland associated promoter capture Hi-C interaction data was downloaded from Jung et. al<sup>70</sup> Significant interactions between promoter-other and promoter-promoter provided in supplementary Table 3 and 4 were used.

### **Genomic Annotation**

Promoters were defined based on 1000 bp upstream of the transcription start site (hg38 gencode v41) based on strand information. Enhancers for respective cell lines were defined based on the overlap between H3K27ac and H3K4me1 peaks using bedtools intersect<sup>71</sup>.

### **Public Data**

ATAC Seq data (SRA: SRR10215668, SRR10215669) and H3K4me1 data (SRA: SRR10217411, SRR10217413) for KELLY was downloaded from NCBI GEO<sup>45</sup>. ChIP-seq data for GATA3, ISL1, HAND2, n-Myc, PHOX2B and TBX2 data for KELLY was downloaded from NCBI GEO<sup>8</sup>. ATAC Seq data (SRA: SRR10215682, SRR10215683), H3k4me1 and HK3K27ac (SRA: SRR10217389, SRR10217391, SRR10217393) data for SKNAS was downloaded from NCBI GEO<sup>45</sup>.

### **Data availability**

RNA, ChIP and ATAC sequencing data are available online through the Gene Expression Omnibus (GEO) portal. The accession number of this SuperSeries is GSE222212, GSE222212, GSE222214.

### **Immunoprecipitation-mass spectrometry analysis**

Kelly and SK-N-AS cell lines were culture to 90% confluency in 15 cm dishes per biological replicate prior to harvesting. Immunoprecipitation of TCF4 was performed as described earlier in the Co-immunoprecipitation method section. IP-MS protocol was performed using 1 mg of whole cell lysate immunoprecipitations in triplicate plus IgG control. Antibody: bead complex samples were sent to the University of Tennessee health science center Proteomics Core for Label Free Quantification (LFQ) mass spectrometry protein identification. We performed On-bead Trypsin Digestion by add 1  $\mu$ L of 1  $\mu$ g/  $\mu$ L MS grade trypsin. Mix gently and incubate with the sample overnight at 37 °C while rocking on a nutator. Mass spectrometry protein identification results were analyzed with Proteome Discoverer 2.4, (Thermo Fisher). Peptide Abundance represents MS Peak Area, normalization mode is the total peptide amount, and the protein abundance is the summed abundances of assigned peptides. TCF4 interaction partners are included in the final list (Supplementary Table 4) if they are present in at least two out of three TCF4 complex purifications and show at least two-fold enrichment by protein abundance in the TCF4 purified sample over the control sample. Cytoskeletal and cytoplasmic proteins (Uniprot) were removed.

### **Statistical analysis**

We used the unpaired, two-tailed Student t test to determine the statistical significance using GraphPad Prism 9.0 software. A p-value of less than 0.05 was considered statistically significant.

### **AUTHOR CONTRIBUTIONS**

Conception and design, K.W.F. and N.A.; development of methodology, K.W.F., and N.A.; experimental design, K.W.F., N.A., M.W.; performing experiments, N.A., S.A., R.O.; analysis and interpretation of data (e.g., statistical analysis, sequencing data, computational analysis), K.W.F., N.A., D.S., Y.C.; writing of the manuscript, K.W.F. and N.A.; review, and/or revision of the manuscript, K.W.F., N.A., M.W., R.O., D.S., Y.C.; administrative and technical support (reporting or organizing data and constructing databases), N.A., and D.S.; study supervision, K.W.F. and N.A.

### **ACKNOWLEDGMENTS**

The authors disclose receipt of the following financial support for the research, authorship, and/or publication of this article: US National Institutes of Health (R073239038 to K.W.F.). The content is solely the responsibility of the authors and does not necessarily represent the official views of the NIH. We thank the staff of the Molecular Resource Center (MRC) Core at The University of Tennessee Health Science Center (UTHSC) for their dedication and expertise. We thank Dr. Anang A. Shelat for providing us with the BETi drug SJ018. We thank R Dean Franz for help in optimizing TCF4 acetylation experiments.

## DECLARATION OF INTEREST

The authors declare no competing interest.

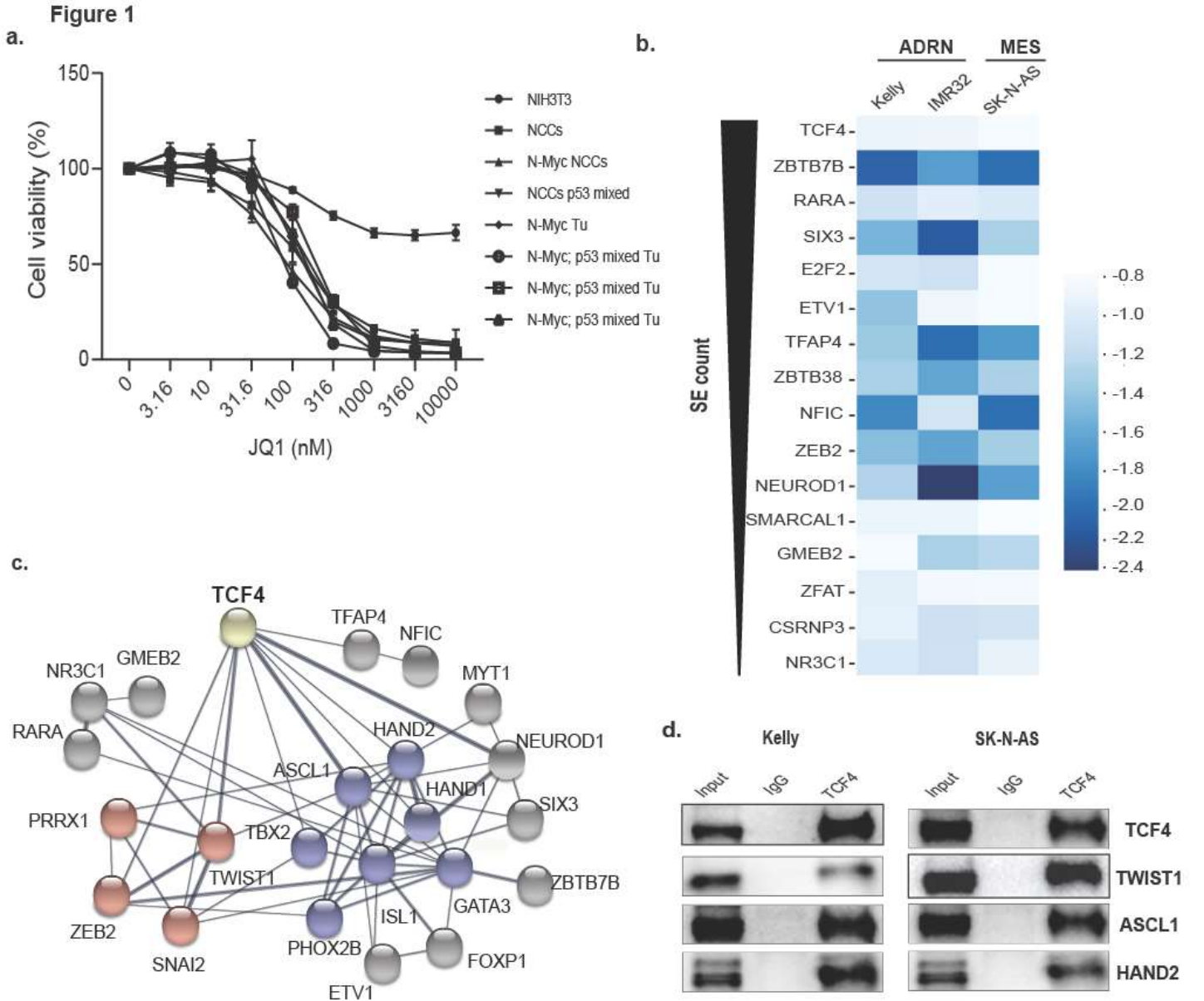
## References:

1. Maris, J.M., Hogarty, M.D., Bagatell, R. & Cohn, S.L. Neuroblastoma. *Lancet* **369**, 2106-20 (2007).
2. Brodeur, G.M. Neuroblastoma: biological insights into a clinical enigma. *Nat Rev Cancer* **3**, 203-16 (2003).
3. Wylie, L.A., Hardwick, L.J., Papkovskaia, T.D., Thiele, C.J. & Philpott, A. Ascl1 phospho-status regulates neuronal differentiation in a *Xenopus* developmental model of neuroblastoma. *Dis Model Mech* **8**, 429-41 (2015).
4. Dong, R. *et al.* Single-Cell Characterization of Malignant Phenotypes and Developmental Trajectories of Adrenal Neuroblastoma. *Cancer Cell* **38**, 716-733.e6 (2020).
5. Bertrand, N., Castro, D.S. & Guillemot, F. Proneural genes and the specification of neural cell types. *Nat Rev Neurosci* **3**, 517-30 (2002).
6. Saint-André, V. *et al.* Models of human core transcriptional regulatory circuitries. *Genome Res* **26**, 385-96 (2016).
7. Hnisz, D. *et al.* Convergence of developmental and oncogenic signaling pathways at transcriptional super-enhancers. *Mol Cell* **58**, 362-70 (2015).
8. Durbin, A.D. *et al.* Selective gene dependencies in MYCN-amplified neuroblastoma include the core transcriptional regulatory circuitry. *Nat Genet* **50**, 1240-1246 (2018).
9. van Groningen, T. *et al.* Neuroblastoma is composed of two super-enhancer-associated differentiation states. *Nat Genet* **49**, 1261-1266 (2017).
10. Wang, L. *et al.* ASCL1 is a MYCN- and LMO1-dependent member of the adrenergic neuroblastoma core regulatory circuitry. *Nat Commun* **10**, 5622 (2019).
11. Boeva, V. *et al.* Heterogeneity of neuroblastoma cell identity defined by transcriptional circuitries. *Nat Genet* **49**, 1408-1413 (2017).
12. van Groningen, T. *et al.* A NOTCH feed-forward loop drives reprogramming from adrenergic to mesenchymal state in neuroblastoma. *Nat Commun* **10**, 1530 (2019).
13. DuBois, S.G., Macy, M.E. & Henderson, T.O. High-Risk and Relapsed Neuroblastoma: Toward More Cures and Better Outcomes. *Am Soc Clin Oncol Educ Book* **42**, 1-13 (2022).
14. Jubierre, L. *et al.* Targeting of epigenetic regulators in neuroblastoma. *Exp Mol Med* **50**, 1-12 (2018).
15. Westerhout, E.M. *et al.* Mesenchymal-Type Neuroblastoma Cells Escape ALK Inhibitors. *Cancer Res* **82**, 484-496 (2022).
16. Puissant, A. *et al.* Targeting MYCN in neuroblastoma by BET bromodomain inhibition. *Cancer Discov* **3**, 308-23 (2013).

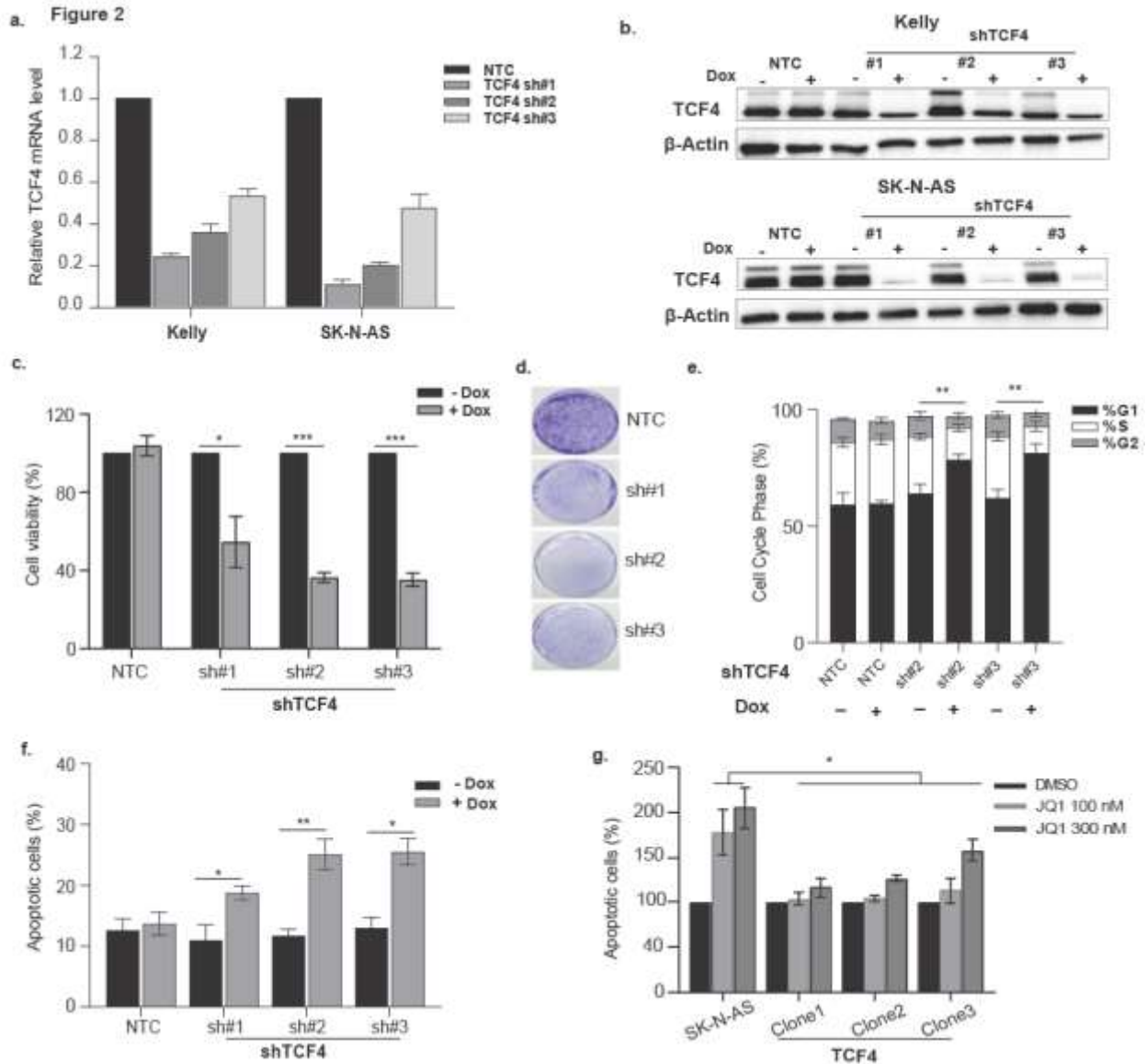
17. Henssen, A. *et al.* Targeting MYCN-Driven Transcription By BET-Bromodomain Inhibition. *Clin Cancer Res* **22**, 2470-81 (2016).
18. Lee, S. *et al.* Bromodomain and extraterminal inhibition blocks tumor progression and promotes differentiation in neuroblastoma. *Surgery* **158**, 819-26 (2015).
19. Greb-Markiewicz, B., Kazana, W., Zarębski, M. & Ożyhar, A. The subcellular localization of bHLH transcription factor TCF4 is mediated by multiple nuclear localization and nuclear export signals. *Sci Rep* **9**, 15629 (2019).
20. Schoof, M. *et al.* The basic helix-loop-helix transcription factor TCF4 impacts brain architecture as well as neuronal morphology and differentiation. *Eur J Neurosci* **51**, 2219-2235 (2020).
21. Persson, P., Jögi, A., Grynfeld, A., Pålman, S. & Axelson, H. HASH-1 and E2-2 are expressed in human neuroblastoma cells and form a functional complex. *Biochem Biophys Res Commun* **274**, 22-31 (2000).
22. Flora, A., Garcia, J.J., Thaller, C. & Zoghbi, H.Y. The E-protein Tcf4 interacts with Math1 to regulate differentiation of a specific subset of neuronal progenitors. *Proc Natl Acad Sci U S A* **104**, 15382-7 (2007).
23. Fan, X. *et al.* TWIST1 and chromatin regulatory proteins interact to guide neural crest cell differentiation. *Elife* **10**(2021).
24. Wedel, M. *et al.* Transcription factor Tcf4 is the preferred heterodimerization partner for Olig2 in oligodendrocytes and required for differentiation. *Nucleic Acids Res* **48**, 4839-4857 (2020).
25. Cano, A. & Portillo, F. An emerging role for class I bHLH E2-2 proteins in EMT regulation and tumor progression. *Cell Adh Migr* **4**, 56-60 (2010).
26. Forrest, M.P., Hill, M.J., Quantock, A.J., Martin-Rendon, E. & Blake, D.J. The emerging roles of TCF4 in disease and development. *Trends Mol Med* **20**, 322-31 (2014).
27. Chen, T. *et al.* Tcf4 Controls Neuronal Migration of the Cerebral Cortex through Regulation of Bmp7. *Front Mol Neurosci* **9**, 94 (2016).
28. Forrest, M.P., Waite, A.J., Martin-Rendon, E. & Blake, D.J. Knockdown of human TCF4 affects multiple signaling pathways involved in cell survival, epithelial to mesenchymal transition and neuronal differentiation. *PLoS One* **8**, e73169 (2013).
29. Zhuang, Y., Cheng, P. & Weintraub, H. B-lymphocyte development is regulated by the combined dosage of three basic helix-loop-helix genes, E2A, E2-2, and HEB. *Mol Cell Biol* **16**, 2898-905 (1996).
30. Bergqvist, I. *et al.* The basic helix-loop-helix transcription factor E2-2 is involved in T lymphocyte development. *Eur J Immunol* **30**, 2857-63 (2000).
31. Quevedo, M. *et al.* Mediator complex interaction partners organize the transcriptional network that defines neural stem cells. *Nat Commun* **10**, 2669 (2019).
32. Ceribelli, M. *et al.* A Druggable TCF4- and BRD4-Dependent Transcriptional Network Sustains Malignancy in Blastic Plasmacytoid Dendritic Cell Neoplasm. *Cancer Cell* **30**, 764-778 (2016).
33. Vicent, S. *et al.* A novel lung cancer signature mediates metastatic bone colonization by a dual mechanism. *Cancer Res* **68**, 2275-85 (2008).

34. Pajtler, K.W. *et al.* The KDM1A histone demethylase is a promising new target for the epigenetic therapy of medulloblastoma. *Acta Neuropathol Commun* **1**, 19 (2013).
35. Fang, Y., Liao, G. & Yu, B. Targeting Histone Lysine Demethylase LSD1/KDM1A as a New Avenue for Cancer Therapy. *Curr Top Med Chem* **19**, 889-891 (2019).
36. Suraweera, A., O'Byrne, K.J. & Richard, D.J. Combination Therapy With Histone Deacetylase Inhibitors (HDACi) for the Treatment of Cancer: Achieving the Full Therapeutic Potential of HDACi. *Front Oncol* **8**, 92 (2018).
37. Sarnik, J., Popławski, T. & Tokarz, P. BET Proteins as Attractive Targets for Cancer Therapeutics. *Int J Mol Sci* **22**(2021).
38. Olsen, R.R. *et al.* MYCN induces neuroblastoma in primary neural crest cells. *Oncogene* **36**, 5075-5082 (2017).
39. Bradner, J.E., Hnisz, D. & Young, R.A. Transcriptional Addiction in Cancer. *Cell* **168**, 629-643 (2017).
40. Jiang, Y. *et al.* SEDb: a comprehensive human super-enhancer database. *Nucleic Acids Res* **47**, D235-d243 (2019).
41. Slavish, P.J. *et al.* Bromodomain-Selective BET Inhibitors Are Potent Antitumor Agents against MYC-Driven Pediatric Cancer. *Cancer Res* **80**, 3507-3518 (2020).
42. Durbin, A.D. *et al.* EP300 Selectively Controls the Enhancer Landscape of MYCN-Amplified Neuroblastoma. *Cancer Discov* **12**, 730-751 (2022).
43. Wang, C. *et al.* EZH2 Mediates epigenetic silencing of neuroblastoma suppressor genes CASZ1, CLU, RUNX3, and NGFR. *Cancer Res* **72**, 315-24 (2012).
44. Kuleshov, M.V. *et al.* Enrichr: a comprehensive gene set enrichment analysis web server 2016 update. *Nucleic Acids Res* **44**, W90-7 (2016).
45. Upton, K. *et al.* Epigenomic profiling of neuroblastoma cell lines. *Sci Data* **7**, 116 (2020).
46. Sussman, R.T. *et al.* CAMKV Is a Candidate Immunotherapeutic Target in MYCN Amplified Neuroblastoma. *Front Oncol* **10**, 302 (2020).
47. Bradney, C. *et al.* Regulation of E2A activities by histone acetyltransferases in B lymphocyte development. *J Biol Chem* **278**, 2370-6 (2003).
48. Tsherniak, A. *et al.* Defining a Cancer Dependency Map. *Cell* **170**, 564-576.e16 (2017).
49. Alleboina, S., Aljouada, N., Miller, M. & Freeman, K.W. Therapeutically targeting oncogenic CRCs facilitates induced differentiation of NB by RA and the BET bromodomain inhibitor. *Mol Ther Oncolytics* **23**, 181-191 (2021).
50. Sen, N., Gui, B. & Kumar, R. Role of MTA1 in cancer progression and metastasis. *Cancer Metastasis Rev* **33**, 879-89 (2014).
51. Maes, T. *et al.* ORY-1001, a Potent and Selective Covalent KDM1A Inhibitor, for the Treatment of Acute Leukemia. *Cancer Cell* **33**, 495-511.e12 (2018).
52. Wei, L. *et al.* Cancer CRC: A Comprehensive Cancer Core Transcriptional Regulatory Circuit Resource and Analysis Platform. *Front Oncol* **11**, 761700 (2021).
53. Zeid, R. *et al.* Enhancer invasion shapes MYCN-dependent transcriptional amplification in neuroblastoma. *Nat Genet* **50**, 515-523 (2018).

54. Liu, Y., Liu, D. & Wan, W. MYCN-induced E2F5 promotes neuroblastoma cell proliferation through regulating cell cycle progression. *Biochem Biophys Res Commun* **511**, 35-40 (2019).
55. Sadasivam, S., Duan, S. & DeCaprio, J.A. The MuvB complex sequentially recruits B-Myb and FoxM1 to promote mitotic gene expression. *Genes Dev* **26**, 474-89 (2012).
56. Leone, G. *et al.* Myc requires distinct E2F activities to induce S phase and apoptosis. *Mol Cell* **8**, 105-13 (2001).
57. Wang, Z. *et al.* FoxM1 in tumorigenicity of the neuroblastoma cells and renewal of the neural progenitors. *Cancer Res* **71**, 4292-302 (2011).
58. Gualdrini, F. *et al.* Addiction of MYCN amplified tumours to B-MYB underscores a reciprocal regulatory loop. *Oncotarget* **1**, 278-88 (2010).
59. Decaestecker, B. *et al.* TBX2 is a neuroblastoma core regulatory circuitry component enhancing MYCN/FOXM1 reactivation of DREAM targets. *Nat Commun* **9**, 4866 (2018).
60. Wang, H. *et al.* The HDAC inhibitor depsipeptide transactivates the p53/p21 pathway by inducing DNA damage. *DNA Repair (Amst)* **11**, 146-56 (2012).
61. Luchenko, V.L. *et al.* Histone deacetylase inhibitor-mediated cell death is distinct from its global effect on chromatin. *Mol Oncol* **8**, 1379-92 (2014).
62. Wood, P.J. *et al.* A phase I study of panobinostat in pediatric patients with refractory solid tumors, including CNS tumors. *Cancer Chemother Pharmacol* **82**, 493-503 (2018).
63. García-López, J. *et al.* Large 1p36 Deletions Affecting Arid1a Locus Facilitate Mycn-Driven Oncogenesis in Neuroblastoma. *Cell Rep* **30**, 454-464.e5 (2020).
64. Dobin, A. *et al.* STAR: ultrafast universal RNA-seq aligner. *Bioinformatics* **29**, 15-21 (2013).
65. Liao, Y., Smyth, G.K. & Shi, W. featureCounts: an efficient general purpose program for assigning sequence reads to genomic features. *Bioinformatics* **30**, 923-30 (2014).
66. Love, M.I., Huber, W. & Anders, S. Moderated estimation of fold change and dispersion for RNA-seq data with DESeq2. *Genome Biol* **15**, 550 (2014).
67. Subramanian, A. *et al.* Gene set enrichment analysis: a knowledge-based approach for interpreting genome-wide expression profiles. *Proc Natl Acad Sci U S A* **102**, 15545-50 (2005).
68. Li, H. & Durbin, R. Fast and accurate short read alignment with Burrows-Wheeler transform. *Bioinformatics* **25**, 1754-60 (2009).
69. Zhang, Y. *et al.* Model-based analysis of ChIP-Seq (MACS). *Genome Biol* **9**, R137 (2008).
70. Jung, I. *et al.* A compendium of promoter-centered long-range chromatin interactions in the human genome. *Nat Genet* **51**, 1442-1449 (2019).
71. Quinlan, A.R. & Hall, I.M. BEDTools: a flexible suite of utilities for comparing genomic features. *Bioinformatics* **26**, 841-2 (2010).



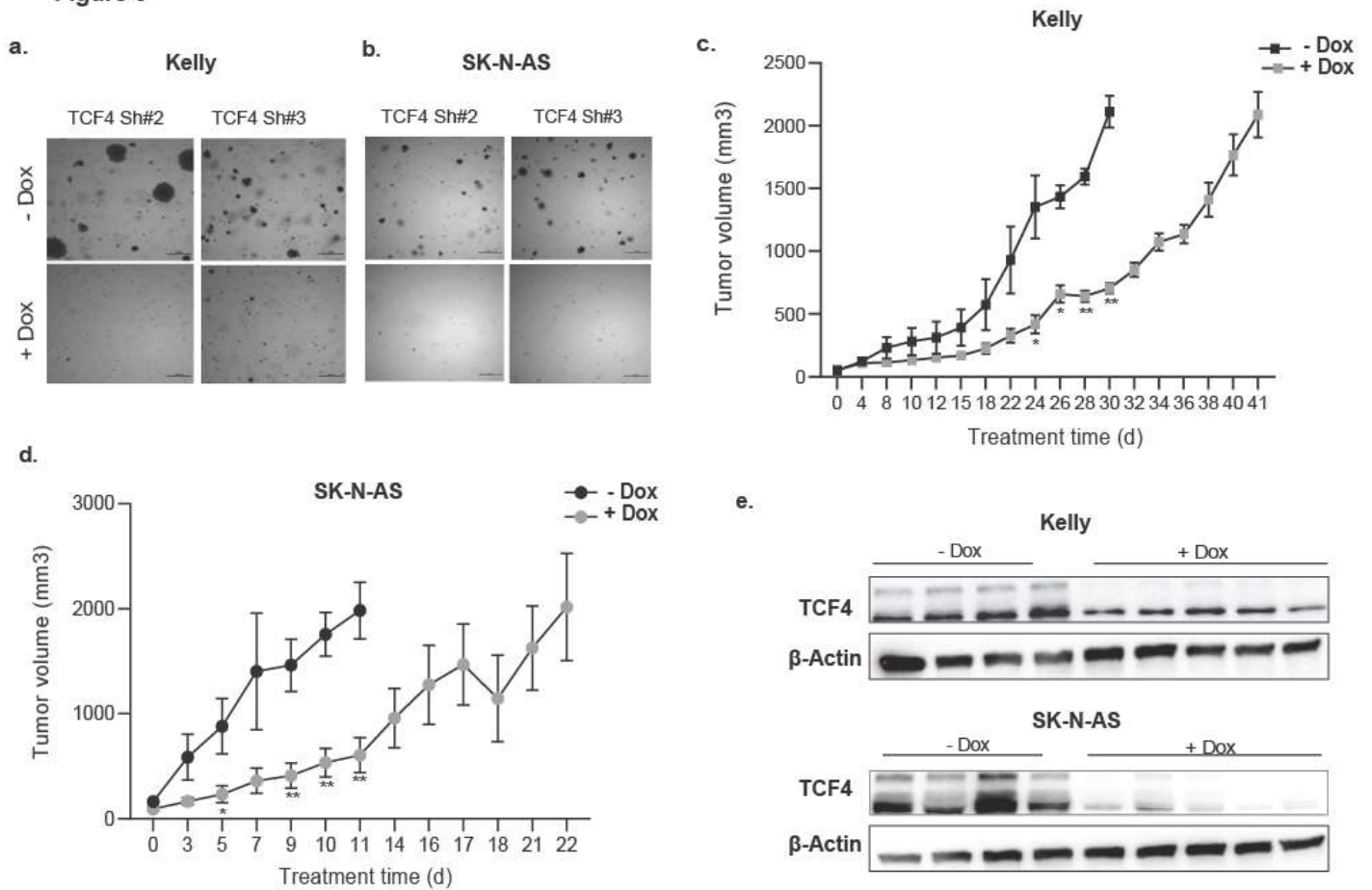
**Figure 1. TCF4 is a critical determinant of JQ1 sensitivity in NB cells.** **a** Dose response of cells after 4-day treatment with half-log dilutions of JQ1. Cell lines include NCCs, NCCs overexpressing N-Myc (N-Myc NCC), NCCs pooled from p53<sup>-/-</sup> and p53<sup>+/-</sup> embryos (NCC p53 mixed, cell line from N-Myc tumor (N-Myc Tu), cell lines from N-Myc p53 mixed tumors (N-Myc; p53 mixed Tu) and control NIH3T3. Results were normalized to control + SE. *n* = 3 independent experiments. **b** Heatmap of log<sub>2</sub> fold change in gene expression of shared transcription factors that are downregulated in Kelly, IMR32 cells (ADRN), and SK-N-AS (MES) after 3 hours of JQ1 treatment. Shared TFs were arranged in a heatmap based on the number of SEs identified for each factor in multiple NB cell lines using the super-enhancer database (SEdb). Data are representative of three independent biological replicates. **c** STRING database analysis demonstrates TCF4 putative protein-protein interactions. Red nodes indicate known MES TFs, blue nodes indicate known ADRN TFs. **d** Immunoprecipitation of TCF4 using Kelly and SK-N-AS whole lysate. WB is probed with the indicated antibodies. Control IP by rabbit IgG and 10% input are also shown.



**Figure 2. TCF4 is essential for NB viability.** **a** Quantitative PCR analysis showing TCF4 expression in Kelly and SK-N-AS stable cells treated with or without 1  $\mu$ g/mL doxycycline for 3 days. **b** Whole-cell protein lysates were analyzed by western blotting using TCF4 antibody 5 days after 1  $\mu$ g/mL doxycycline treatment. **c** CyQuant proliferation assay performed using SK-N-AS TCF4 sh #1, #2, #3 stable cell lines compared to empty vector control (NTC) cell line 7 days after doxycycline treatment. **d** Colony formation assays were performed following TCF4 knockdown in SK-N-AS. Cells were cultured for 10 days in the presence or absence of 1  $\mu$ g/mL of doxycycline. **e** % of cells in each phase of the cell cycle 5 days following TCF4 knockdown in the SK-N-AS cell line. Cell cycle was assayed by flow cytometry. Statistical test is based on G1 phase percentage. Data are presented as the mean  $\pm$  S.E. (\* $p$ <0.05\*\* $p$ <0.01, \*\*\* $p$ <0.001 vs. control) **f** Quantitative analysis of the percentage of apoptotic cells (Annexin V + /FITC +) in SK-N-AS TCF4 stable cell lines treated with or without 1  $\mu$ g/mL doxycycline for 7 days. **g** Annexin V/FITC staining of parental SK-N-AS cells and SK-N-AS overexpressing TCF4 cultured in the presence of increasing concentrations of JQ1 for 4 days. Data are presented as the means  $\pm$  SE from three independent experiments. (\* $p$ <0.05\*\* $p$ <0.01, \*\*\* $p$ <0.001 vs. control).

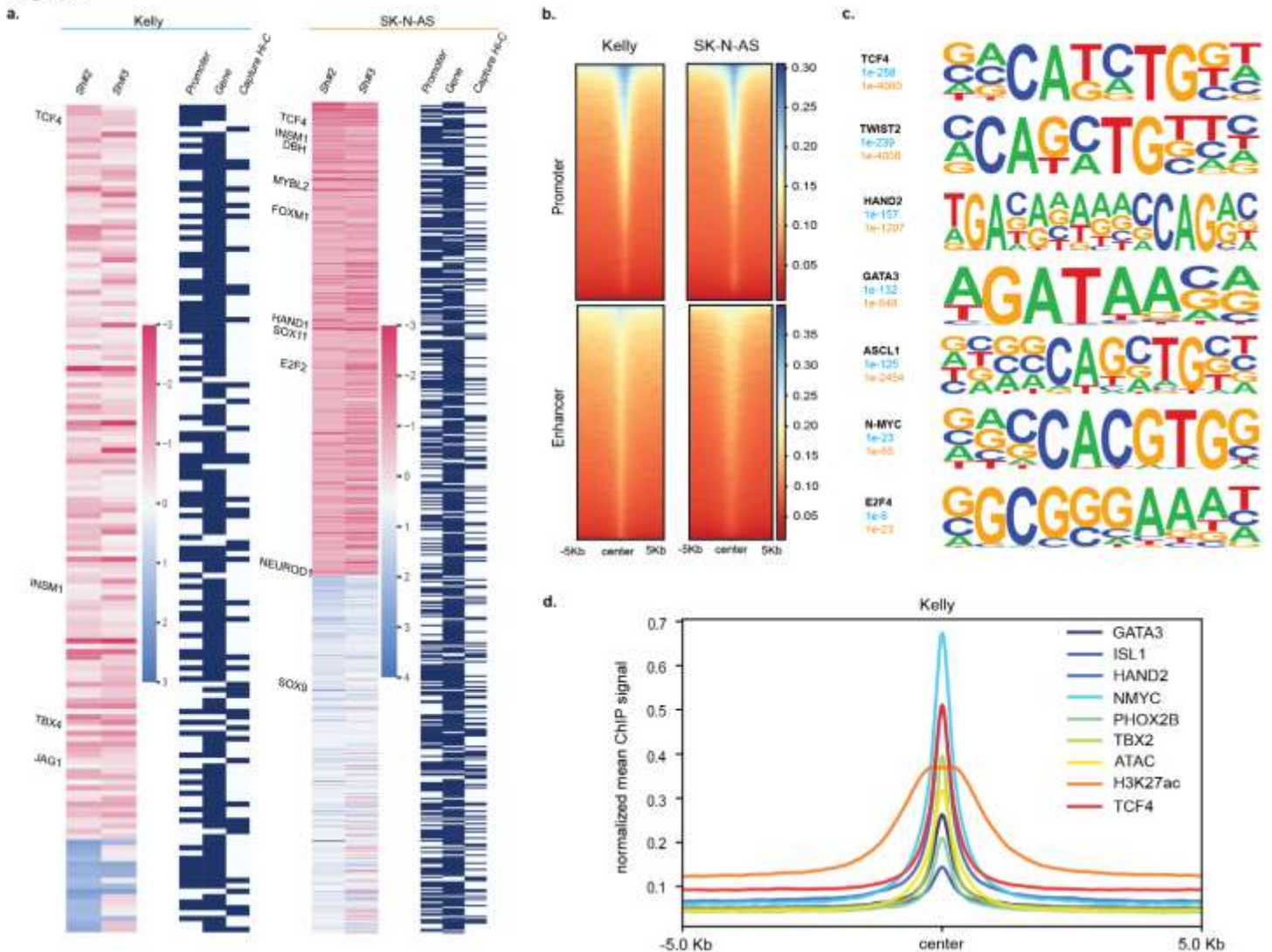


**Figure 3**



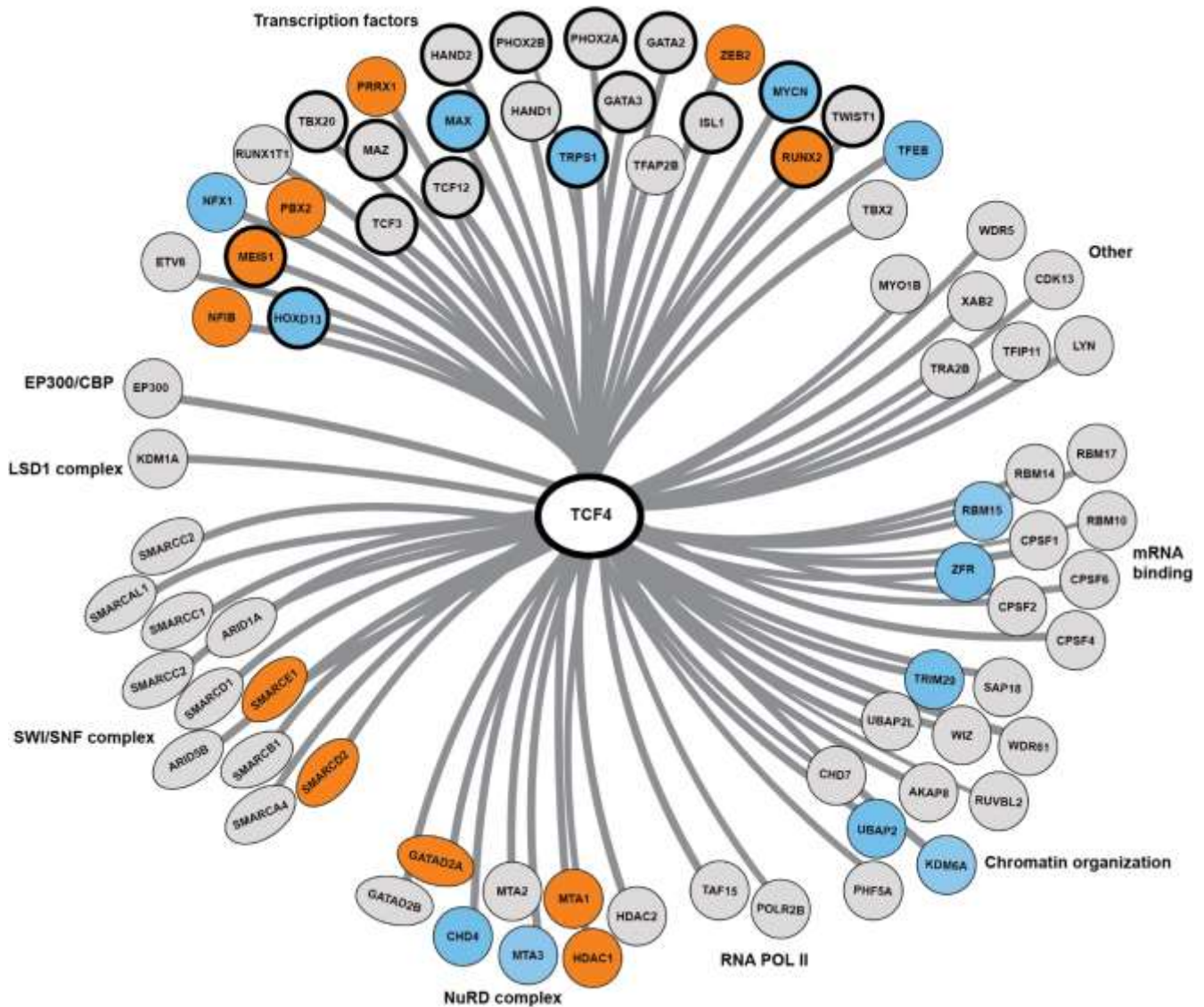
**Figure 3. TCF4 knockdown suppresses tumor growth in vivo.** **a, b** Soft-agar colony formation assay (Clonogenic Assay) of the Kelly and SK-N-AS TCF4 stable cell lines at 21 days after doxycycline treatment. Brightfield microscopy, Bar 500  $\mu$ m. Growth curves for subcutaneous xenograft transduced with **c** Kelly TCF4 sh2, **d** SK-N-AS sh2 injected in the flank region of nude mice. One week after the injections, mice were assigned to either (-Dox) or (+Dox) feed (Con group= 4 mice, Dox group= 5 mice). Data is presented as the means  $\pm$  SE (\* $p$ <0.05, \*\* $p$ <0.01). **e** TCF4 knockdown after doxycycline treatment was confirmed by immunoblot in tumors formed from Kelly and SK-N-AS NB cells, control or transduced cells with an shRNA targeting TCF4.

**Figure 4**



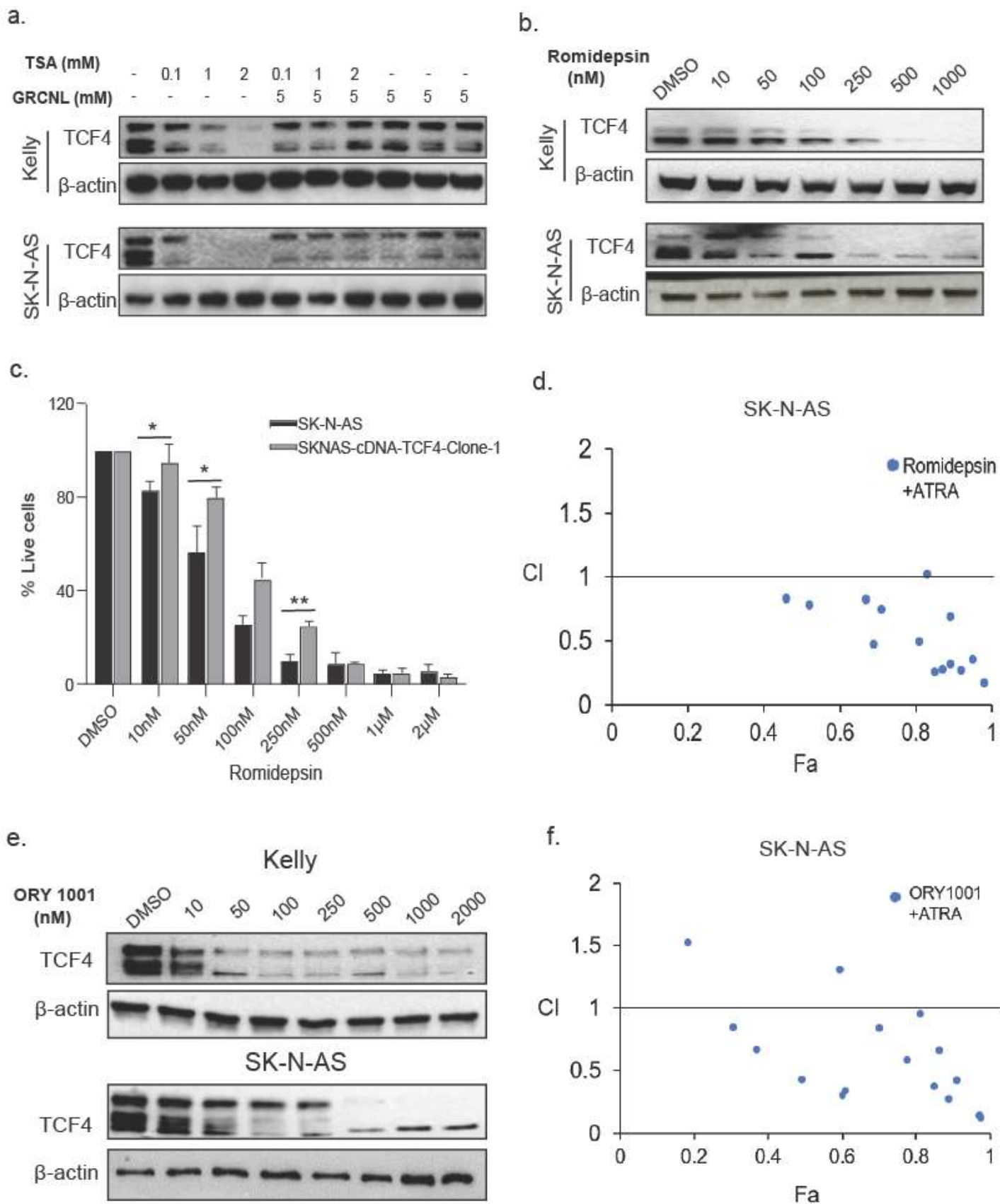
**Figure 4. TCF4-dependent regulatory network in NB.** **a** Heatmap image represents genes down- or up-regulated in both Kelly and SK-N-AS cells after TCF4 KD using 2 different shRNAs (#2, #3), containing a TCF4 ChIP-seq peak within the promoter (1000bp from TSS based on gene orientation), the gene body or capture Hi-C data. **b** Heatmap indicating the binding intensity of TCF4 at promoters or enhancers (Homer annotation) within 5 kb of ChIP-seq peaks in the Kelly and SK-N-AS cell lines. The color scale shows the intensity of the distribution signal. **c** Enriched DNA-binding motifs identified by HOMER corresponding to known transcription factors. **d** Aggregated ChIP-seq signals for TCF4, H3K27ac, ATAC, MYCN, and the CRC members HAND2, PHOX2B, GATA3, ISL1, ASCL1 peaks in the Kelly cell line for the regions (- +5000bp) from the TCF4 peak summits of all TCF4 peaks.

Figure 5



**Figure 5. TCF4 interactome in NB. a** Proteins interacting with TCF4 in both Kelly and SK-N-AS NB cells, identified by immunoprecipitation coupled to mass spectrometry (IP-MS). Normal rabbit IgG was used as a negative control. Identified proteins are high-confidence proteins identified in at least two independent (IP-MS) reactions per cell line, found in both Kelly and SK-N-AS cells. n = 3 independent experiments. TCF4 interaction partners shared between Kelly and SK-N-AS cells are denoted in gray, TCF4 interactors identified in Kelly cells only are in blue, and SK-N-AS only are in orange. Bold circles represent TFs identified as TCF4 interactors in the (IP-MS) analysis and have enriched DNA-binding motifs identified in the TCF4 ChIP-seq in both cell lines.

**Figure 6**



**Figure 6. Histone deacetylase inhibitors (HDACi) and lysine demethylase 1A (KDM1A) inhibitors affect TCF4 protein stability** **a** Western blot for levels of TCF4 following treatment of Kelly and SK-N-AS cell lines with increasing doses of Trichostatin A (TSA) with or without 5 uM doses of garcinol for 24 hours. **b** Western blot for levels of TCF4, TCF3, and TCF12 following treatment of Kelly and SK-N-AS cell lines with increasing doses of the HDACi (romidepsin) for 24 hours. **c** CyQuant proliferation assay of parental SK-N-AS cells and SK-N-AS clone1 stable cell line overexpressing TCF4 following treatment with increasing doses of romidepsin for 4 days. **d** Fraction affected (Fa) versus CI plots were generated to determine the extent of synergy following the combinatorial treatment of romidepsin + ATRA in SK-N-AS cells. Representative data were analyzed by CompuSyn software. Synergistic effects are defined as  $CI < 1$ . The dotted line indicates a reference point of a CI value of 1. **e** Western blot for levels of TCF4 following treatment of Kelly and SK-N-AS cell lines with increasing doses of the KDM1A inhibitor (ORY1001) for 24 hours. **f** Fraction affected (Fa) versus CI plots were generated to determine the extent of synergy following the combinatorial treatment of ORY1001 + ATRA in SK-N-AS cells. Synergistic effects are defined as  $CI < 1$ . The dotted line indicates a reference point of a CI value of 1. Data are presented as the means  $\pm$  SE from three independent experiments. \* $p < 0.05$ , \*\* $p < 0.01$ .

## Supplementary File

Supplementary figure 1

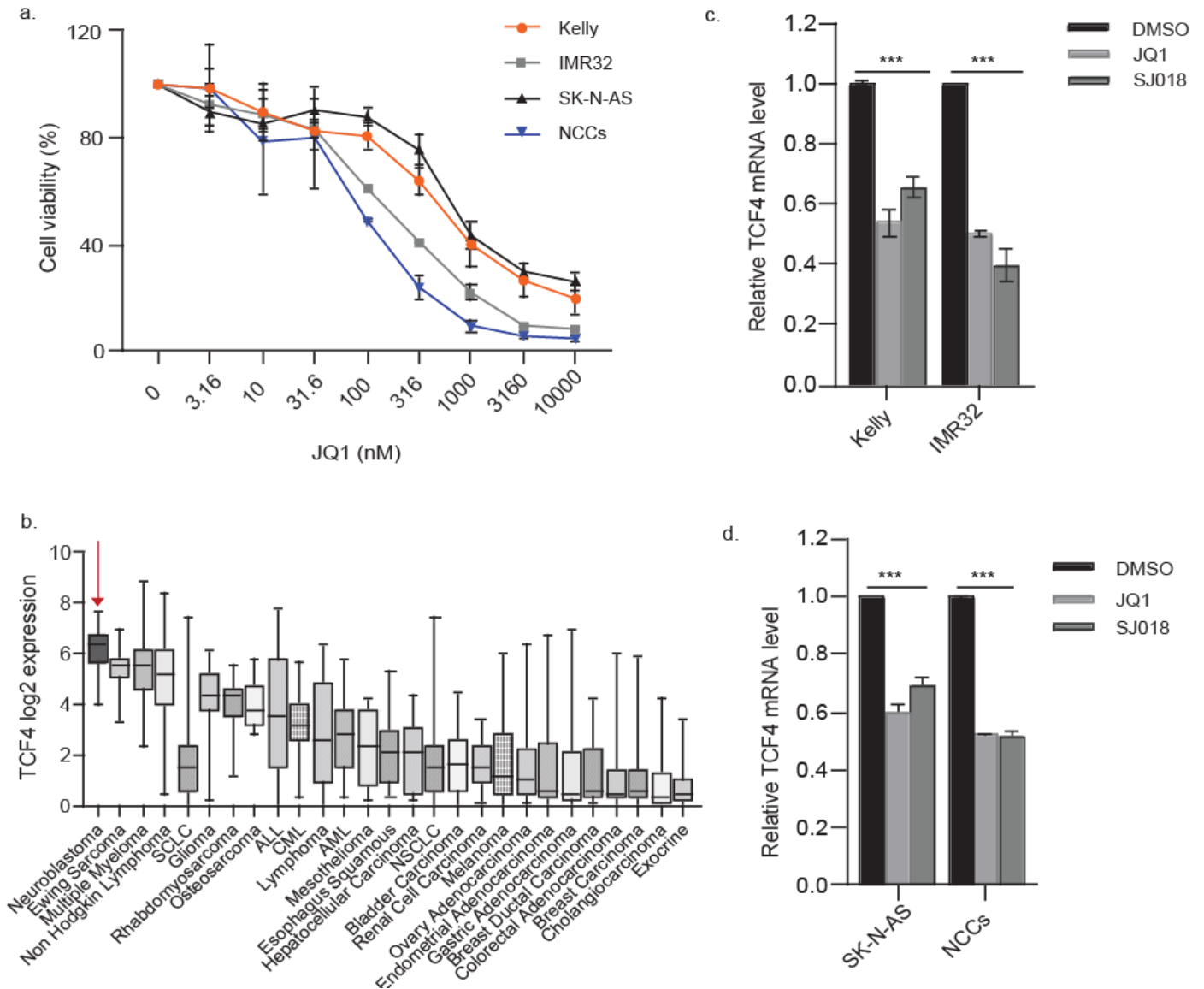


**Figure 1. TCF4 is highly expressed in neuroblastoma and JQ1 suppresses the expression of TCF4 in multiple NB lineage cells.** **a** Dose response curve of cells 4-days following treatment with half-log dilutions of JQ1. Cell lines include Kelly, IMR32 (ADRN), SK-N-AS and mouse NCCs (MES/STEM). Results were normalized to control  $\pm$  S.E.  $n = 3$  independent experiments. **b** TCF4 expression (log<sub>2</sub>) in NB tumors and NB cell lines as compared to other tumors or cell lines. **c, d** TCF4 mRNA levels were determined by quantitative real-time PCR after neuroblastoma cell lines and primary NCCs were treated with DMSO, 1 $\mu$ M JQ1 or SJ018 for 3 hours. Expression values are shown relative to the DMSO condition for each cell line. Data are presented as the mean  $\pm$  S.E. (\* $p < 0.05$  \*\* $p < 0.01$ , \*\*\* $p < 0.001$  vs. control).

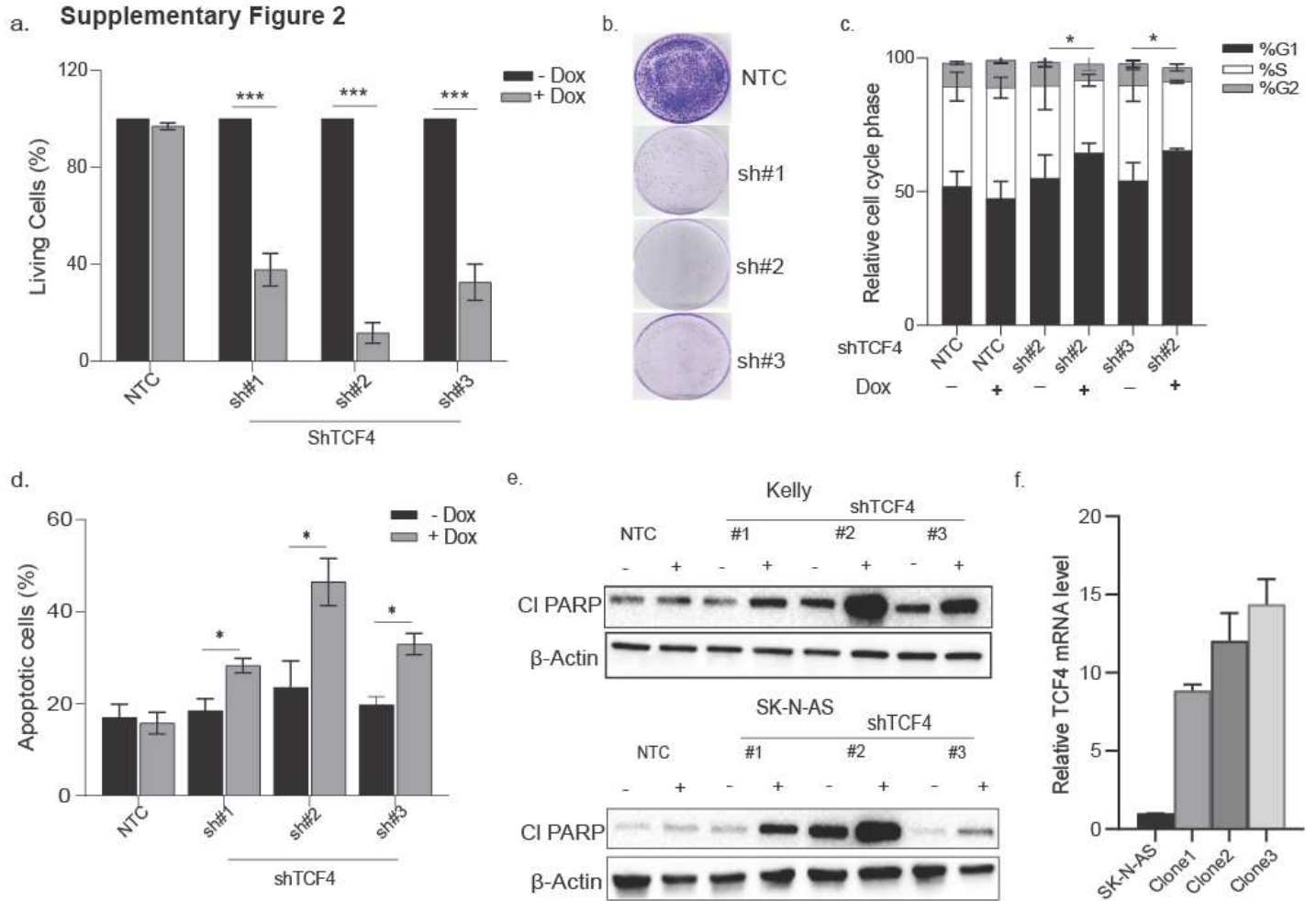


**Figure 2. Knockdown of TCF4 dramatically decreases cell proliferation and induces apoptosis.** **a** CyQuant proliferation assay performed using Kelly TCF4 sh #1, #2, #3 cell lines compared to empty vector control (NTC) cell line 5 days after doxycycline treatment. Results were normalized to control + S.E.  $n = 3$  independent experiments. **b** Colony formation assays were performed following TCF4 knockdown in Kelly cells. Cells were cultured for 10 days with or without 1  $\mu\text{g}/\text{mL}$  of doxycycline. **c** % of cells in each phase of the cycle 3 days following TCF4 knockdown in the Kelly cell line. Cell cycle was assayed by flow cytometry. Statistical test is based on G1 phase percentage. Data are presented as the mean  $\pm$  S.E. (\* $p < 0.05$ \*\* $p < 0.01$ , \*\*\* $p < 0.001$  vs. control) **d** Quantitative analysis of the percentage of apoptotic cells (Annexin V + /FITC +) in Kelly TCF4 stable cell lines treated with or without 1  $\mu\text{g}/\text{mL}$  doxycycline for 5 days. **e** Western blot of cleaved PARP protein levels in Kelly and SK-N-AS cells 5 days after doxycycline treatment. Data are presented as the mean  $\pm$  S.E. (\* $p < 0.05$ \*\* $p < 0.01$ , \*\*\* $p < 0.001$  vs. control). **f** TCF4 mRNA level determined using real-time PCR following TCF4 overexpression in SK-N-AS cells. These cells were transfected with TCF4 cDNA vector. Three resistant clones stably overexpressing TCF4 were culture and expanded. Results were normalized to parental SK-N-AS cell line  $\pm$  S.E.

Supplementary figure 3

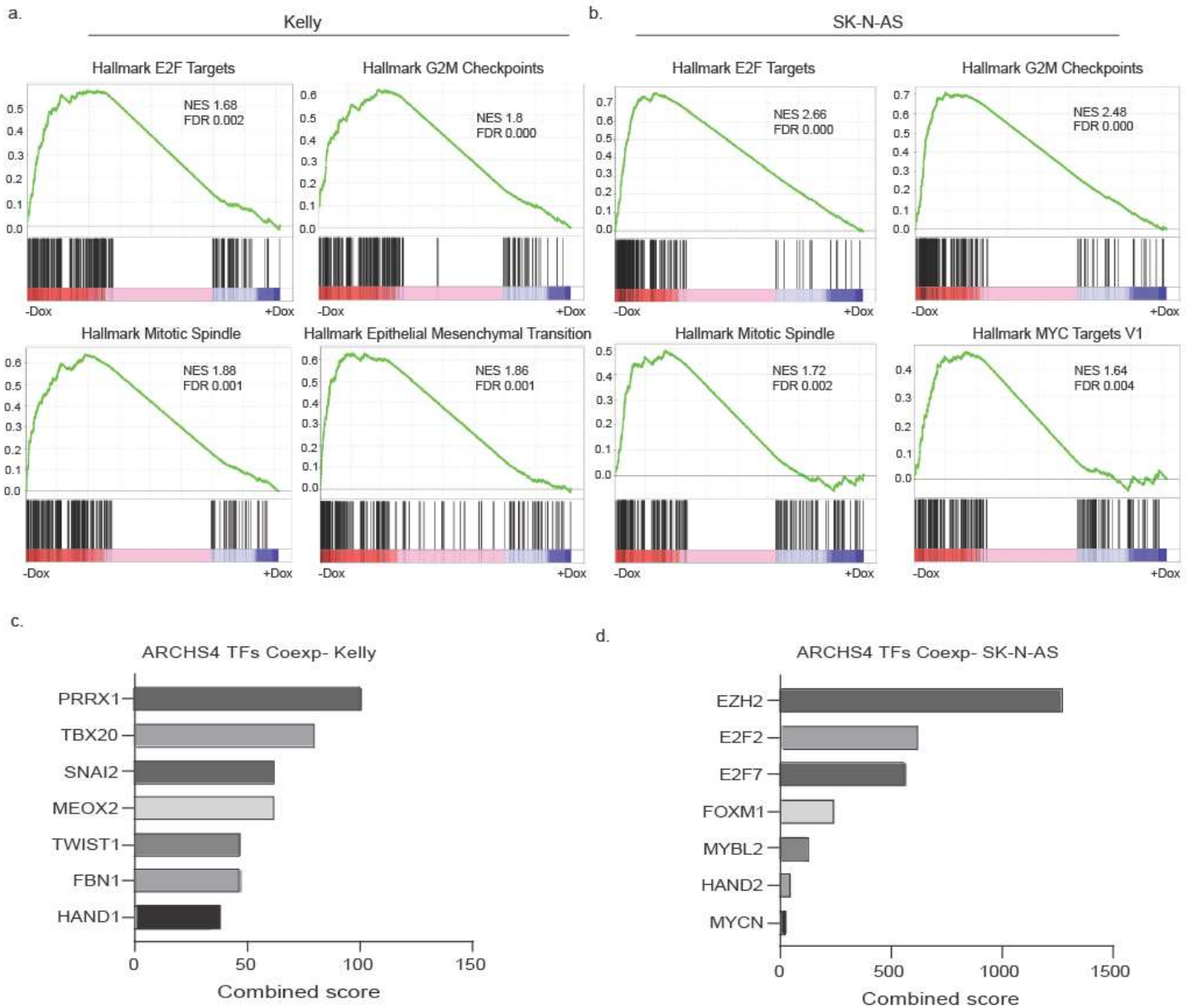


**Figure 3. Knockdown of TCF4 deregulates gene expression of MYC target genes as well as genes involved in cell cycle.** a,b Enrichment plots acquired from the gene set enrichment analysis (GSEA). Four significant pathways enriched in vehicle-treated cells compared to doxycycline-treated cells upon TCF4 knockdown in Kelly and SK-N-AS. FDR < 0.01 was defined as statistically significant. c,d Enrichr pathway analysis of downregulated differentially expressed genes (DEG) following TCF4 knockdown in Kelly and SK-N-AS cells using the ARCHS4 TF Coexp. The lists of genes were analyzed based on the combined score ranking. p-value < 0.05 was used as the significance threshold.



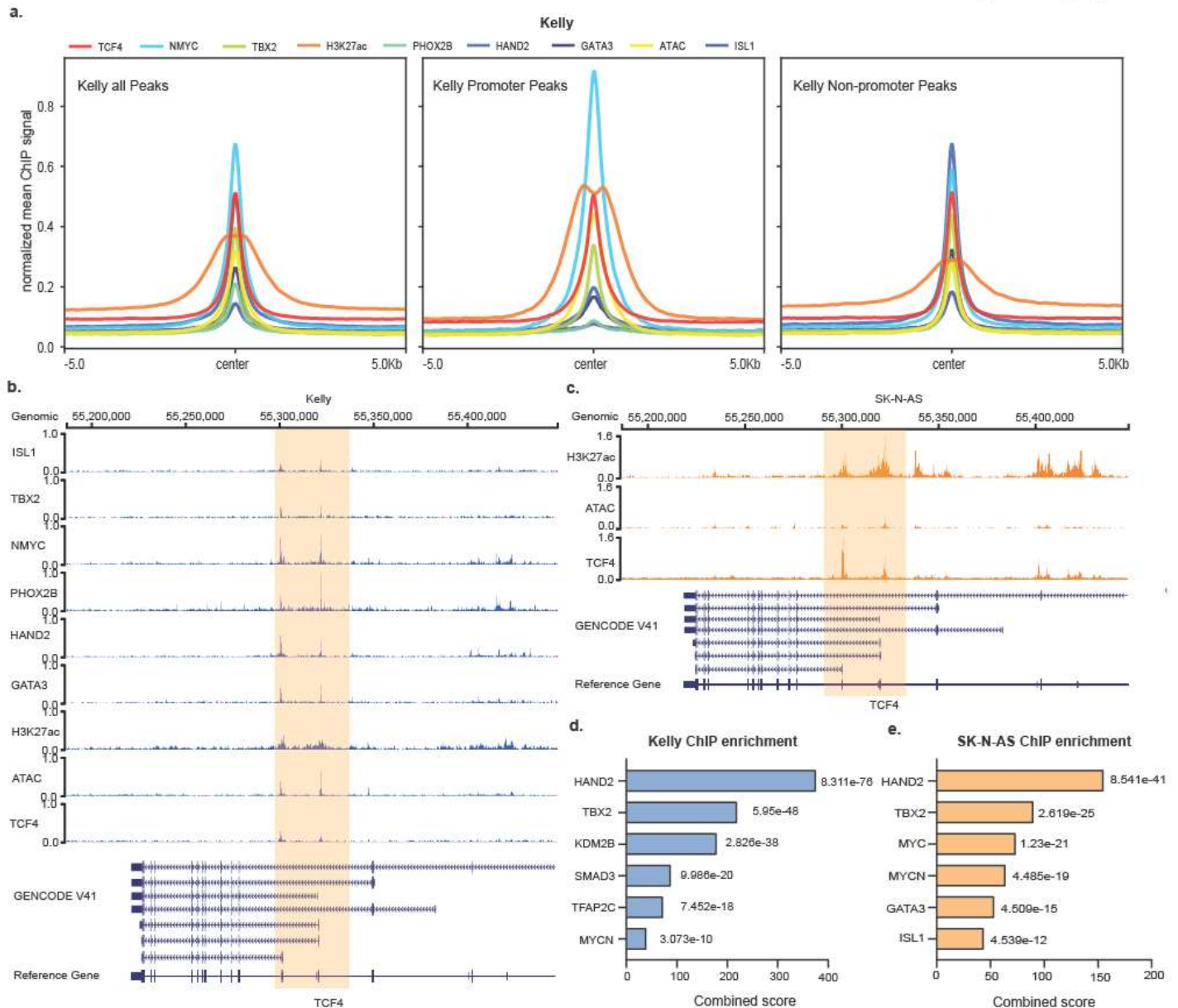


**Figure 4. TCF4 is showing a high concordance of DNA occupancy with CRC proteins.** **a** Aggregated ChIP-seq signals for TCF4, H3K27ac, ATAC, MYCN, and the CRC members HAND2, PHOX2B, GATA3, ISL1, ASCL1 peaks in the Kelly cell line for the regions ( $\pm 5.0$  Kb) from the TCF4 peak summits of all TCF4 peaks (left), peaks located at promoter (center), and peaks located at enhancers (right). **b** ChIP-seq gene tracks showing the binding locations of ADRN CRC members at the TCF4 gene locus in Kelly cells. Also shown is the enhancer marker (H3K27ac) and open chromatin (ATAC-seq) at the TCF4 gene locus in Kelly cells. **c** ChIP-seq gene tracks showing the enhancer marker (H3K27ac) and open chromatin (ATAC-seq) at the TCF4 gene locus in SK-N-AS cells. **d,e** Enrichr pathway analysis of TCF4 peaks that overlap with MYCN peaks at SEs in Kelly and SK-N-AS cells using the ChIP Enrichment Analysis (ChEA). The lists of genes were analyzed based on the combined score ranking. p-value  $< 0.05$  was used as the significance threshold.

## Supplementary figure 5

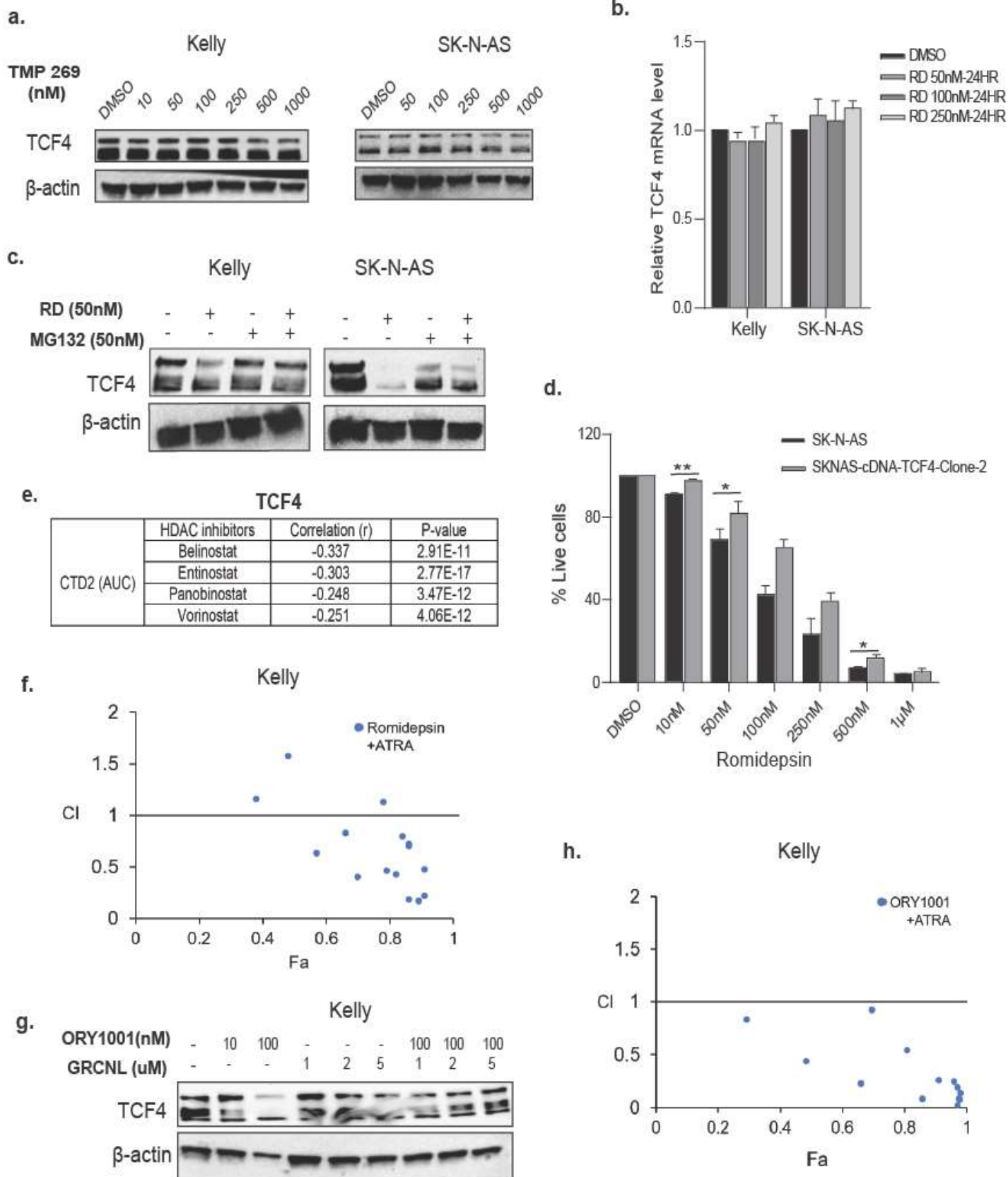


**Figure 5. Effects of HDACi and KDM1A inhibitors are post-translational and based on protein stability.** **a** Western blot for levels of TCF4 following treatment of Kelly and SK-N-AS cell lines with increasing doses of the class II HDACi TMP 269 for 24 hours. **b** TCF4 mRNA level determined using quantitative RT-PCR after treating Kelly and SK-N-AS with increasing doses of romidepsin for 24 hours. **c** Western blot for levels of TCF4 following treatment of Kelly and SK-N-AS cell lines with 50 nM romidepsin with or without 50 nM doses of the proteasome inhibitor MG132 for 24 hours. **d** CyQuant proliferation assay of parental SK-N-AS cells and SK-N-AS clone 2 stable cell line overexpressing TCF4 following treatment with increasing doses of romidepsin for 4 days. **e** TCF4 expression across all cancers correlates with multiple HDAC inhibitors as determined using the Cancer Dependency Map (DepMap). **f** Fraction affected (Fa) versus CI plots were generated to determine the extent of synergy following the combinatorial treatment of romidepsin + ATRA in Kelly cells. Synergistic effects are defined as  $CI < 1$ . The dotted line indicates a reference point of a CI value of 1. **g** Western blot for levels of TCF4 following treatment of Kelly cell line with increasing doses of the KDM1A inhibitor ORY1001 with or without increasing doses of garcinol for 24 hours. **h** Fraction affected (Fa) versus CI plots were generated to determine the extent of synergy following the combinatorial treatment of ORY1001 + ATRA in SK-N-AS cells. Synergistic effects are defined as  $CI < 1$ . The dotted line indicates a reference point of a CI value of 1. Data are presented as the means  $\pm$  standard error from three independent experiments. \* $p < 0.05$ , \*\* $p < 0.01$ .

## APPENDIX B. CHAPTER 4 ARTICLE

**NOTE:** Navigation with Adobe Acrobat Reader or Adobe Acrobat Professional: To return to the last viewed page, use key commands Alt/Ctrl+Left Arrow on PC or Command+Left Arrow on Mac. For “Next view,” use Alt/Ctrl+Right Arrow on PC or Command+Right Arrow on Mac. See [Preface](#) for further details. If needed, use this link to return to **Chapter 4** after navigating within this appendix.

### Introduction

Final submission reused with permission. Alleboina S, Aljouda N, Miller M, Freeman KW. Therapeutically targeting oncogenic CRCs facilitates induced differentiation of NB by RA and the BET bromodomain inhibitor. *Mol Ther Oncolytics*. 2021 Sep 25;23:181-191. DOI: <https://doi.org/10.1016/j.omto.2021.09.004>.

### Article

**Therapeutically targeting oncogenic cell regulatory circuitries facilitates induced differentiation of neuroblastoma by retinoic acid and BET bromodomain inhibitor.**

Satyanarayana Alleboina, Nour Aljouda, Mellessa Miller, Kevin W Freeman\*

Department of Genetics, Genomics and Informatics, University of Tennessee Health Science Center, Memphis, TN, United States

\*Correspondence should be addressed K.W.F. (kfreem22@uthsc.edu)

University of Tennessee Health Science Center, 19 S Manassas St, CRB-326, Memphis, TN 38163 Email: kfreem22@uthsc.edu, Phone: 901-448-5024

**Short title:** CRC disruption facilitates NB differentiation.

## Abstract

Retinoic acids (RA) are the most successful therapeutics for cancer differentiation therapy and used in high-risk neuroblastoma (NB) maintenance therapy but are limited in effectiveness. This study identifies a strategy for improving efficacy through disruption of cancer cell identity using BET inhibitors. Mutations that block development are theorized to cause NB through retention of immature cell identities contributing to oncogenesis. NB has two interchangeable cell identities, maintained by two different core transcriptional regulatory circuitries (CRCs); a therapy resistant mesenchymal/stem cell state, and a proliferative adrenergic cell state. MYCN amplification is a common mutation of high-risk NB and recently found to block differentiation by driving high expression of the adrenergic CRC transcription factor ASCL1. We investigated whether disruption of immature CRCs can promote RA induced differentiation since only a subset of NB patients respond to RA. We found silencing ASCL1, a critical member of the adrenergic CRC, or global disruption of CRCs with the BET inhibitor JQ1, suppresses gene expression of multiple CRC factors, improving RA mediated differentiation. Further, that JQ1 and RA synergistically decrease proliferation and induce differentiation in NB cell lines. Our findings support preclinical studies of RA and BET inhibitors as a combination therapy in treating NB.

## Introduction

Neuroblastoma (NB) is the most common extracranial solid tumor of infancy. It is purported to arise from a block in normal development during differentiation of neural crest cells (NCCs) into cells of the sympathetic nervous system. NB is responsible for about 15% of childhood mortality<sup>1-3</sup> and approximately 50-60% of children with high-risk NB develop treatment resistance<sup>1,4,5</sup>. Current multimodal therapies such as chemotherapy, radiation and immune therapies prolong the survival rate in about 40% of patients<sup>6</sup>. However, the increased risk of treatment related toxicity, long-term complications and the development of resistance in disease prevention and progression has been a major concern in the clinical setting<sup>7,8</sup>. Maintenance therapy using retinoic acid (RA), a well-known differentiating agent, reduces the risk of recurrent disease after intensive multimodal treatment; however, only a subset of NB patients is responsive to RA induced differentiation.

During development, transcription factors establish core transcriptional regulatory circuitries (CRC) that generate and maintain cell identity, by establishing and reinforcing super-enhancers upstream of other mutually regulated members. One model for NB oncogenesis is that a subset of NB mutations inappropriately reinforces early developmental CRCs which lock NB into a developmentally immature state. For the purposes of development that state is highly proliferative, resistant to apoptosis, migratory and invasive. While those traits are important to achieve proper development, they are dangerous if perpetuated in cancer<sup>9</sup>. For example, MYCN gene amplification, a common mutation in high-risk NB, drives ASCL1 expression thus preventing its reduction which is required for cell differentiation of sympathoadrenal neuroblasts into mature neurons<sup>10-12</sup>. ASCL1 along with transcription factors such as PHOX2B, GATA3, and TBX2, are all part of the immature sympathoadrenal CRC observed in NB<sup>13</sup>.

In addition to the proliferative sympathoadrenal identity state, NB can acquire a more immature cell migratory, therapy resistant mesenchymal state, which is regulated by a separate CRC.

These two identity states, adrenergic and mesenchymal, likely capture NCCs early in their commitment to the sympathoadrenal lineage<sup>14</sup>. At this stage, NCCs are transitioning from an epithelial to mesenchymal transition (EMT) program that is migratory into neuroblasts that are highly proliferative. In normal development these cells would respond to differentiation cues like RA to become mature neurons and Schwann cells of the sympathetic nervous system<sup>15</sup>. To differing degrees both of these identity states co-occur as distinct cell populations within neuroblastoma cell lines (NBCL) and within tumors. NBCL and tumors can skew towards one identity state over another suggesting that different mutations favor different identity states. One underutilized strategy for treating NB is to push the cells into a more differentiated and less dangerous state is through differentiation therapy. RA can drive maturation of some NBs through transition of an immature CRC to a more differentiated CRC<sup>16</sup>, but how NB mutations interfere with RA induced differentiation is not well understood. We investigated a novel therapeutic strategy for NB based on the hypothesis that blocks in differentiation are due to pathogenic CRCs, caused by multiple mechanisms including N-Myc induced ASCL1 overexpression and that these interfere with RA mediated differentiation. BET bromodomain inhibitor JQ1 inhibits the epigenetic reader bromodomain containing protein 4 (BRD4)<sup>17</sup>, which accumulates at super-enhancers to promote gene transcription. BET bromodomain inhibitors disrupt super-enhancer function and in turn CRCs. These inhibitors also show prominent anticancer activity in NB including promoting cellular differentiation in some NBCL<sup>18,19</sup>. We found that disrupting CRCs either with genetic silencing of ASCL1, or with BET bromodomain inhibitors, facilitates RA differentiation; thereby identifying a promising therapeutic approach for treating NB.

## Results

**Basal differences of adrenergic vs mesenchymal core regulatory transcription factors in NB cells.** To confirm recently reported findings<sup>20</sup>, we examined protein expression in NBCL that have various genomic signatures and differences in MYCN gene amplification for their identity states. We selected MYCN amplified cell lines Kelly, and SK-N-BE2, and MYCN wild-type SKNAS, GIMEN and SY5Y cell lines to determine the basal protein expression of ASCL1, GATA3, TBX2, PHOX2B, which are prominent adrenergic markers and SOX10, TWIST1, PRRX1, SNAI2 and Vimentin which are prominent mesenchymal markers (**Figure S1**). Higher levels of ASCL1 and PHOX2B protein expression were observed in Kelly, which were also marked by low protein expression of SOX10, TWIST1, SNAI2, and Vimentin indicating these cells favor an adrenergic cell identity. SKNAS showed a markedly lower basal protein expression of ASCL1, PHOX2B and higher protein expression of SOX10, TWIST1, PRRX1, SNAI2, and Vimentin indicating a more mesenchymal type of identity. The other cell lines SK-N-BE2, GIMEN and SY5Y showed an intermediate identity with a more mixed expression of adrenergic and mesenchymal markers (**Figure S1**). Kelly cells, an MYCN-amplified NB, had higher ASCL1 expression and the most adrenergic type of identity thus were chosen for our ASCL1 studies.

**Suppression of ASCL1 by shRNA results in the inhibition of cell proliferation and switching of cell identity core regulatory transcription factors:** Kelly cells were subjected to doxycycline (Dox)-inducible shRNA mediated silencing of *ASCL1*. After 72hrs in the presence +Dox or absence -Dox, quantitative PCR (qPCR) gene expression of *ASCL1* normalized to *ACTIN* demonstrated 57% knockdown in Sh6 and 61% knockdown in Sh8 stably transfected

cells (**Figure 1A and B**). Protein expression of ASCL1 was analyzed at day 4 with Dox treated cells showing a significant knockdown of ASCL1 protein expression in Sh6 and Sh8 (**Figure 1C and D**). To understand the role of the proneural and neurogenic effects of *ASCL1* suppression on the cells, we analyzed the expression of PHOX2B which marks early sympathoadrenal commitments<sup>21</sup>; GATA3 which is downstream of both ASCL1 and PHOX2B and later in sympathoadrenal commitment<sup>22</sup>; SOX10 which is a NCC stemness marker that is lost during neuronal commitment but retained during early mesenchymal commitment<sup>23, 24</sup>; and finally, TWIST1, a marker of mesenchymal commitment<sup>25</sup>. Knockdown of *ASCL1* by Sh6 and Sh8 showed a significant increase in the gene expression of GATA3 and TWIST1 but a significant decrease of SOX10. Specifically, Sh6 ASCL1 showed a significant effect on gene expression of core transcription factors GATA3 Sh6(-Dox 1) vs knockdown (+Dox 1.23±0.03), p<0.05, SOX10 fold change expression Sh6(-Dox 1) vs knockdown (+Dox 0.53±0.10), and TWIST1 fold change expression in Sh6(-Dox 1) vs knockdown (+Dox 1.22±0.06), p<0.05 (**Figure 1E**). Similarly, Sh8 ASCL1 knockdown showed a significant effect on gene expression of core transcription factors with an upregulation in adrenergic vs mesenchymal identity (**Figure 1F**). These results suggested a loss of stemness and gain of both more mesenchymal and adrenergic differentiation.

Due to the well documented labile nature of TWIST1 protein<sup>26</sup>, we wanted to determine if we observed the same changes by protein as in mRNA expression. We also expanded the number of factors that we tested for adrenergic vs mesenchymal identity core regulatory transcription factors adding GATA3 in the adrenergic core and PRRX1 in the mesenchymal core identity. We also analyzed the rate-limiting enzyme in catecholamine biosynthesis, tyrosine hydroxylase (TH) since its used as an expression marker that increases in accordance with further sympathoadrenal commitment<sup>27</sup>. By protein expression, loss of ASCL1 again caused loss of the stemness marker SOX10, but a gain of multiple sympathoadrenal markers, TBX2, GATA3 and TH at 96-hours (**Figure 1G and H**). However, we did not observe obvious and consistent increases in the mesenchymal markers, TWIST1 and PRRX1 suggesting silencing of ASCL1 promotes sympathoadrenal differentiation.

**Treatment of ATRA in cells with ASCL1 suppression results in upregulation of the differentiation marker TH and the inhibition of proliferation:** From the observation that the knockdown of *ASCL1* promoted adrenergic differentiation we wanted to ascertain if the differentiating agent ATRA would augment differentiation when *ASCL1* is silenced. We incubated the cells in the presence or absence of doxycycline and with and without ATRA to determine the effects of ATRA on *ASCL1* expression. We observed that ATRA reduces *ASCL1* gene expression to almost the same extent as caused by silencing of *ASCL1* with further diminishment seen when Dox induced silencing was combined with ATRA (**Figure 2A**). Next, we tested *TH* expression using the same combinations and observed a significant upregulation in both Sh6 and Sh8 when *ASCL1* silencing was combined with ATRA (**Figure 2B**). By Western blot we also observe ATRA reducing ASCL1 expression and causing a further increase in TH expression when combined with *ASCL1* silencing (**Figure 2C**). Finally, we tested the effect of suppression of *ASCL1* on cell proliferation after 4 days by CyQuant assay in the presence or absence of doxycycline along with ATRA treatment. We observed a significant inhibition in proliferation by either *ASCL1* knockdown or ATRA treatment in both Sh-*ASCL1* cell lines. The treatment of ATRA in the presence of doxycycline showed a significant

inhibitory effect in proliferation compared to the treatments of doxycycline or ATRA alone in both shASCL1 Kelly cell lines (**Figure 2D**).

**Combinatorial treatment with JQ1 and ATRA alters core regulatory transcription factors in adrenergic cell types:** Since the results of shRNA mediated *ASCL1* suppression on reducing proliferation and inducing differentiation in combination with ATRA was encouraging, this prompted us to test the potential of JQ1 and JQ1+ATRA combinations in NBCL. While silencing of *ASCL1* would be predicted to disrupt a pathogenic adrenergic CRC caused by *MYCN* amplification, we wanted to determine if broad disruption of CRCs using BET inhibitor in combination with ATRA would recapitulate the findings observed with genetic silencing of *ASCL1*. Additionally, we wanted to assess if this drug combination could affect other NBCL that are not *MYCN* amplified. To this end we performed a series of experiments on Kelly, and two *MYCN* wild-type cell lines SY5Y and SKNAS to determine the potential effect of ATRA and JQ1 either alone or in combination on core regulatory transcription factor gene expression, proliferation, and differentiation.

A 10-fold dilution series of JQ1, ATRA and JQ1+ATRA was performed to determine a concentration that led to significant reduction of proliferation at 4 days of treatment but that would allow assessment for changes in gene expression on Day 3 (**Figure S2A**). We also performed a baseline analysis of N-MYC protein expression in Kelly, SKNAS, GIMEN and SY5Y cells to confirm differential gene expression of *MYCN* (**Figure S2B**). We then used the optimized concentration of 100nM of JQ1 in combination with ATRA to test their effectiveness in causing differentiation and changes in core regulatory transcription factor expression. First, we tested the gene expression of *ASCL1*, *GATA3* and *SOX10* in the three cell lines after 72 hours of treatment. The treatment of ATRA in the presence of JQ1 in Kelly and SY5Y cells showed a significant suppression of *ASCL1* expression, a significant increase in *GATA3* expression, and a significant decrease in the expression of *SOX10* (**Figure 3A and B**) recapitulating what was observed with gene silencing of *ASCL1* (**Figure 1E-H**). For *GATA3*, which is regulated by a super-enhancer in a subset of NBCLs, we do observe a reduction of *GATA3* in response to JQ1 in SY5Y cells that is offset when also treated by ATRA (**Figure 3B**). While JQ1 is expected to cause reduced gene expression by disrupting the *GATA3* super-enhancer in SY5Y the *GATA3* promoter seems directly or indirectly responsive to ATRA in SY5Y cells after JQ1 treatment. In contrast the most mesenchymal type of cell line tested, SKNAS, did not show any significant changes in the mRNA expression of *ASCL1*, *GATA3* or *SOX10* genes (**Figure 3C**). However, SKNAS has the most divergent basal expression of these factors with low protein expression of *ASCL1* and *GATA3* in comparison to the other cell lines tested and the highest *SOX10* expression which suggests SKNAS has a different developmental block from the other cells lines (**Figure S1**).

We next wanted to determine if the cells were differentiating, therefore gene expression of TH and myelin basic protein (MBP), a Schwann cell marker, was analyzed in cells treated for three days demonstrating significant upregulation of both markers in Kelly and SY5Y (**Figure 4A and B**) after combinatorial JQ1/ATRA treatment in comparison to independent treatments. While combination treatment in SKNAS showed a significant increase in TH expression (**Figure 4A**) no change in MBP expression was observed (**Figure 4B**). The combinatorial treatment of JQ1 100nM with ATRA 1 $\mu$ M for four days showed by western blot analysis a significant suppression of *SOX10* in Kelly, SY5Y and SKNAS cells with more modest effects for TH in SY5Y and for *ASCL1* in SKNAS (**Figure 4C, D and E**). The differences in results



between protein and mRNA for SOX10 in SKNAS cells in response to JQ1 with ATRA could be due to timing of the experiments with RT-PCR being done at three days and western blot at four days, or it might indicate that ATRA promotes SOX10 protein turnover when cells are also treated with JQ1. In Kelly cells N-Myc is regulated by a super-enhancer that can be suppressed by BET inhibitors, which we confirmed, interestingly we noted that ATRA does not further affect N-Myc expression, suggesting other factors besides N-Myc are responsible for the results of the combinatorial therapy (**Figure S2C**)<sup>19</sup>. Under combinatorial therapy we do observe significant reduction of SOX10 protein expression across the cell lines indicating a loss of mesenchymal/stem identity.

We further confirmed the effect of combination treatment on differentiation by immune fluorescent staining of TH with images captured after four days of treatment in Kelly and SY5Y cells (**Figure S3A**). The combination of JQ1 and ATRA promoted an increase in differentiation across the three genetically diverse NBCL. In addition, our data indicates they do so by overcoming a different developmental block in SKNAS than occurs in Kelly cells based on their divergent responses to treatment with JQ1 and ATRA for the CRC factors we assayed (**Figure 3A, B and C**) and based on their different basal expression of CRC factors and N-MYC expression pattern (**Figure S1 and S2A**).

**Combinatorial treatment of ATRA with JQ1 are synergistic in inhibition of proliferation in NB cells:** Next, we tested the effect of ATRA, JQ1 or combinations on the inhibition of cell number. A significant reduction in cell number was observed in all cell lines with a further significant decrease with combined JQ1+ATRA therapy for Kelly (**Figure 5A**), SY5Y (**Figure 5B**), and SKNAS (**Figure 5C**) versus single agent treatments. Clinically, high-risk NB patients are treated with high-dose 13-cis-retinoic acid (isotretinoin) as maintenance therapy, which converts into all-trans-retinoic acid (ATRA) and 9-cis-retinoic acid (9-cis-RA), a stereoisomer of ATRA<sup>28, 29</sup>. Both 9-cis-RA and ATRA can promote differentiation. Therefore, we tested 9-cis-retinoic acid versus ATRA in combination with JQ1 to compare their effects on differentiation in the presence of JQ1 in Kelly and SY5Y cells. The combination of JQ1 with either ATRA or 9-cis-RA lead to comparable increases in TH and GATA3 expression, and loss of ASCL1 and SOX10 expression indicating similar effects on cell differentiation (**Figure S3B and S3C**). Next, we determined the combination index (CI) for median effect concentration of JQ1 with ATRA or 9-cis-RA using Chou and Talalay method (compusyn software)<sup>30</sup>. We found a CI of 0.56 against Kelly and 0.61 against SKNAS cells with Dose vs Fraction affected (Fa) curves for Kelly (**Figure 5D**) and SKNAS (**Figure 5E**) indicating this combination is synergistic *in vitro*. The findings of CI values against Fa indicate combinatorial treatment of low dose JQ1 (100nM) with either 100nM, 500nM or 1000nM of ATRA has CIs of 0.33, 0.40 and 0.29 respectively indicating effective synergies while high-dose JQ1 (1 $\mu$ M) in combination with 100nM or 500nM ATRA having CIs of 1.39, 1.03 respectively indicating an antagonistic affect when Kelly cells are treated with high concentrations of JQ1 and lower concentrations of ATRA (**Figure 5F**). We had similar findings for SKNAS where low dose JQ1 was synergistic with ATRA, but high dose was antagonistic (**Figure 5G**). Additionally, we screened 9-cis-RA in combination with JQ1 analyzing the dose vs effect with CI values in Kelly and SKNAS cells finding similar effects as we observed with ATRA (**Figure S4A-D**). However, we found 9-cis-RA to be less effective than ATRA showing higher CI but still synergistic values at combinations of 100nM JQ1 with either 100nM or 500nM of 9-cis-RA (CI values 0.82, 0.81).

Due to our observations that combinations of JQ1 and ATRA lead to a reduction in SOX10 expression, which is a marker for stemness, we next performed two assays that are surrogate tests for cancer stem/progenitor cell behavior, a colony-forming assay and a tumor-sphere assay. For the colony forming assay we continuously treated cells with combinations of JQ1 and ATRA for 10 days with concentrations ranging from 10nM to 1 $\mu$ M for both compounds and showed a complete growth inhibition in the crystal violet assay image pattern of Kelly and SKNAS cells at a combination treatment of 10nM JQ1 with 100nM ATRA, which was not observed at equivalent concentrations of single agents (**Figure 6A** and **S5**). To determine the long-term treatment effects, we performed a soft-agar tumor-sphere forming assay treating with JQ1 and ATRA combinations from 10nM, 100nM to 1 $\mu$ M concentrations for 25 days. The combination of 10nM JQ1 with 100nM ATRA significantly inhibited tumor-sphere formation and growth in soft agar similar to what was observed with the colony forming assay (**Figure 6B**). Both the colony-forming and tumor-sphere assays indicate that BET inhibitors with retinoic acid treatment can reduced stem/progenitor behavior in NBCLs.

**Discussion:** Dysregulated expression of CRC transcription factors in NB that control neural cell maturation is proposed to retain cells in immature oncogenic identity states. One underutilized strategy for treating NB is to push the cells into a more differentiated and less dangerous state through differentiation therapy. Though limited, RA treatments are the most successful therapeutics for differentiation therapy in cancer and this study identifies a novel strategy to improve the efficacy of retinoids<sup>31-33</sup>. NB is characterized by two identity states, an adrenergic proliferative state; and a mesenchymal pro-migratory, therapy resistant state that are maintained by different CRCs. In aggressive NB, MYCN is a frequently amplified transcription factor which can enforce high expression of ASCL1 in certain NB cell types including Kelly<sup>34</sup>. In this study, after knockdown of ASCL1 in the MYCN amplified Kelly cell line, we observed opposite responses of gene and protein expression in the core regulatory transcription factors GATA3 and SOX10, which regulate cell identity during development. Silencing of ASCL1 in combination with ATRA further increased TH and reduced proliferation in Kelly cells. This indicated that disrupting the developmental block caused by high ASCL1 expression in combination with ATRA is an effective strategy to drive differentiation of Kelly cells. Other subtypes of NB that do not have a defined oncogenic driver like N-Myc and whose etiology is not as well understood, also have immature CRCs<sup>35</sup>. We investigated whether resistance to ATRA induced differentiation could be overcome by disrupting developmentally immature CRCs irrespective of the NB subtype using the BET inhibitor JQ1. BET inhibitors suppress the super-enhancers that often increase the expression of transcription factors that regulate identity states. Treatment with JQ1 and retinoids (ATRA or 9-cis RA) resulted in the three cell lines showing, 1) a significant loss of SOX10, a key neural stem cell marker that plays a prominent role in multipotency and inhibition of neuronal differentiation<sup>36</sup>, 2) a gain of the differentiation marker TH and 3) a significant inhibition in cell growth in multiple *in vitro* assays. We observed that JQ1 was sufficient to cause decreased gene expression of the mesenchymal/ stem marker SOX10 in Kelly and SY5Y cells, while, in the timeframe tested, protein levels only decreased when cells were treated with both JQ1 and ATRA. Similarly, we observe that SKNAS does not show loss of *SOX10* mRNA expression but does show loss of SOX10 protein when treated by the combination. This suggests ATRA promotes protein turnover of SOX10. RA has previously been shown to promote protein degradation of the insulin receptor substrate (IRS-1) and, in neuroblastoma cell lines, repressor element-1 silencing

transcription factor (REST)<sup>37-39</sup>. The reduced SOX10 expression, loss of colony formation and loss of tumor-sphere formation in response to combinatorial treatment indicates a loss of stem/progenitor cells, the proposed cause of metastatic spread and relapse disease<sup>40</sup>.

We have demonstrated that Kelly cells are dependent on ASCL1 expression and the changes we observe with ASCL1 silencing are also seen with JQ1/ATRA combinatorial treatment in Kelly cells. Though we have not demonstrated that SY5Y is ASCL1 dependent, this cell line has similar responses to JQ1/ATRA treatment as Kelly for the markers we have analyzed, suggesting SY5Y might have a similar developmental block as Kelly cells. In contrast, SKNAS shows multiple differing behavior with the other two cell lines in its response to JQ1/ATRA suggesting this line has a different developmental block. It is known that SKNAS cells have a chromosomal translocation that places c-Myc under the control of the HAND2 super-enhancer, which may explain its differential response to JQ1/ATRA treatment<sup>40</sup>. Overall, these findings suggests that the JQ1/ATRA drug combination can overcome different developmental blocks in cell differentiation that occur in NBCL and therefore could be broadly useful in treating NB with different underlying mutations.

Neuroblastoma patients are treated with 13-cis-retinoic acid (isotretinoin), which is metabolized into all trans RA and 9-cis-retinoic acid (9-cis-RA) a stereoisomer of ATRA and has been shown in some instances to be more effective than ATRA in differentiating NB cell lines. ATRA binds the retinoic acid receptor (RAR) while 9-cis-RA binds both RAR and the RAR heterodimerization partner retinoid x receptor (RXR). We observed similar responses to both ATRA and 9-cis-RA in our studies; however, ATRA was more potent at lower concentrations. Interestingly, high doses of JQ1 were antagonistic to lower doses of both retinoids. We speculate that high dose JQ1 interferes with the ability of ATRA to establish a more differentiated CRC, since BET inhibitors indiscriminately affect CRCs. This suggests that timing and dosing of BET inhibitors with retinoids will be critical in their effectiveness and should be further explored in preclinical models.

## Methods and Materials

**Cell lines and culture methods:** Human neuroblastoma cell lines Kelly, SY5Y, SKNAS from European collection of cell cultures and American Type Culture Collection (ATCC, Manassas, VA, USA) and Gimen cells were purchased from Cell line Service GmbH, Germany. These NB Cells were cultured as previously described<sup>41, 42</sup>. Briefly Kelly cell culture media includes RPMI with 10% FBS, SY5Y cells cultured in MEM $\alpha$  with HAM'S F12, NEAA, 10% FBS. SKNAS cells in DMEM, 1% NEAA and 10% FBS. Gimen Cells were grown on DMEM plus 10% FBS. **Doxycycline-inducible shRNA system:** Two different mission shRNAs from the TRC1 library (Sigma-Aldrich, TRCN0000013550, TRCN0000235656, referred in the manuscript as sh6, sh8 respectively) targeting ASCL1 and one non-targeting shRNA control (NTC) were used to generate Kelly NB cell lines with ASCL1 KD. ASCL1-specific short hairpin RNAs were cloned into the Tet-pLKO-puro plasmid (Addgene). Lentiviral particles were produced in 293T cells, and Kelly cells were infected and incubated with viral particles for 24 h with 4 $\mu$ g/ml Polybrene. Selection with puromycin (Invitrogen) at 500 ng/ml, was performed 48 h after infection and maintained during all culture experiments. ASCL1 knockdown efficacy was assessed by immunoblot 72 h after the addition of doxycycline (1 $\mu$ g/ml).

**Drug treatments:** Retinoic acid from Sigma, Cat#R2625, BET inhibitor JQ1 from Cayman chemical company cat#11232. Puromycin (Cat#11138-10, Gibco), Doxycycline (Cat#D9891 Sigma), DMSO (Cat#BP231-100 Fischer Scientific). The drugs were prepared in 10mM or 10mg/ml stocks depending on requirements, filter sterilized and stored in -80°C until further use.

**Cell proliferation assays:** In a 96-well tissue culture plate,  $1 \times 10^4$  cells were plated in each well. Plates were incubated for 4 days in the presence of DMSO, Retinoic acid, JQ1 drug treatments and then submitted to CyQuant Cell Direct Proliferation Assay (Thermo Fisher Scientific) according to manufacturer's instructions and read with a Synergy HT Multi-mode microplate reader (Bio-Tek instruments).

**Soft Agar and crystal violet staining assay:** Kelly and SKNAS cells  $5 \times 10^4$  were incubated in soft agar mixture of 0.3% upper layer and 0.6% agar quoted 12 well culture plates. Cells were incubated for 21 days in DMSO, ATRA, JQ1 and combinations, changing the media every 3 days. Images of tumor-sphere were observed and captured by (Nikon, Microphot FX) by treating the plates with 0.01% crystal violet and subsequent gentle washing with PBS. A ten-day incubation of Kelly and SKNAS in drug treatments was done in normal plates and stained the plates with crystal violet to observe the effect of drug treatments on proliferation.

**Immunofluorescence and Confocal microscopy:** Kelly and SY5Y cells were cultured on 8 well chamber slides under the treatments of DMSO, RA, JQ1 and JQ1+RA condition for 4-7 days. After completion of the time-course cells were immune stained with TH primary antibody, Alexa Flour 488 secondary antibody (Invitrogen) and for the imaging under confocal microscopy (Zeiss 5000) at the UTHSC neuro imaging facility.

**Gene expression analysis:** RNA was isolated using RNeasy Mini Kit (Qiagen USA), following the manufacturers protocol. 1ug of total RNA from each sample was converted to cDNA using SuperScript III first-strand synthesis supermix (Thermo Fisher Scientific). The resulting cDNA sample served as a template for real-time qPCR using TaqMan probes and accompanying Taqman Master Mix (Applied Biosystems, Foster City, CA). PCR amplification was carried out using Quantstudio3 (Applied Biosystems) system with cycle conditions of the initial cycle: 50 °C for 2min, and initial denaturation at 95 °C for 15 sec. This was followed by 40 cycles of denaturation at 95 °C for 15 sec and annealing/extension of 60 °C for 1min. The expression levels of target gene transcripts were determined using  $2^{-DDCt}$  method and normalized to PPIB. Taqman probes used in the study (Applied Biosystems) includes PPIB cat#Hs00168719, TH cat#Hs00165941, ASCL1 Cat#Hs04187546, GATA3 cat# Hs Hs00231122, SOX10 cat#Hs00366918, TWIST1 cat#Hs04989912, MBP cat#Hs00921945, GFAP cat#Hs00157674.

**Protein blot analysis:** After incubation of the cells with designated treatment conditions, the lysates were prepared and protein expression was measured by Western blot analysis using anti-ASCL1 (Cat#ABE1025, Sigma/Millipore), anti-TH Cat# 2792 (CST -Cell Signaling Technology, Danvers, MA, USA), anti-GATA3 (Cat# 5852, CST), anti-PHOX2B (Cat#AB227719, Abcam), anti-SOX9 (Cat#82630, CST) anti-SOX10 antibody (Cat#89356, CST), anti-Vimentin (Cat#5741,CST), anti-SNAI2 (CST#9585), anti-TWIST1 (Cat#4670, CST), anti-ACTIN Cat#3700, anti-PRRX1 (cat# B2380, LS Bio), Secondary goat anti rabbit Alexa fluor488 antibody (BD Bioscience), secondary antibodies with IR Dyes 700 (mouse) 800 (rabbit) were purchased from Li-COR Bioscience. Western blot images were captured on Nitrocellulose (Whatman) by Odyssey Infrared Imaging System (LI-COR Biosciences, Lincoln, NE, USA). Quantification of the protein bands on blots were performed by Image Studio Lite version 5.2 (Li-COR Odyssey).

**Statistics:** All experiments were replicated three times. Differences were tested for statistical significance using ANOVA groups or as unpaired t test for two groups (Graph Pad Prism) with data presented as the Mean  $\pm$  standard error of the mean (SEM) with a p-value of  $<0.05$  considered significant from three independent experiments.

**Acknowledgements**

The author(s) disclosed receipt of the following financial support for the research, authorship, and/or publication of this article: This work was supported by the National Institute Health (R01CA216394 to KWF) and the US Department of Defense (W81XWH-18-1-0477 to KWF)

**Disclosure of Potential Conflicts of Interest**

No potential conflicts of interest disclosed by authors.

## Authors' Contributions

Conception and design: K.W.F., S.A.

Development of methodology: K.W.F., S.A, N.A.

Acquisition of data (provided animals, acquired, and managed patients, provided facilities, etc.): S.A.

Analysis and interpretation of data (e.g., statistical analysis, biostatistics, computational analysis): K.W.F., S.A.

Writing, review, and/or revision of the manuscript: K.W.F., S.A.

Administrative, technical support (reporting or organizing data, constructing databases): S.A., N.A., M.M.

Study supervision: K.W.F., S.A.

**Key words:** Neuroblastoma, ASCL1, Retinoic Acid, BET inhibitor JQ1, MYCN

## References

1. Maris JM. Recent advances in neuroblastoma. *N Engl J Med*. Jun 10 2010;362(23):2202-2211.
2. Cheung NK, Dyer MA. Neuroblastoma: developmental biology, cancer genomics and immunotherapy. *Nat Rev Cancer*. Jun 2013;13(6):397-411.
3. Park JR, Eggert A, Caron H. Neuroblastoma: biology, prognosis, and treatment. *Hematol Oncol Clin North Am*. Feb 2010;24(1):65-86.
4. Peaston AE, Gardaneh M, Franco AV, et al. MRP1 gene expression level regulates the death and differentiation response of neuroblastoma cells. *Br J Cancer*. Nov 16 2001;85(10):1564-1571.
5. Applebaum MA, Henderson TO, Lee SM, Pinto N, Volchenbom SL, Cohn SL. Second malignancies in patients with neuroblastoma: the effects of risk-based therapy. *Pediatr Blood Cancer*. Jan 2015;62(1):128-133.
6. Wang K. Integrative genomics identifies LMO1 as a neuroblastoma oncogene. *Nature*. 2011// 2011;469.
7. Laverdiere C, Cheung NK, Kushner BH, et al. Long-term complications in survivors of advanced stage neuroblastoma. *Pediatr Blood Cancer*. Sep 2005;45(3):324-332.
8. Pinto NR, Applebaum MA, Volchenbom SL, et al. Advances in Risk Classification and Treatment Strategies for Neuroblastoma. *J Clin Oncol*. Sep 20 2015;33(27):3008-3017.
9. Tomolonis JA, Agarwal S, Shohet JM. Neuroblastoma pathogenesis: deregulation of embryonic neural crest development. *Cell Tissue Res*. May 2018;372(2):245-262.
10. Huang HS, Redmond TM, Kubish GM, et al. Transcriptional regulatory events initiated by Ascl1 and Neurog2 during neuronal differentiation of P19 embryonic carcinoma cells. *J Mol Neurosci*. Mar 2015;55(3):684-705.

11. Decaestecker B, De Preter K, Speleman F. DREAM target reactivation by core transcriptional regulators supports neuroblastoma growth. *Mol Cell Oncol.* 2019;6(2):1565470.
12. Almutairi B, Charlet J, Dallosso AR, et al. Epigenetic deregulation of GATA3 in neuroblastoma is associated with increased GATA3 protein expression and with poor outcomes. *Sci Rep.* Dec 12 2019;9(1):18934.
13. Boeva V. Heterogeneity of neuroblastoma cell identity defined by transcriptional circuitries. *Nat Genet.* 2017// 2017;49.
14. Soldatov R, Kaucka M, Kastriti ME, et al. Spatiotemporal structure of cell fate decisions in murine neural crest. *Science.* Jun 7 2019;364(6444).
15. Maden M. Retinoic acid in the development, regeneration and maintenance of the nervous system. *Nat Rev Neurosci.* Oct 2007;8(10):755-765.
16. Zimmerman MW, Durbin AD, He S, et al. Retinoic acid rewires the adrenergic core regulatory circuitry of neuroblastoma but can be subverted by enhancer hijacking of *MYC* or *MYCN*. *bioRxiv.* 2020:2020.2007.2023.218834.
17. Filippakopoulos P, Qi J, Picaud S, et al. Selective inhibition of BET bromodomains. *Nature.* Dec 23 2010;468(7327):1067-1073.
18. Lee S, Rellinger EJ, Kim KW, et al. Bromodomain and extraterminal inhibition blocks tumor progression and promotes differentiation in neuroblastoma. *Surgery.* Sep 2015;158(3):819-826.
19. Puissant A, Frumm SM, Alexe G, et al. Targeting MYCN in neuroblastoma by BET bromodomain inhibition. *Cancer Discov.* Mar 2013;3(3):308-323.
20. van Groningen T, Koster J, Valentijn LJ, et al. Neuroblastoma is composed of two super-enhancer-associated differentiation states. *Nat Genet.* Aug 2017;49(8):1261-1266.
21. Amiel J, Laudier B, Attie-Bitach T, et al. Polyalanine expansion and frameshift mutations of the paired-like homeobox gene PHOX2B in congenital central hypoventilation syndrome. *Nat Genet.* Apr 2003;33(4):459-461.
22. Moriguchi T, Takako N, Hamada M, et al. Gata3 participates in a complex transcriptional feedback network to regulate sympathoadrenal differentiation. *Development.* Oct 2006;133(19):3871-3881.
23. Aquino JB, Hjerling-Leffler J, Koltzenburg M, Edlund T, Villar MJ, Ernfors P. In vitro and in vivo differentiation of boundary cap neural crest stem cells into mature Schwann cells. *Exp Neurol.* Apr 2006;198(2):438-449.
24. Aldskogius H, Berens C, Kanaykina N, et al. Regulation of boundary cap neural crest stem cell differentiation after transplantation. *Stem Cells.* Jul 2009;27(7):1592-1603.
25. Isenmann S, Arthur A, Zannettino AC, et al. TWIST family of basic helix-loop-helix transcription factors mediate human mesenchymal stem cell growth and commitment. *Stem Cells.* Oct 2009;27(10):2457-2468.
26. Diaz VM, Vinas-Castells R, Garcia de Herreros A. Regulation of the protein stability of EMT transcription factors. *Cell Adh Migr.* 2014;8(4):418-428.
27. Iwase K, Nagasaka A, Nagatsu I, et al. Tyrosine hydroxylase indicates cell differentiation of catecholamine biosynthesis in neuroendocrine tumors. *J Endocrinol Invest.* Apr 1994;17(4):235-239.

28. Veal GJ, Cole M, Errington J, et al. Pharmacokinetics and metabolism of 13-cis-retinoic acid (isotretinoin) in children with high-risk neuroblastoma - a study of the United Kingdom Children's Cancer Study Group. *Br J Cancer*. Feb 12 2007;96(3):424-431.
29. Matthay KK, Villablanca JG, Seeger RC, et al. Treatment of high-risk neuroblastoma with intensive chemotherapy, radiotherapy, autologous bone marrow transplantation, and 13-cis-retinoic acid. Children's Cancer Group. *N Engl J Med*. Oct 14 1999;341(16):1165-1173.
30. Chou TC. Drug combination studies and their synergy quantification using the Chou-Talalay method. *Cancer Res*. Jan 15 2010;70(2):440-446.
31. Matthay KK, Reynolds CP, Seeger RC, et al. Long-term results for children with high-risk neuroblastoma treated on a randomized trial of myeloablative therapy followed by 13-cis-retinoic acid: a children's oncology group study. *J Clin Oncol*. Mar 1 2009;27(7):1007-1013.
32. Kohler JA, Imeson J, Ellershaw C, Lie SO. A randomized trial of 13-Cis retinoic acid in children with advanced neuroblastoma after high-dose therapy. *Br J Cancer*. Nov 2000;83(9):1124-1127.
33. Peinemann F, van Dalen EC, Tushabe DA, Berthold F. Retinoic acid post consolidation therapy for high-risk neuroblastoma patients treated with autologous hematopoietic stem cell transplantation. *Cochrane Database Syst Rev*. Jan 29 2015;1:CD010685.
34. Westermann F, Muth D, Benner A, et al. Distinct transcriptional MYCN/c-MYC activities are associated with spontaneous regression or malignant progression in neuroblastomas. *Genome Biol*. Oct 13 2008;9(10):R150.
35. Wang L, Tan TK, Durbin AD, et al. ASCL1 is a MYCN- and LMO1-dependent member of the adrenergic neuroblastoma core regulatory circuitry. *Nat Commun*. Dec 9 2019;10(1):5622.
36. Kim J, Lo L, Dormand E, Anderson DJ. SOX10 maintains multipotency and inhibits neuronal differentiation of neural crest stem cells. *Neuron*. Apr 10 2003;38(1):17-31.
37. del Rincon SV, Guo Q, Morelli C, Shiu HY, Surmacz E, Miller WH. Retinoic acid mediates degradation of IRS-1 by the ubiquitin-proteasome pathway, via a PKC-dependant mechanism. *Oncogene*. Dec 9 2004;23(57):9269-9279.
38. Singh A, Rokes C, Gireud M, et al. Retinoic acid induces REST degradation and neuronal differentiation by modulating the expression of SCF(beta-TRCP) in neuroblastoma cells. *Cancer*. Nov 15 2011;117(22):5189-5202.
39. Wang Y, Zhang D, Tang Z, et al. REST, regulated by RA through miR-29a and the proteasome pathway, plays a crucial role in RPC proliferation and differentiation. *Cell Death Dis*. May 1 2018;9(5):444.
40. Visvader JE, Lindeman GJ. Cancer stem cells: current status and evolving complexities. *Cell Stem Cell*. Jun 14 2012;10(6):717-728.
41. Edsjo A, Nilsson H, Vandesompele J, et al. Neuroblastoma cells with overexpressed MYCN retain their capacity to undergo neuronal differentiation. *Lab Invest*. Apr 2004;84(4):406-417.



42. Biedler JL, Helson L, Spengler BA. Morphology and growth, tumorigenicity, and cytogenetics of human neuroblastoma cells in continuous culture. *Cancer Res.* Nov 1973;33(11):2643-2652.

### List of Figures Captions

**Figure 1. Evaluation of the ASCL1 Knockdown and its effects on CRC factors by Sh6 and Sh8 in Kelly.** Sh6 and Sh8 induced knockdown of ASCL1 in the presence of doxycycline at Day4 as assessed by (A and B) RT-PCR and (C and D) western blot analysis. (E and F) Gene expression of ASCL1, SOX10 and GATA3 in Sh6 and Sh8 inducible Kelly cells by RT-PCR analysis. (G and H) Protein expression of CRC transcription factors in Sh6 and Sh8 cells. (All statistical data presented as Mean  $\pm$  SEM with n=3, \*\*p< 0.01 or \*p< 0.05).

**Figure 2. Effect of ASCL1 knockdown and treatment of ATRA on proliferation and differentiation.** (A and B) The gene expression of ASCL1 and TH in day3 treatments of Dox vs Dox+ATRA in Sh6 and Sh8 inducible cells by RT-PCR assay. (C) Protein expression of ASCL1 and TH as assessed by Western blots. (D) Proliferation percentage in Sh6 and Sh8 inducible cells at day4 treatment of doxycycline and Dox+ATRA combination as measured by CyQuant. (n=3, \*\*p< 0.01 or \*p< 0.05).

**Figure 3. Effect of JQ1 and ATRA combinations on gene expression of CRC in NB cells.** (A-C). Gene expression by RT-PCR of ASCL1, GATA3 and SOX10 in (A) Kelly, (B) SY5Y and (C) SKNAS cells under the treatment of independent and combinations of JQ1+ATRA. (All data presented as Mean  $\pm$  SEM with n=3, \*\*p< 0.01 or \*p< 0.05)

**Figure 4. Evaluation of Differentiation markers under JQ1 and ATRA combinatorial treatments in NB cells.** (A and B) Gene expression by RT-PCR of *TH* and *MBP* in Kelly, SY5Y and SKNAS cells under the treatment of independent and combinations of JQ1+ATRA. (C, D and E) Protein expression analyzed by western blots of TH and ASCL1 in the three cell lines under the treatment of independent and combinations of JQ1+ATRA. (Data presented as Mean  $\pm$  SEM with n=3, \*\*p< 0.01)

**Figure 5. Determination of Dose vs Response effect of JQ1+ATRA combinatorial treatments on NB cells.** (A, B and C) Combinatorial treatment of JQ1 and ATRA on Kelly, SKNAS and SY5Y on % proliferation by CyQuant assay data. (D and E) Dose vs Response curves in the treatments of JQ1 with ATRA combinations on Kelly and SKNAS cells. X-axis represents the concentration of drugs used; Y-axis represents the % inhibition of cells as fraction affected (Fa). (F and G) The combinatorial treatment of JQ1+ATRA in Kelly and SKNAS on the quantitative outcomes of combination Index (CI) values. X- axis represents % inhibition of cells as Fa, Y-axis represents combination index, which generates drug effect values with differing ratio of drug combinations. Representative data were analyzed by Compusyn software. (Data presented as Mean  $\pm$  SEM with n=3, \*\*p< 0.01 or \*p< 0.05, \*significant difference between JQ1 vs JQ1+ATRA).

**Figure 6. Effect of JQ1 and ATRA combinatorial treatments on tumor sphere formation.** (A) Tumor sphere formation in 25 days after treating cells with JQ1, ATRA

and combinations from 10nM to 1 $\mu$ M. (B) Proliferation inhibition measured by CyQuant assay of Kelly with JQ1 and ATRA combinatorial treatments for 10 days. Representative images of tumor spheres and proliferating colony of Kelly cells. Cells were imaged after adding crystal violet dye and washing procedure.

**Supplementary Figure 1. Comparison of basal core regulatory transcription factor expression in NB cell lines:** Western blot analysis of protein expression of core regulatory transcription factors ASCL1, GATA3, TBX2 and PHOX2B that drive adrenergic identity and core regulatory transcription factors SOX10, TWIST1, PRRX1, SNAI2 that drive mesenchymal identity including the mesenchymal marker vimentin in the NB cell lines Kelly, SKNAS, SKNBE2, GIMEN and SY5Y cells.

**Supplementary Figure 2. Effect of ATRA and JQ1 combinations on NB cell proliferation.** (A) Drug Titrations from 10nM to 10 $\mu$ M concentrations were analyzed by CyQuant assay to optimize effective combinations for checking the expression of stemness and differentiation markers. Representative data of 10, 100, 1 $\mu$ M JQ1 and ATRA on NB cells. (B) Representative western blot showing a basal protein expression of MYCN between NB cells Kelly, SKNAS, GIMEN and SY5Y. (C) Protein expression of MYCN in Kelly cells treated with ATRA and JQ1 combinations.

**Supplementary Figure 3. Comparison of all trans retinoic acid vs 9 cis retinoic acid in NB cell differentiation and loss of stemness.** (A) Analysis of TH expression by Immune fluorescence staining in Kelly and SY5Y cells treated with JQ1 and ATRA combinations after four days. Representative images were obtained by confocal microscopy. (B) Representative western blots of protein expression of ASCL1, TH and GATA3 in Kelly cells under the treatment of all trans retinoic acid vs 9 cis retinoic acid in combination with JQ1. (C) protein expression of TH and SOX10 in SY5Y cells treated with all trans retinoic acid vs 9 cis retinoic acid in combination with JQ1.

**Supplementary Figure 4. Effect of all trans retinoic acid vs 9 cis retinoic acid treatments on dose vs response and combination index in Kelly and SKNAS cells.** (A) Effect of 9 cis retinoic acid independently and in combination with JQ1 on dose vs response in Kelly cells. (B) effect of 9 cis retinoic acid independently and combination with JQ1 on dose vs response in SKNAS cells. (C) Treatment effect of 9 cis retinoic acid with JQ1 on combination index in Kelly cells. (D) Treatment effect of 9 cis retinoic acid with JQ1 on combination index in SKNAS cells. The effect of dose vs response on NBCL was analyzed by Compusyn software according to Chau and Talalay method.

**Supplementary Figure 5. Effect of ATRA and JQ1 combinations on NB cell proliferation and differentiation.** (A) Representative images of 10-day duration treatment effect of ATRA, JQ1 and combinations on proliferation of SKNAS cells analyzed by crystal violet staining.

**Figure 1**

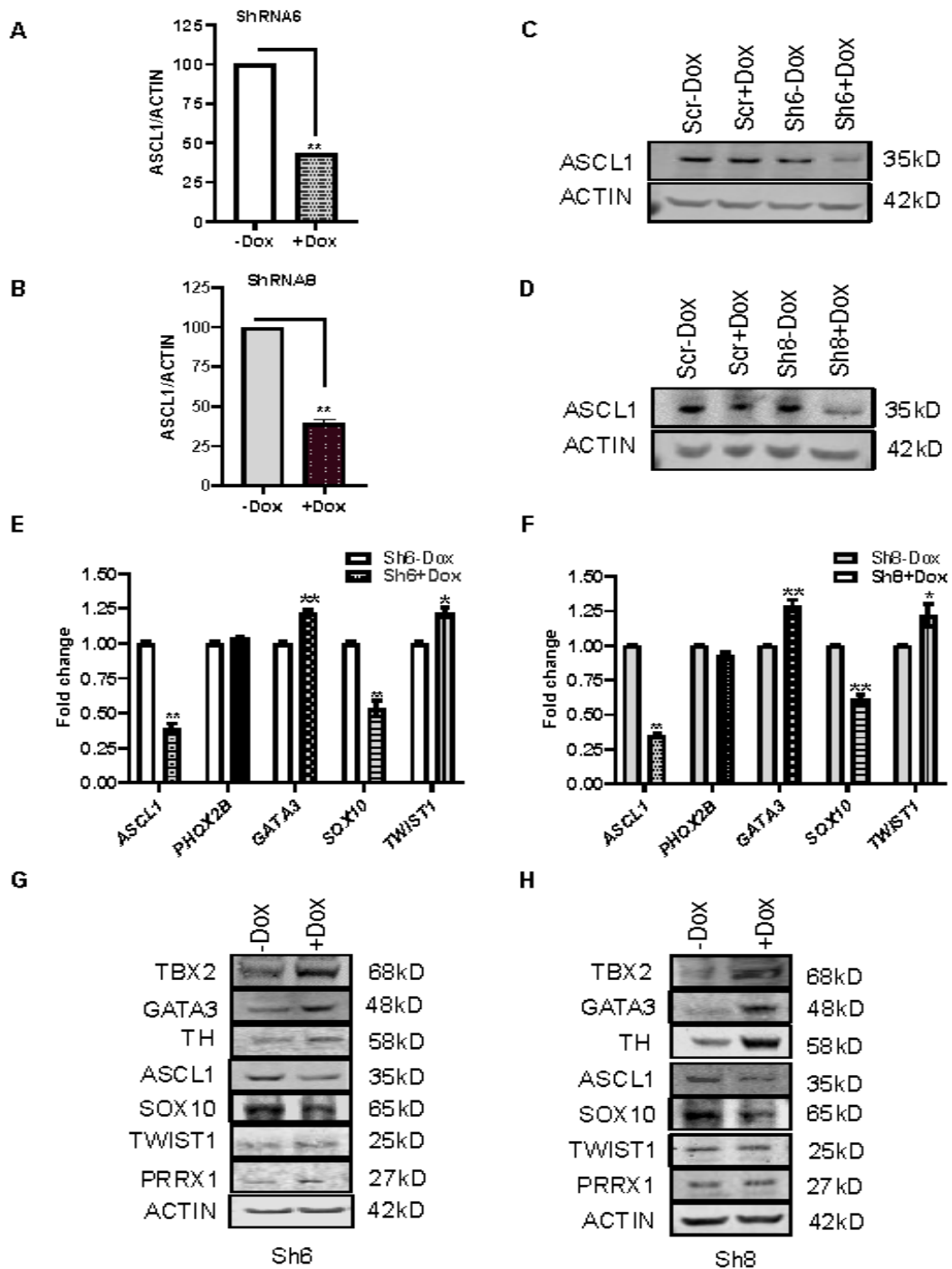


**Figure 2**

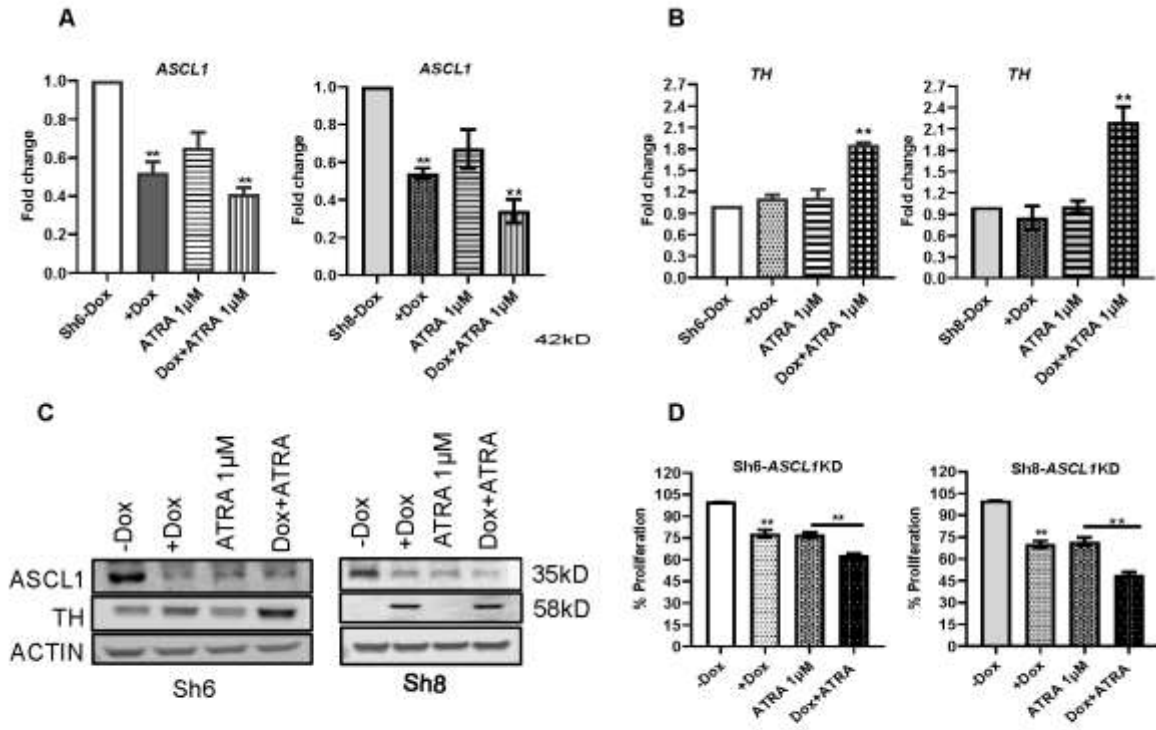


Figure 3

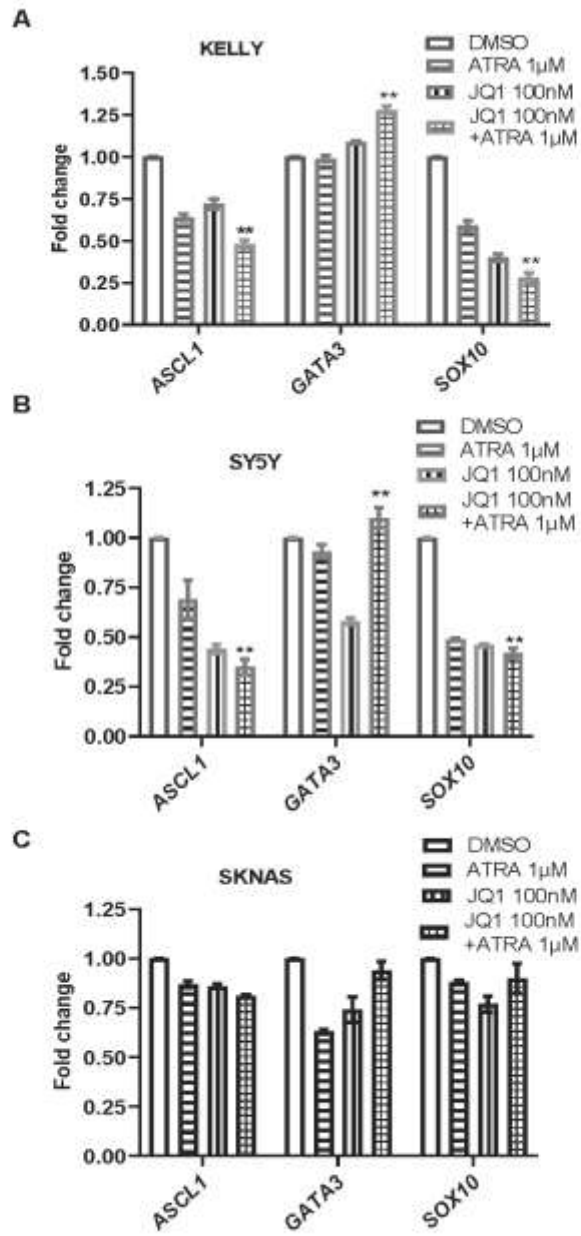


Figure 4

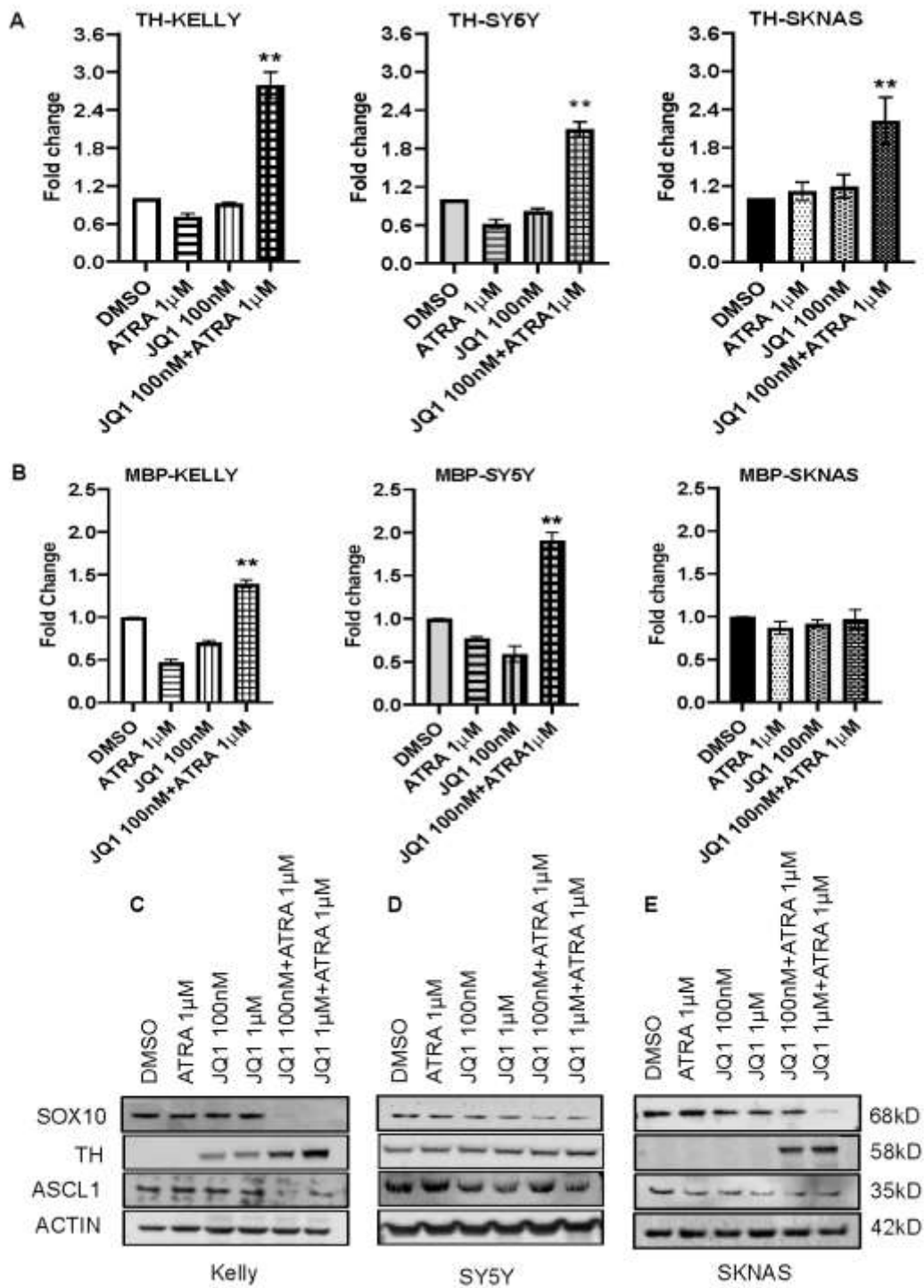


Figure 5

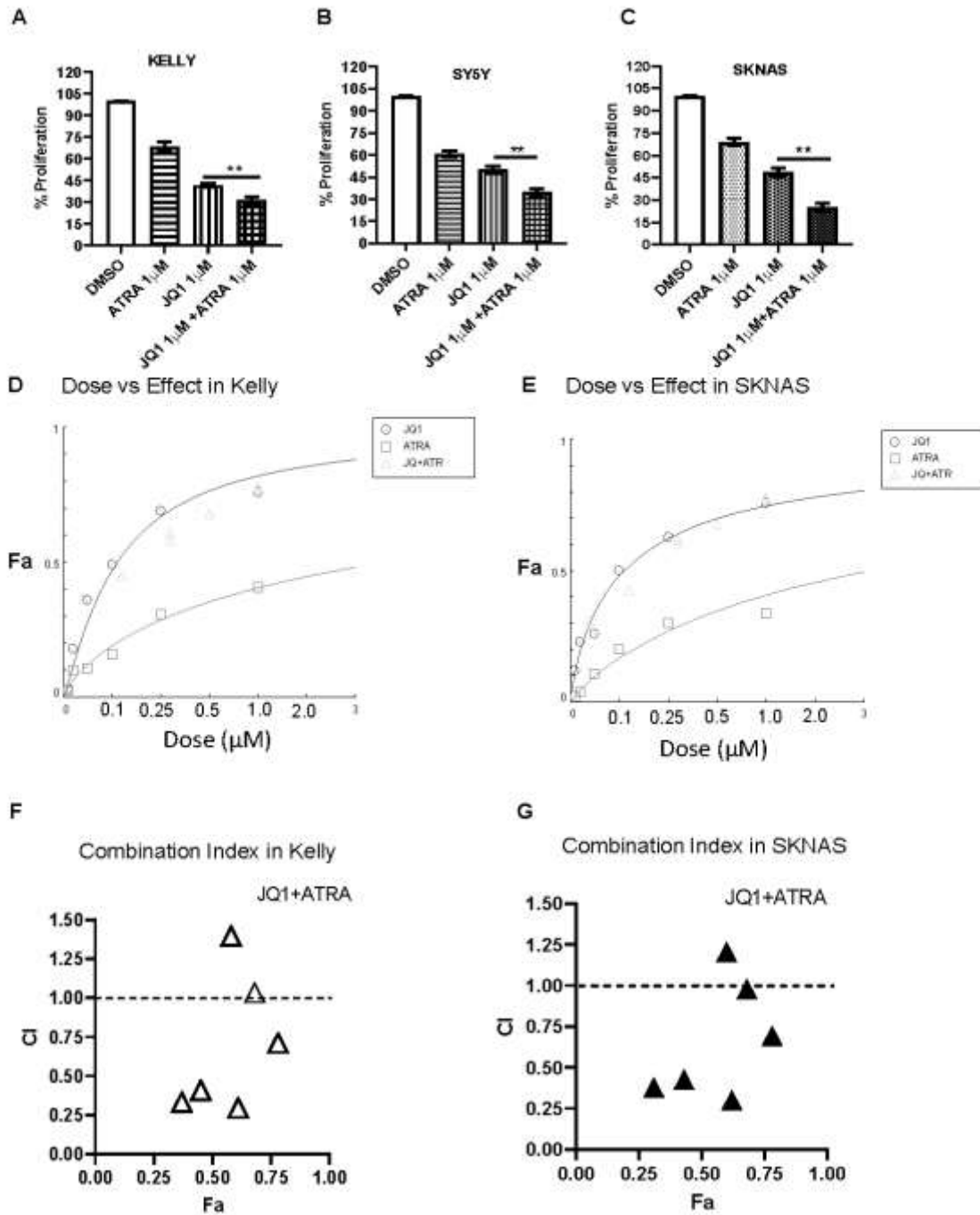
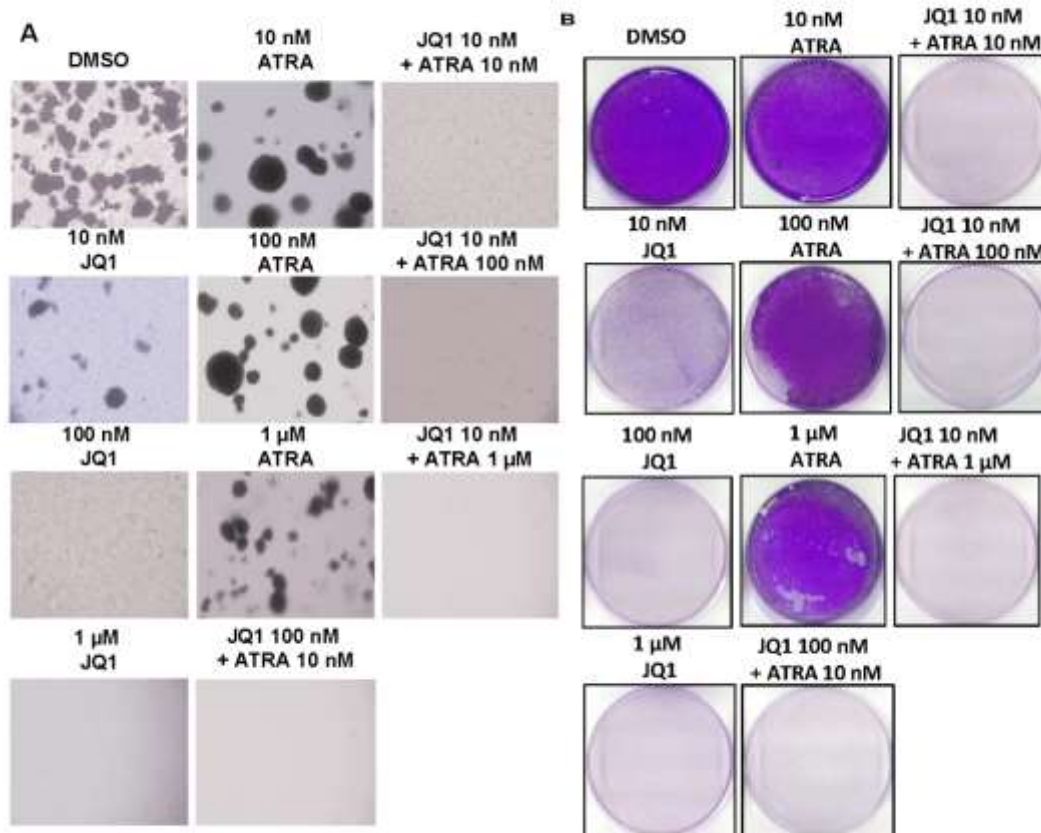


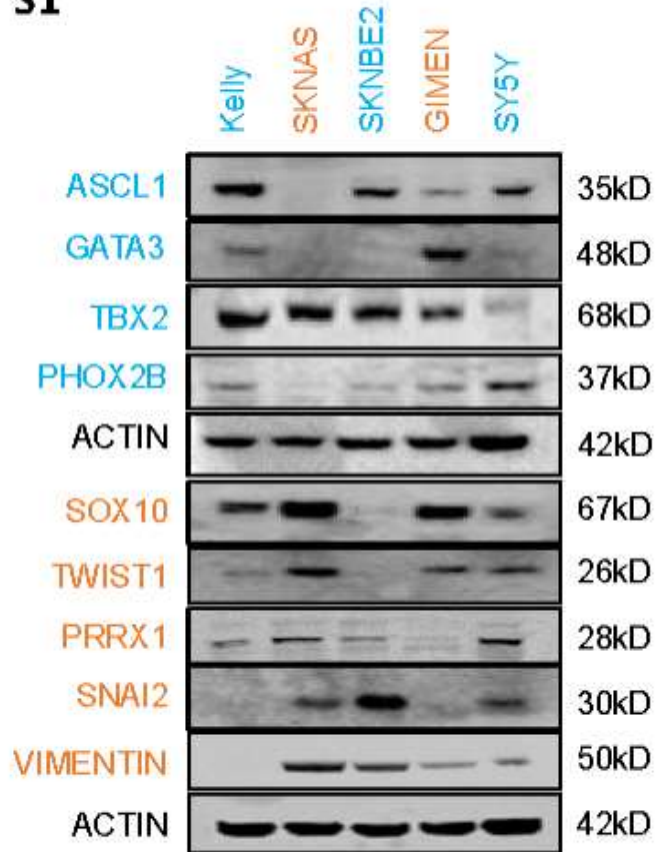
Figure 6



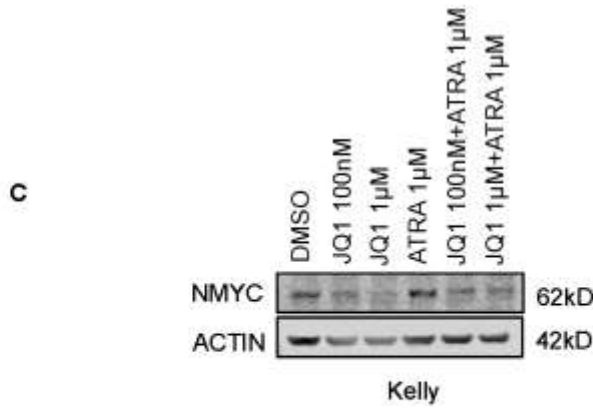
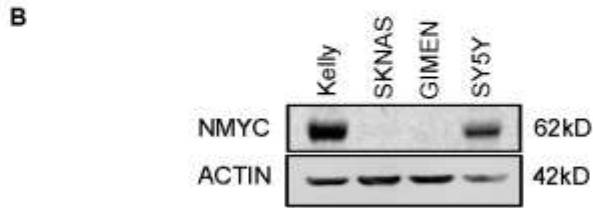
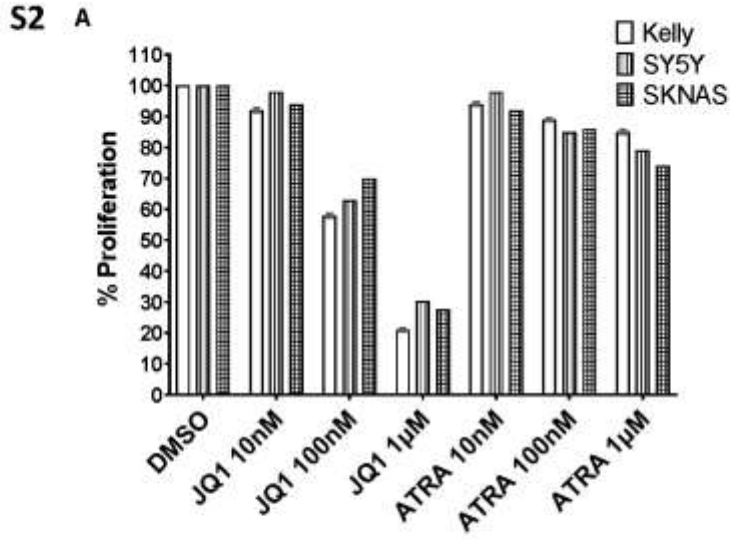


Supplementary figure 1

**S1**

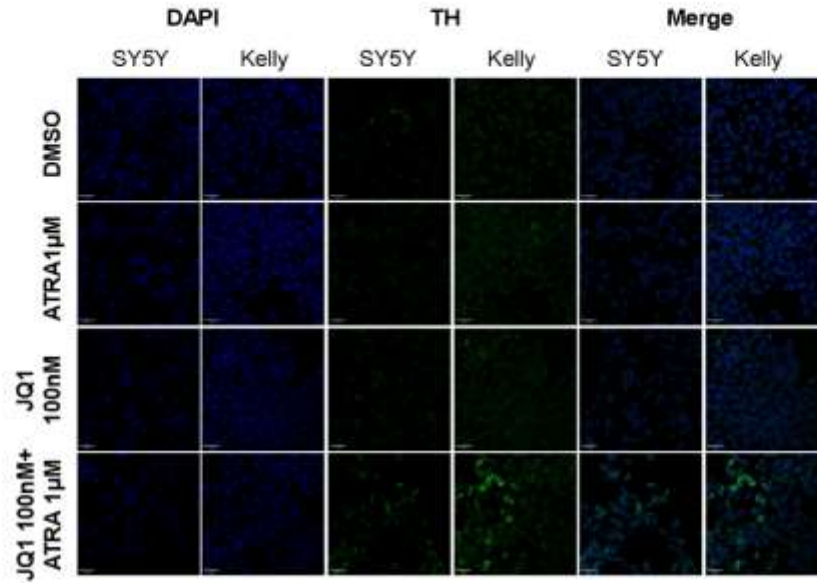


Supplementary figure 2

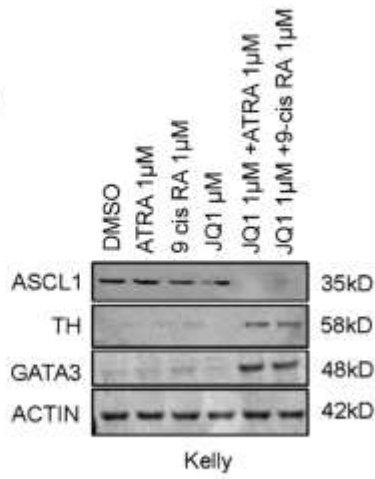


Supplementary figure 3

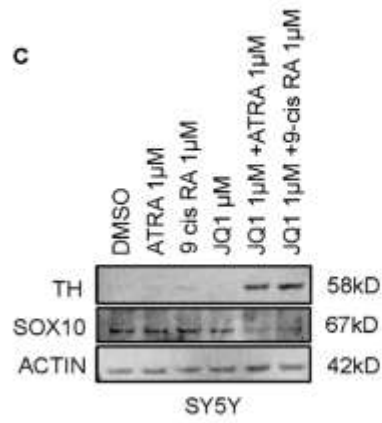
S3 A



B



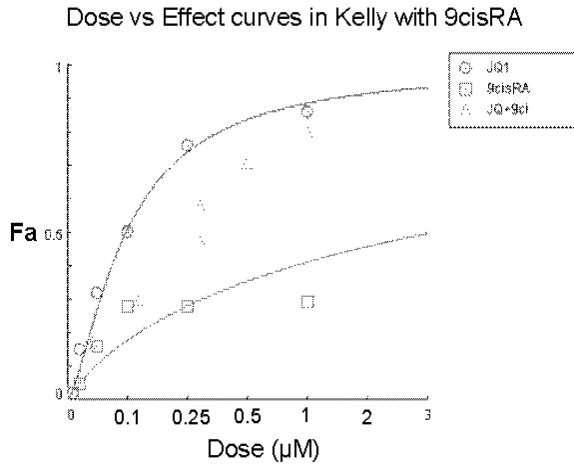
C



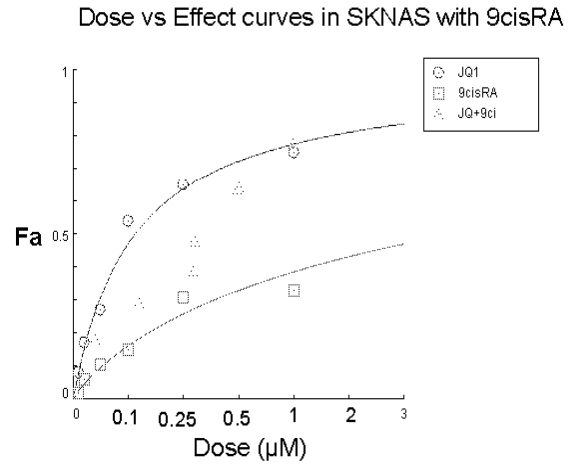
Supplementary figure 4

S4

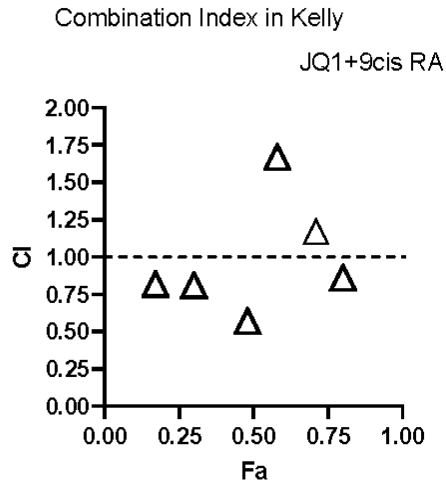
A



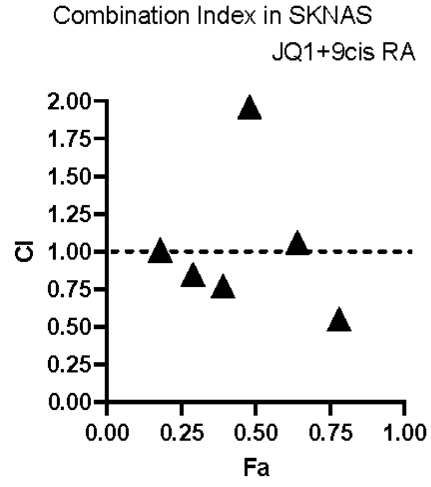
B



C

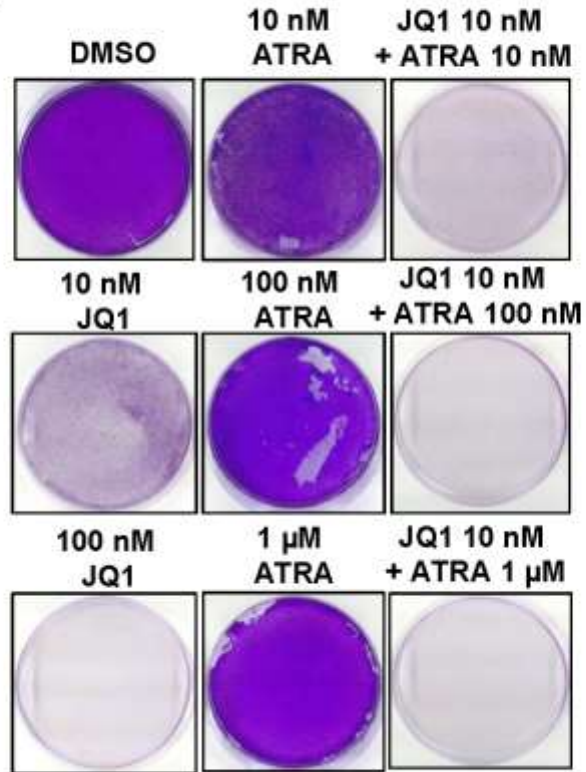


D



Supplementary figure 5

S5



## VITA

Nour A Aljouda was born in Nablus, Palestine in 1988. Following her graduation from Pharmacy school at the An-Najah National university she began working as a pharmacist at the Nablus Specialty Hospital. In the summer of 2012, she moved to the United States of America with her husband Abdul so that she could pursue her dream of earning a graduate degree from the University of Missouri Kansas City (UMKC), specializing in Pharmacology with a minor in pharmaceutical sciences. In early 2015, Nour was compelled to leave her graduate program at UMKC when multiple allegations concerning her prior PI led to the closure of the department. However, being determined to continue a career in science, Nour joined the Integrated Biomedical Sciences Program at the University of Tennessee Health Science Center (UTHSC) in 2018. She was awarded the 1st place for the top presentation at Graduate Research Day UTHSC, best graduate student in the Genetics department, an Imhotep Society Membership, and served as the Vice President Education at the UTHSC Toastmaster club, and the honor council president at the Graduate Health Sciences Executive Council for 3 years. She expects to complete her doctoral degree by May of 2023.